

IDENTIFICATION OF SIRT1 AS A NOVEL REGULATOR OF NFAT5 DEPENDENT  
ALDOSE REDUCTASE EXPRESSION UNDER OSMOTIC STRESS

by

AHMET CAN TİMUÇİN

Submitted to Graduate School of Engineering and Natural Sciences

in partial fulfilment of the requirements for the degree of

Doctor of Philosophy

Sabancı University

July 2015

IDENTIFICATION OF SIRT1 AS A NOVEL REGULATOR OF NFAT5 DEPENDENT  
ALDOSE REDUCTASE EXPRESSION UNDER OSMOTIC STRESS

APPROVED BY:

Prof. Dr. Hüveyda BAŞAĞA  
(Thesis Supervisor)



Asst. Prof. Dr. Alpay TARALP



Assoc. Prof. Dr. Batu ERMAN



Asst. Prof. Dr. Özgür KÜTÜK



Prof. Dr. Uğur SEZERMAN



DATE OF APPROVAL: 23/07/2015

© Ahmet Can Timuçin 2015

All Rights Reserved

## ABSTRACT

### IDENTIFICATION OF SIRT1 AS A NOVEL REGULATOR OF NFAT5 DEPENDENT ALDOSE REDUCTASE EXPRESSION UNDER OSMOTIC STRESS

AHMET CAN TİMUÇİN

Biological Sciences and Bioengineering, PhD Dissertation, July 2015

Thesis Supervisor: Prof. Dr. Hüveyda BAŞAĞA

Keywords: NFAT5, SIRT1, aldose reductase, osmotic stress, deacetylation

Until now, numerous diverse molecules modulating NFAT5 and its targets have been characterized. Among these widespread NFAT5 modifiers, SIRT1 has been proposed to be a promising candidate to play a role in NFAT5 dependent events, yet the exact machinery still remains inconclusive. Hence, in this thesis, we aimed to delineate the link between SIRT1 and NFAT5-Aldose Reductase (AR) axis under osmotic stress. A unique osmotic stress model was generated and its mechanistic components were deciphered in U937 monocytes. By utilization of pharmacological modulators in this model, we showed that AR expression and stabilization of nuclear NFAT5, were revealed to be positively regulated by SIRT1. Overexpression and co-transfection studies of NFAT5 and SIRT1, further validated contribution of SIRT1 on NFAT5 dependent AR expression. Involvement of SIRT1 activity in these events was mediated via modification of DNA binding of NFAT5 to AR ORE region. Besides, NFAT5 and SIRT1 were also shown to co-immunoprecipitate under isosmotic conditions and this interaction was disrupted by osmotic stress. Subsequently, *in silico* experiments were conducted for investigating if SIRT1 directly targets NFAT5. In this regard, certain lysine residues of NFAT5, when kept deacetylated, were found to contribute to its DNA binding and SIRT1 was shown to target acetylated lysine 282 of NFAT5. Based on *in vitro* and *in silico* findings, we identified SIRT1, for the first time, as a novel contributor to NFAT5 dependent AR expression under osmotic stress.

## ÖZET

### OZMOTİK STRES ALTINDA, SIRT1`İN NFAT5 BAĞIMLI ALDOZ REDÜKTAZ ANLATIMININ YENİ DÜZENLEYİCİSİ OLARAK TANIMLANMASI

AHMET CAN TİMUÇİN

Biyoloji Bilimleri ve Biyomühendislik, Doktora Tezi, Temmuz 2015

Tez Danışmanı: Prof. Dr. Hüveyda BAŞAĞA

Anahtar Kelimeler: NFAT5, SIRT1, aldoz redüktaz, ozmotik stres, deasetilasyon

Bugüne kadar, çeşitli moleküllerin NFAT5`i ve hedeflerini düzenlendiği tanımlanmıştır. Bu yaygın NFAT5 düzenleyicileri arasından, NFAT5 bağımlı olaylarda rol almak üzere, SIRT1, umut verici bir aday olarak önerilmiş fakat bunun kesin mekanizması ortaya konmamıştır. Bu nedenle, bu tezde, ozmotik stress altında, SIRT1 ve NFAT5-Aldoz Redüktaz (AR) eksenli ilişkisinin açıklanması hedeflenmiştir. Özgün ozmotik stress modeli oluşturulmuş ve bu modelin mekanizmasının bileşenleri U937 monositlerinde araştırılmıştır. Bu modelde, SIRT1 düzenleyicileri kullanılarak, AR anlatımının ve nükleer NFAT5 stabilizasyonunun, SIRT1 tarafından pozitif yönde etkilendiği gösterilmiştir. NFAT5 ve SIRT1`in aşırı anlatım ve ko-transfeksiyon çalışmaları ile SIRT1`in NFAT5 bağımlı AR anlatımı üzerindeki etkisi doğrulanmıştır. SIRT1`in bu olaylara, NFAT5`in AR geninin ORE bölgesine bağlanmasını sağlayarak katıldığı ortaya konmuştur. Öte yandan, izozmotik koşullarda, NFAT5 ve SIRT1 ko-immunopresipitasyonu gösterilmiş ve bu ilişkinin ozmotik stress altında bozulduğu gözlemlenmiştir. Bunları takiben, *in siliko* deneyler ile, NFAT5`in SIRT1 tarafından doğrudan etkilenmesi araştırılmıştır. Bu bağlamda, belli NFAT5 lizinlerinin, deasetilasyon durumunda iken, NFAT5`in DNA`ya bağlanmasına katkıda bulunduğu ve SIRT1`in asetillenmiş lizin 282`yi hedeflediği gösterilmiştir. Bu *in vitro* ve *in siliko* gözlemler ışığında, SIRT1`in, ilk defa, NFAT5 bağımlı AR anlatımına, ozmotik stress altında, katkıda bulunduğu belirlenmiştir.

## ACKNOWLEDGEMENTS

Completing this dissertation has been a long journey for me. Much has changed in my life from the beginning of this project, up to this time. Extraordinarily, from oscillating back and forth in between experiments, now I turned out to be the father of a young man... Each of the experiences I have been into during this period, taught me to be more courageous and to be stubborn as a bull, which I guess, are settled in me during this journey and assisted me to go through and complete this work. Unquestionably, I could not have succeeded without invaluable support of several.

I would like to, first, thank sincerely, to my thesis supervisor, Prof. Dr. Hüveyda Başağa for her guidance, support, caring and flexibility throughout this thesis, enabling me to bring this dissertation into reality. Only with her encouragement and motivation on me, I was able to handle and face the hardest obstacles in this work. I would also like to express my special thanks to Assoc. Prof. Dr. Batu Erman, Asst. Prof. Dr. Alpay Taralp, Prof. Dr. Uğur Sezerman and Asst. Prof. Dr. Özgür Kütük for their comments on the thesis and for accepting to be my jury members.

I would like to also thank Faculty of Engineering and Natural Sciences of Sabanci University for providing me financial support and scholarship to complete this thesis. I would like to thank to Basağa lab members for their support in this work, Cagri Bodur, Beyza Vuruşaner Aktaş, Bahriye Karakaş, Tuğçe Ayça Tekiner and Yelda Birinci.

Finally, I would like to thank to my family, Emel, Yaman, Ahmet, Ece, Burak, Hazal, Sumru, Seher, Ali, Deniz and Haydar for their endless love and caring.

## TABLE OF CONTENTS

1. INTRODUCTION .....	1
1.1. Osmosis .....	1
1.2. Regulation of cell volume .....	2
1.2.1. Accumulation of compatible osmolytes .....	4
1.3. Creating a hypertonicity with high NaCl .....	6
1.3.1. Hyperosmotic environment induced modifications of cytoskeleton .....	7
1.3.2. Hyperosmotic environment induced oxidative stress .....	10
1.3.3. Hyperosmotic environment induced DNA damage .....	10
1.3.4. Hyperosmotic environment induced apoptosis .....	11
1.4. The transcription factor, NFAT5 and its activation under osmotic stress.....	12
1.4.1. Structure of NFAT5.....	13
1.4.2. Regulation of NFAT5 mRNA and protein .....	14
1.4.3. Regulation of NFAT5 phosphorylation and other post translational modifications .....	15
1.4.4. Regulation of intracellular localization of NFAT5 .....	16
1.4.5. Regulation of NFAT5 transactivational activity .....	17
1.4.6. Interactions of NFAT5 .....	20
1.4.7. Inhibition of NFAT5.....	20
1.5. NFAT5, AR and diabetic vascular complications.....	20
1.5.1. Diabetic vascular complications.....	21
1.5.2. Role of AR under diabetic vascular complications .....	23
1.6. Protein acetylation and deacetylation.....	24
1.6.1. Reaction mechanisms of acetylation and deacetylation .....	25

1.6.2. Roles acetylation and deacetylation in cellular processes .....	27
1.6.3. NAD <sup>+</sup> dependent deacetylase SIRT1 .....	27
1.6.4. Structure of SIRT1 .....	29
1.6.5. Enzymatic mechanism of SIRT1 .....	30
1.6.6. Interplay of SIRT1 with NAD <sup>+</sup> dependent poly (ADP-ribose) polymerase, PARP1 .....	31
1.7. Scope and aim of thesis .....	32
2. MATERIALS AND METHODS .....	36
2.1. Materials .....	36
2.1.1. Summary of the materials used in this thesis .....	36
2.1.2. Chemicals and Media .....	37
2.1.3. Antibodies .....	37
2.1.4. Molecular biology kits and reagents .....	37
2.1.5. Expression vectors .....	37
2.1.6. Oligonucleotides .....	37
2.1.7. Buffers and solutions .....	37
2.1.8. Equipment and computer software .....	38
2.2. Methods .....	38
2.2.1. Cell Culture and Treatments .....	38
2.2.2. Metabolic activity, cell death and oxidative stress assays .....	38
2.2.3. Protein extraction and immunoblotting .....	39
2.2.4 Measurement of protein concentration .....	40
2.2.5. Transfections .....	40
2.2.6. Electrophoretic mobility shift assay (EMSA) .....	41
2.2.7. Co-immunoprecipitation .....	41

2.2.8. Prediction of acetylated lysines of NFAT5 .....	42
2.2.8.1. Detailed methodology of algorithms for acetyllysine prediction .....	43
2.2.9. FoldX calculations.....	44
2.2.10. Structure Preparation and Docking .....	45
2.2.11. Molecular dynamics simulations.....	46
2.2.12. Statistical Analysis .....	46
2.2.13. Densitometric analysis.....	47
2.2.14. Illustrations.....	47
<b>3. RESULTS.....</b>	<b>48</b>
3.1. Osmotic stress model to study the role of SIRT1 on NFAT5 .....	48
3.1.1. 16 hours of 100 mM NaCl treatment generates osmotic stress dependent intracellular stress.....	48
3.1.2. 16 hours of 100 mM NaCl treatment simultaneously upregulates NFAT5 and SIRT1 in osmotic stress dependent manner .....	51
3.2. SIRT1 activity contributes to AR expression during osmotic stress in U937 and HeLa cells.....	53
3.2.1. Osmotic stress model dependent changes on intracellular NFAT5 and SIRT1 localizations, AR expression and oxidative stress generation.....	53
3.2.2. SIRT1 activity promotes AR expression during 16 hours of 100 mM NaCl treatment in U937 cells.....	54
3.2.3. SIRT1 activity promotes AR expression during 16 hours of 100 mM NaCl treatment in Hela cells .....	58
3.3. SIRT1 activity enhances nuclear NFAT5 stabilization during osmotic stress in U937 and HeLa cells.....	58
3.3.1. SIRT1 activity augments stabilization of nuclear NFAT5 in U937 cells.....	58
3.3.2. SIRT1 activity augments stabilization of nuclear NFAT5 in Hela cells .....	59

3.4. Enzymatic activity of SIRT1 regulates myc-NFAT5 induced AR expression through stabilizing nuclear NFAT5 and allowing more NFAT5 to bind AR ORE in HeLa cells .62	
3.4.1. myc-NFAT5 induced AR expression was regulated by SIRT1 activity in HeLa cells.....62	62
3.4.2. Stabilization nuclear of myc-NFAT5 expression was regulated by SIRT1 activity in HeLa cells.....62	62
3.4.3. DNA binding of myc-NFAT5 to AR ORE was regulated by SIRT1 activity in HeLa cells.....63	63
3.5. 16 hours of osmotic stress disrupts the interaction of NFAT5 with SIRT1, but enhances its acetylated lysine status and interaction with PARP1 in U937 cells .....67	67
3.6. In silico prediction of deacetylated lysines of NFAT5 that stabilize NFAT5-DNA complex .....69	69
3.7. In silico prediction of lysine 282 of NFAT5 as a potential SIRT1 target site .....72	72
4. DISCUSSION AND CONCLUSION .....79	79
4.1. A unique osmotic stress model .....79	79
4.2. Functional interplay of SIRT1 and PARP1 under osmotic stress .....80	80
4.3. Complementary <i>in vitro</i> and <i>in silico</i> data for NFAT5 as direct target of SIRT1 enzymatic activity .....81	81
4.4. Proposed Mechanism .....82	82
4.5. Conclusions .....83	83
4.6. Future Studies.....84	84
5. REFERENCES .....85	85
APPENDIX A .....110	110
APPENDIX B .....113	113
APPENDIX C .....114	114
APPENDIX D .....115	115
APPENDIX E.....118	118

APPENDIX F.....	119
APPENDIX G.....	124

## TABLE OF FIGURES

Figure 1.1. Flow of water across a semipermeable membrane and directions of hydrostatic and osmotic pressure.....	2
Figure 1.2. Regulation of cell volume is maintained through electrolyte accumulation. ....	3
Figure 1.3. Illustration of the difference between the impacts of a perturbing (P) and compatible (C) solute on the native conformation of a protein. ....	4
Figure 1.4. Glucose and some of the main compatible osmolytes found in animal cells. Glucose is reduced to sorbitol by AR. ....	5
Figure 1.5. Regulation of accumulation and loss of compatible organic osmolytes. ....	6
Figure 1.6. Brx dependent regulation of p38 and NFAT5 under hyperosmotic environment. ....	9
Figure 1.7. Structure of NFAT5.....	14
Figure 1.8. Structure of NFAT5-DNA complex, depicted from PDB ID: 1IMH.....	15
Figure 1.9. High NaCl causes NFAT5 transcriptional activity via several mechanisms and upregulates osmoprotective gene expression, including AR, SMIT and BGT1.....	19
Figure 1.10. Mechanisms of diabetic vascular complications. ....	22
Figure 1.11. Involvement of AR in polyol pathway. ....	23
Figure 1.12. Acylation of proteins. ....	24
Figure 1.13. Mechanism of lysine acetylation. ....	25
Figure 1.14. Deacetylation by class I, II and IV HDACs. ....	26
Figure 1.15. Deacetylation by class III HDACs. ....	26
Figure 1.16. Structure of SIRT1. ....	28
Figure 1.17. Structure of SIRT1, depicted from PDB ID: 4IG9 Chain A. ....	29
Figure 1.18. Mechanism of SIRT1 based deacetylation of the acetylated protein. ....	30
Figure 3.1. Measurement of osmolality of RPMI 1640 for validation of generation of hyperosmotic environment. ....	49
Figure 3.2. 48 hours of 100 mM NaCl treatment generates osmotic stress dependent intracellular stress. ....	50

Figure 3.3. 16 hours of 100 mM NaCl treatment simultaneously upregulates NFAT5 and SIRT1 in osmotic stress dependent manner.....	52
Figure 3.4. Osmotic stress dependent changes on intracellular NFAT5 and SIRT1 localizations. ....	54
Figure 3.5. Osmotic stress dependent changes on AR expression and oxidative stress generation.....	55
Figure 3.6. SIRT1 activity promotes AR expression during 16 hours of 100 mM NaCl treatment in U937 cells. ....	56
Figure 3.7. SIRT1 activity promotes AR expression during 16 hours of 100 mM NaCl treatment in HeLa cells. ....	57
Figure 3.8. SIRT1 activity augments stabilization of nuclear NFAT5 in U937 during 16 hours 100 mM N treatment.....	60
Figure 3.9. Validation of SIRT1 based stabilization of nuclear NFAT5 in U937 and HeLa cells during 16 hours 100 mM N treatment. ....	61
Figure 3.10. myc-NFAT5 induced AR expression was regulated by SIRT1 activity in HeLa cells. ....	64
Figure 3.11. Stabilization nuclear of myc-NFAT5 expression was regulated by SIRT1 activity in HeLa cells. ....	65
Figure 3.12. DNA binding of myc-NFAT5 to AR ORE was regulated by SIRT1 activity in HeLa cells. ....	66
Figure 3.13. 16 hours of osmotic stress weakened the interaction of NFAT5 containing complex with SIRT1, but increased its acetylated lysine status and its interaction with PARP1. ....	68
Figure 3.14. Acetylation and deacetylation mimicry mutations of NFAT5 lysine residues regulate the stability of NFAT5-DNA complex. ....	71
Figure 3.15. RMSD of backbone atoms of p65(AK)-SIRT1(F414) and all NFAT5(AK)-SIRT1 (F414) complexes were calculated from 10 ns of MD simulations, depicted in legend. ....	73
Figure 3.16. RMSF of Ca atoms of p65 in p65(AK)-SIRT1(F414) complex and NFAT5 in all NFAT5(AK)-SIRT1(F414) complexes were calculated from 10 ns of MD simulations, depicted in legends.....	74

Figure 3.17. RMSF of C $\alpha$  atoms of SIRT1 in p65(AK)-SIRT1(F414) complex and in all NFAT5(AK)-SIRT1(F414) complexes were calculated from 10 ns of MD simulations, depicted in legend. ....75

Figure 3.18. AK282 and AK373 of NFAT5 docked to SIRT1 substrate binding site F414 showed similar AK to F414 (gray, magenta and black) distance compared to p65 (AK310)-SIRT1 (F414) complex during 10 ns MD simulations. ....76

Figure 3.19. AK282 of NFAT5 docked to SIRT1 substrate binding site F414 showed lower RMSF values for AK and F414 atoms, compared to p65 (AK310)-SIRT1 (F414) complex during 10 ns MD simulations.....77

Figure 3.20. Representative snapshots of whole complexes taken from the last 1 ns of simulations were shown in upper panels, while AK282, AK310 and SIRT1 substrate binding site (F414) were shown in lower panels. ....78

Figure 4.1. Proposed mechanism of SIRT1 based regulation of NFAT5 dependent AR expression in U937 cells under 16 hours of osmotic stress. ....83

## LIST OF TABLES

Table 3. 1. Results of acetylated lysine predictions.....	70
---	----

## LIST OF SYMBOLS AND ABBREVIATIONS

AADPR	O-acetyl-ADP-ribose
ATM	Ataxia telangiectasia mutated
ATP	Adenosine triphosphate
ADP	Adenosine diphosphate
AED	Auxiliary export domain
AMP	Adenosine monophosphate
AP-1	Activator protein 1
AR	Aldose Reductase
AQP	Aquaporin
Bax	Bcl-2-like protein 4
Bcl2	B-cell lymphoma 2
BGT1	Betaine/ gamma-aminobutyric acid transporter
BRCA1	Breast cancer type 1 susceptibility protein
Brx	A-kinase anchor protein 13
Cdc42	Cell division control protein 42 homolog
chk2	Checkpoint kinase 2
CIP	Calf intestinal phosphatase
Cl <sup>-</sup>	Chloride ion
CRM1	Exportin 1 / Chromosomal maintenance 1
DAG	Diglyceride
DHAP	Dihydroxyacetone phosphate

DNA	Deoxyribonucleic acid
Egr-1	Early growth response protein 1
F-actin	Filamentous actin
FOXO	Forkhead box O
FSP27	Fat-specific protein 27
Fyn	Tyrosine-protein kinase Fyn / Src-like kinase
GABA	Gamma-aminobutyric acid
Gadd45	Growth Arrest and DNA Damage 45
GAPDH	Glyceraldehyde 3-phosphate dehydrogenase
GFAT	Glutamine fructose-6-phosphate amidotransferase
GSH	Glutathione
GSSG	Glutathione disulfide
GTP	Guanosine-5'-triphosphate
H <sup>+</sup>	Hydrogen ion
H <sub>2</sub> O	Water
HCO <sub>3</sub> <sup>-</sup>	Bicarbonate anion
HSP90	Heat shock protein 90
IL	Interleukin
JIP4	C-jun-amino-terminal kinase-interacting protein 4
K <sup>+</sup>	Potassium ion
kDa	Kilo dalton
KCl	Potassium chloride
MAPK	Mitogen-activated protein kinase

MEKK3	Mitogen-activated protein kinase kinase kinase 3
MKK3	Mitogen-activated protein kinase kinase 3
MKK6	Mitogen-activated protein kinase kinase 6
mIMCD3	Mouse inner medullary collecting duct cells
mRNA	Messenger ribonucleic acid
Na <sup>+</sup>	Sodium ion
NaCl	Sodium chloride
NAC	N-acetylcysteine
NAD	Nicotinamide adenine dinucleotide
NAM	Nicotinamide
NADP	Nicotinamide adenine dinucleotide phosphate
NES	Nuclear export sequence
NFAT	Nuclear factor of activated T-cells
NFAT5	Nuclear factor of activated T-cells 5
NFκB	Nuclear factor κB
NLS	Nuclear localization sequence
ORE	Osmotic response element
OREBP	Osmotic response element binding protein
OSM	Osmosensing scaffold for MEKK3
p38	Mitogen-activated protein kinase p38
p53	Cellular tumor antigen p53
p65	Transcription factor p65
PARP1	Poly (ADP-ribose) polymerase 1

PI3K	Phosphatidylinositol-3-kinase
PIP <sub>2</sub>	Phosphatidylinositol 4,5-bisphosphate
PIP <sub>3</sub>	Phosphatidylinositol 3,4,5-trisphosphate
PKA	Protein Kinase A
PP1	Protein phosphatase 1
Rac	Ras-related C3 botulinum toxin substrate
RHR	Rel homology region
ROS	Reactive oxygen species
SIRT1	Sirtuin 1
Sho1	High osmolarity signaling protein
Sln1	Osmosensing histidine protein kinase
Src	Sarcoma
SDH	Sorbitol dehydrogenase
SMIT	Sodium-myo-inositol transporter
TAB1	Protein kinase 1 binding protein
TAD	Transactivation domain
TAZ	Transcriptional coactivator with PDZ-binding motif
TNF- $\alpha$	Tumor necrosis factor alpha
TonEBP	Tonicity-responsive enhancer binding protein
UTR	Untranslated region
Zn <sup>2+</sup>	Zinc ion

## 1. INTRODUCTION

### 1.1. Osmosis

Movement of water across a semi-permeable membrane is defined as osmosis. In an ideal case, only water can pass through a semipermeable membrane. For instance, if there are two different concentrations of NaCl in water, separated by a semipermeable membrane, the direction of water will be towards to the compartment, with higher NaCl concentration (Figure 1.1). This is due to the condition called “concentration gradient of water” in which solution with the low NaCl concentration has higher concentration of water compared to the high NaCl containing solution. This phenomena can be prevented by applying a hydrostatic pressure, for example using a hypothetical piston applied from high NaCl compartment (Figure 1.1). In line with these, osmotic pressure is defined as the total pressure to prevent the water flow through this membrane, assuming no kinetic barrier for water flow through the membrane is present (Figure 1.1, right). Total concentration of solute particles in the solvent is what generates osmotic pressure.

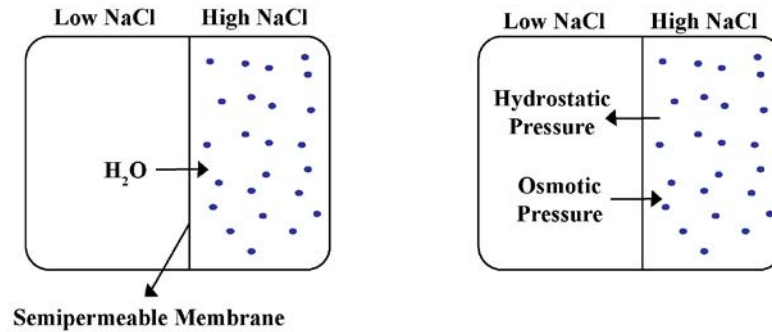


Figure 1.1. Flow of water across a semipermeable membrane and directions of hydrostatic and osmotic pressure.

Under steady state conditions, intracellular and extracellular concentrations of solutes are similar. Any perturbation of these concentrations results in an osmotic gradient between membrane and extracellular fluid. In response, cells try to go back to their steady state condition, via flowing water in or out of the cell. Nonetheless, unlike plant cells with a cell wall, mammalian cells cannot generate enough hydrostatic pressure to overcome such gradients and they swell or shrink, depending on the case.

## 1.2. Regulation of cell volume

Modifications of cellular volume are categorized in mainly two groups. Anisotonic volume changes are the ones, generated via changes in extracellular solute concentrations. In healthy state, almost all mammalian cells, except the ones in renal medulla and gastrointestinal tract, are sheltered from anisotonic perturbations via control of solute concentration of plasma by kidney. On the other hand, isotonic volume changes are defined by the perturbations on intracellular solute concentrations. Cells protect themselves from such a threat by solute transport to inside or to outside of the cell and also by synthesizing osmotically active compounds.

Amount of water inside the cell, thus, cellular volume is regulated by concentrations of intracellular osmotically active compounds and extracellular solute. Membrane of the

animal cells are generally accepted to be permeable to water. The permeability of water into animal cells is much higher than the permeability of  $\text{Na}^+$  and  $\text{Cl}^-$ . In this regard, presence of AQPs has been shown to increase intracellular water content upon exposure to hypotonicity (King et al., 2004, Liu et al., 2006, Galizia et al., 2008). Moreover, the “pump and leak” hypothesis states that, cells protect themselves from swelling induced lysis via both constituting low  $\text{Na}^+$  mobility across membrane and via active pumping of  $\text{Na}^+$  out of the cell by  $\text{Na}^+\text{-K}^+\text{-ATPase}$  (Leaf, 1959, Tosteson et al., 1960). Nevertheless, almost all cells are exposed to volume changes due to changes in environmental or intracellular osmolarity. When swollen, cells extrude water and  $\text{KCl}$  via activation of  $\text{K}^+$  and  $\text{Cl}^-$  channels, as well as  $\text{KCl}$  cotransporter, thus try to minimize their volume, in process called regulatory volume decrease (RVD) (Figure 1.2, right). On the contrary, shrunken cells, try to increase their volume by taking up more  $\text{KCl}$ ,  $\text{NaCl}$  and water through employing  $\text{Na}^+\text{-H}^+$  and  $\text{Cl}^-/\text{HCO}_3^-$  exchangers, as well as,  $\text{Na-K-2Cl}$  cotransporter, which has been widely known as regulatory volume increase (RVI) (Figure 1.2, left). These two well established phenomenon of cell volume regulation happens within seconds to minutes after exposure of the cell, hence they can be considered as first line of defense mechanism against osmotic perturbations (Strange, 2004, Hoffmann et al., 2009).

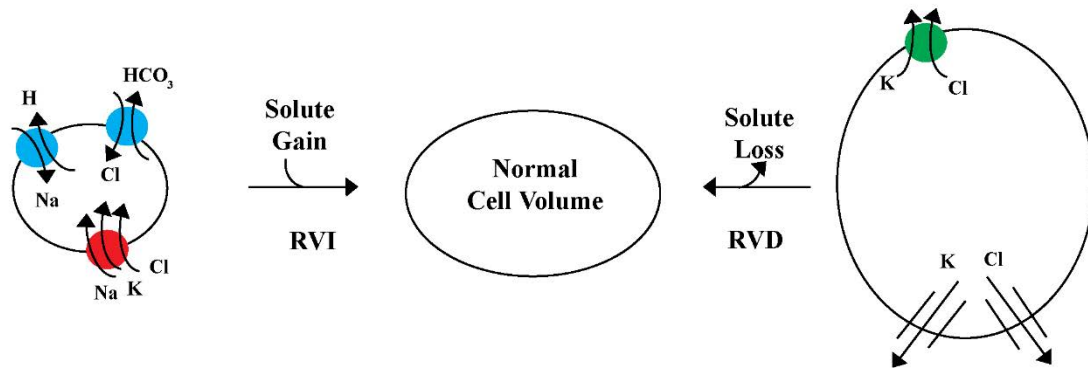


Figure 1.2. Regulation of cell volume is maintained through electrolyte accumulation.

### 1.2.1. Accumulation of compatible osmolytes

Shrinkage is often counteracted by cells through maintaining RVI (Wehner et al., 2003). While this volume increasing modification provides advantage for cell survival within minutes, main disadvantage of RVI is the abnormal increase in concentration of ions within the cell. This condition has deleterious effects on intracellular macromolecules (Figure 1.3, left) (Yancey et al., 1982).

After several hours, instead, compatible organic osmolytes begin to be synthesized (Figures 1.4 and 1.5). Structures of glucose, as well as, major compatible organic osmolytes found in animal cells are shown in Figure 1.4. One major advantage of accumulation these osmolytes is that they do stabilize the native conformation of proteins, unlike perturbing inorganic ions (Figure 1.3, right) (Yancey et al., 1982, Street et al., 2006). Sorbitol, betaine and myo-inositol are widely used osmolytes by kidney for osmoregulation (Bagnasco et al., 1986, Garcia-Perez et al., 1991, Nakanishi et al., 1991).

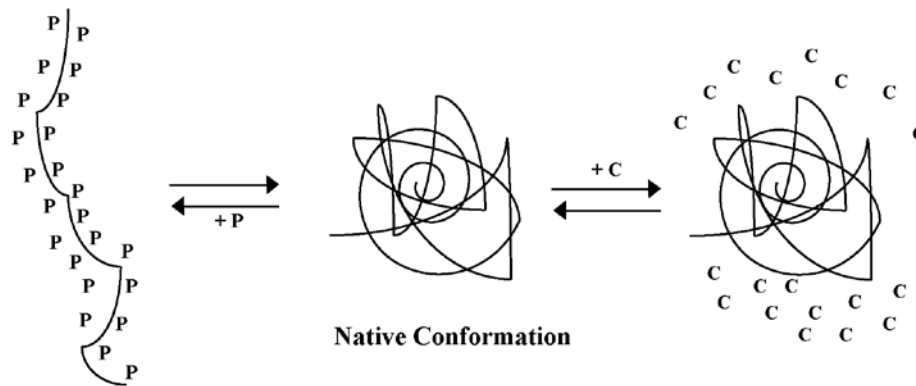


Figure 1.3. Illustration of the difference between the impacts of a perturbing (P) and compatible (C) solute on the native conformation of a protein. Compatible osmolytes tend to be away from protein surface. Sorbitol is produced from glucose, via AR based reduction and sorbitol is converted to glucose by SDH (Figures 1.4 and 1.5) (Garcia-Perez et al., 1991). Cell shrinkage upon osmotic stimuli increases AR enzymatic activity as well as, its mRNA and protein levels. This increase is mainly mediated by the transcription factor NFAT5, also

called TonEBP/OREBP. (See heading 1.4. The transcription factor, NFAT5 and its activation under osmotic stress) Betaine (Figures 1.4 and 1.5) is produced from choline both in liver and kidney (Garcia-Perez et al., 1991). Osmotic stimuli does not affect the rate of production of betaine, but upregulates betaine carrying transporters, such as BGT1 and betaine transporter which increase its intracellular concentration (Figure 1.5) (Yamauchi et al., 1992). Betaine transporter works with symporting NaCl and also regulates BGT1 in osmotic stimuli dependent manner (Figure 1.5) (Strange, 2004, Burg et al., 2007). The transcriptional regulation of BGT1 is also enhanced by the transcription factor NFAT5, under hypertonicity (Uchida et al., 1993, Burg et al., 2007). BGT1 is also controlled by insertion into plasma membrane (Kempson et al., 2004). Upon osmotic stimuli, BGT1 tend to locate to basolateral plasma membrane. This localization of BGT1 is regulated by microtubules and calcium (Kempson et al., 2004, Kempson et al., 2006).

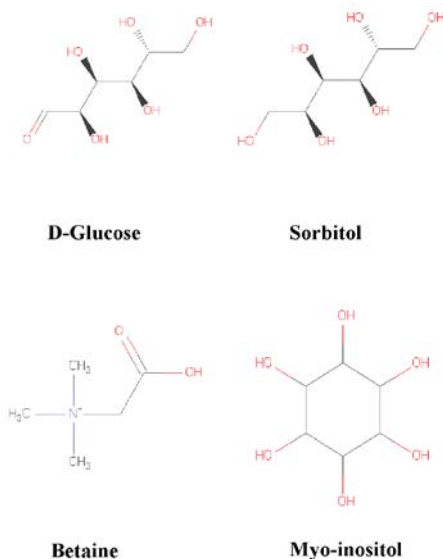


Figure 1.4. Glucose and some of the main compatible osmolytes found in animal cells. Glucose is reduced to sorbitol by AR.

Inositol (Figures 1.4 and 1.5) is produced by renal cells (Garcia-Perez et al., 1991). Nonetheless, its concentration is not dependent on synthesis, but only on its transport upon osmotic stimuli (Figure 1.5). Thus, its presence outside cell is the major determinant for its

accumulation. Hypertonic environment increases its transporter SMIT, which works similar to BGT1, through utilization Na gradient coupling (Kwon et al., 1992, Hager et al., 1995). Osmotic stimuli increases the SMIT gene expression, through employing NFAT5 (Yamauchi et al., 1993).

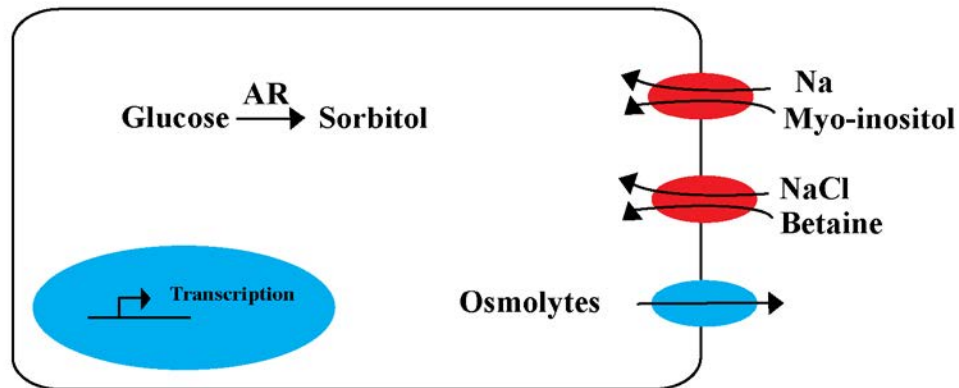


Figure 1.5. Regulation of accumulation and loss of compatible organic osmolytes. Accumulation of compatible osmolytes are interceded mainly by Na<sup>+</sup> coupled membrane transporters or by direct synthesis. This process is relatively slow compared to RVI, and takes several hours from beginning to end. One main reason of this lengthy process is that cells need several hours to complete of transcription and translation of genes, whose products are osmolyte transporters and osmolyte synthesis enzymes. On the contrary, loss of these osmolytes are handled in order of seconds after swelling is sensed by the cell.

### 1.3. Creating a hypertonicity with high NaCl

Hypertonicity occurs of when solute concentration in extracellular environment is hyperosmotic, which results in the water loss, hence cellular volume decreases. Loss of water results in macromolecular crowding and related increased activity of intracellular molecules (Garner et al., 1994). In parallel, intracellular ionic strength and cytoskeletal changes are

accompanied with macromolecular crowding, all of which are primary effects of hypertonicity.

Hypertonic environment for cells can be generated by employing high NaCl which is the main element of osmotic actions of the extracellular fluid. This property of NaCl led us to investigate its impact in this thesis. Nevertheless, Na<sup>+</sup> and Cl<sup>-</sup> has specific effects other than osmotic stress on the cells. For instance, elevated Cl<sup>-</sup> upregulates the  $\alpha$ -Na<sup>+</sup>-K<sup>+</sup>-ATPase (Capasso et al., 2003). In this sense, while NaCl is widely used to create hyperosmotic environment, its impact on the cell may not be just due to generation of hypertonicity. Because of this, other solutes that have relatively low permeability to cells should be utilized in parallel to NaCl treatment, such as mannitol, to differentiate the osmotic stress based effects from other specific effects the agents. In turn, those low permeability solutes like mannitol, may have other specific effects to the cells. Therefore, the concrete approach, when studying osmotic stress generation with high NaCl, is utilization osmotic controls. In our case, we used mannitol, as the osmotic control of NaCl, and mannitol and NaCl, as the osmotic controls of glucose. It is also worth noting that increasing osmolality over 300 mosmol/kgH<sub>2</sub>O may end up with abnormal increase in apoptotic rate in some cells, so viability of the cells should examined carefully, before any analysis (Santos et al., 1998, Michea et al., 2000).

Hyperosmotic environment causes wide variety of changes in many cellular components (Figure 1.9). These changes can be categorized in two categories: a) changes induced as cellular osmoprotection mechanism, b) changes due hypertonicity induced dysfunctions.

### **1.3.1. Hyperosmotic environment induced modifications of cytoskeleton**

Environmental hyperosmotic milieu causes polymerization of microfilament and exerts changes in actin cytoskeleton (Di Ciano et al., 2002, Bustamante et al., 2003, Yamamoto et al., 2006). Nevertheless, mechanism of actin remodeling is handled differently in each cell type. For instance, in glial cells, osmotic stress causes microfilaments from

cortical ring to turn into diffuse actin bundles (Mountain et al., 1998). On the other hand, in fibroblasts, only cortical ring is condensed (Di Ciano et al., 2002). This alterations in cytoskeleton are regulated by GTPases, Rac and Cdc42, F-actin nucleation regulator, actin binding protein (Di Ciano et al., 2002). Rho kinase and p38 also, in part, mediate the osmotic stress dependent localization myosin IIB to cortical region (Pedersen et al., 2002).

Exposure of cells to hyperosmotic stress also induces changes on integrins, which are responsible for interaction of the cell with extracellular matrix. Osmotic stress has been shown to upregulate integrin  $\beta$  mRNA and protein in Madin-Darby canine kidney cells, in NFAT5 dependent manner (Sheikh-Hamad et al., 1997).

Overall, the role of cytoskeleton modifications in cells under hyperosmotic milieu is still unclear (Eggermont, 2003). It is speculated to regulate sensing of cell volume, stabilizing against shrinkage or carrying osmotic stress related signals within the cell. Within these possibilities, cytoskeleton based transmittance of osmotic signals is highly likely due to presence of supportive data. Hyperosmotic stress induces formation of actin interacting complex through assembly of OSM, Rac, MEKK3, MKK3 and p38 (Uhlik et al., 2003). In turn, p38 can contribute to the activation of NFAT5 and experimental evidence suggests that alterations of OSM complex causes inhibition of p38 dependent NFAT5 activation, suggesting that role of cytoskeleton in osmotic signal transmittance (Uhlik et al., 2003). While this data suggests the involvement of p38, more recently, Brx (a guanine nucleotide exchange factor)-JIP4 complex has been shown to regulate activation of p38 under hyperosmotic conditions (Figure 1.6) (Aramburu et al., 2009).

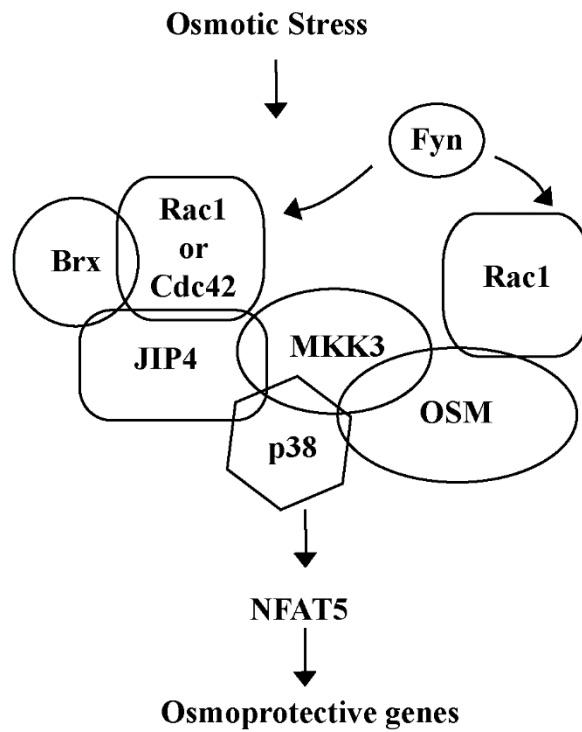


Figure 1.6. Brx dependent regulation of p38 and NFAT5 under hyperosmotic environment. Specifically, Brx-JIP4 complex is a necessary component of Cdc42 and Rac1 based p38 activation. p38, as well other kinases, have the capability of activating NFAT5. Fyn, a kinase of Src family, acts as an upstream effector of Rac1 and Cdc42, hence may also augment them for p38 activation. Brx and JIP4 interacts with Cdc42 or Rac1 for their activation. OSM is required for the actin interacting assembly, thus, also for p38 activation. Sensing of osmotic stress is initiated in the plasma membrane and may be mediated by cytoskeletal change induced Brx activation or by yet undetermined osmosensor molecules, orthologous to the yeast Sln1 and Sho1.

### **1.3.2. Hyperosmotic environment induced oxidative stress**

High NaCl causes oxidative stress, accompanied by increase in ROS (Zou et al., 2001, Zhang et al., 2004, Yang et al., 2005, Zhou et al., 2005, Zhou et al., 2006). DNA bases can be altered by ROS through formation 8-oxoguanine and proteins are also targets for carbonylation by ROS (Levine et al., 2000, Greenberg, 2004). In particular, carbonylation has deleterious effects on stability and function of the proteins (Stadtman et al., 2000). No repair mechanism for carbonylated proteins are present in cells, therefore for protection cell should degrade and resynthesize such proteins (Levine, 2002). In renal medullary cells exposed to high NaCl, oxygen is low compared to other parts of the cells in the body, so they can handle miniscule amounts of ROS and its deleterious effect (Bagnasco et al., 1985) (Burg et al., 2007). Therefore, cells that have higher supply of oxygen, may be prone to hyperosmotic stress driven ROS in highly noticeable amounts.

On the contrary, ROS has been also suggested to be involved in osmoprotection. In line with this notion, antioxidants have been shown to inhibit high NaCl induced NFAT5 transcriptional activity and BGT1 mRNA (Zhou et al., 2005, Zhou et al., 2006). Furthermore, NAC have been shown to suppress high NaCl dependent phosphorylation of ERK1/2 and p38 (Yang et al., 2005).

### **1.3.3. Hyperosmotic environment induced DNA damage**

High NaCl based hyperosmotic stress induces DNA breaks in mIMCD3 cells (Kultz et al., 2001, Dmitrieva et al., 2003). Many DNA breaks exist and kept in cells adapted to long term high NaCl concentrations, interestingly these breaks are not repaired and cells continue to proliferate (Capasso et al., 2001, Santos et al., 2003, Dmitrieva et al., 2004). At normal conditions, DNA damage sites are direct targets for DNA repair complexes. If this repair mechanism cannot be completed, cells initiate the apoptotic machinery. Hence, cells without DNA repair complexes are accepted to be not viable upon DNA damage (Xiao et al., 1997, Luo et al., 1999, Liu et al., 2000, Zhu et al., 2001). Extraordinarily, DNA damage kept as it

is during high NaCl treatment and apoptosis due to these DNA breaks is not initiated (Dmitrieva et al., 2004). In addition, elimination of NaCl from environment activates DNA repair mechanism again, indicating that high NaCl suppresses DNA repair (Dmitrieva et al., 2003, Dmitrieva et al., 2004). This remarkable link between high NaCl and DNA damage, may be explained by the fact that gene rich regions are not subjected to DNA breaks during high NaCl exposure, as suggested previously (Dmitrieva et al., 2011).

High NaCl upregulates and activates several DNA damage response proteins such as Gadd45, p53, ATM and chk2 (Sheen et al., 2006). Other than these DNA damage response related proteins, PARP1, a DNA repair enzyme, has been suggested to negatively involved in high NaCl induced activation of NFAT5 (Malanga et al., 2005, Chen et al., 2007). (See heading 1.4.7. Inhibition of NFAT5)

#### **1.3.4. Hyperosmotic environment induced apoptosis**

When timing of hyperosmotic environment generated hypertonicity is prolonged, cellular death happens. The tolerance of each cell line to hypertonicity greatly varies, but the characteristics of it, are generally same for all cells. Hypertonic cell death demonstrates typical markers of apoptosis (Bortner et al., 1996, Santos et al., 1998, Michea et al., 2000, Galvez et al., 2001). Condensation of DNA, appearance of apoptotic bodies, fragmentation of DNA and increased phosphatidylserine on cell membrane, are some of the apoptotic hallmarks, observed for hypertonic cell death. Both of the two basic cascades of apoptosis, intrinsic and extrinsic pathways have shown to be involved during osmotic stress dependent cell death (Jin et al., 2005). Elevation of osmolality to 700 mosmol/kgH<sub>2</sub>O using NaCl in mIMCD3 cells have shown to cause depolarization of mitochondria, reduced Bcl2/Bax ratio and increased ratio of ADP/ATP (Michea et al., 2002). Elevation of osmolality to 900 mosmol/kgH<sub>2</sub>O using sorbitol in HeLa cells, induced the extrinsic apoptotic machinery and displayed clustering and internalization of TNF- $\alpha$  receptors (Rosette et al., 1996). Moreover, using NaCl to raise osmolality to 500 mosmol/kgH<sub>2</sub>O in U937 cells have been presented to upregulate TNF- $\alpha$ , raising the possibility that this cell line induces cell death on its own (Lang et al., 2002). Employing TNF- $\alpha$  antibody also has shown to inhibit apoptosis in U937 cells,

indicating that internal accumulation of TNF- $\alpha$ , is responsible for initiation of apoptosis in this cell line. It is apparent that hyperosmotic environment induced hypertonicity results initiation of both intrinsic and extrinsic mechanisms of apoptosis, however the selection of the mechanism, depends on the cell line being studied. In our case, we have chosen to work with U937 and HeLa cells, in light of these previous observations.

#### **1.4. The transcription factor, NFAT5 and its activation under osmotic stress**

NFAT5, also called TonEBP/OREBP, belongs to Rel family member of proteins which also includes NF $\kappa$ B. Targets of NFAT5 contain at least one DNA binding region, which is named as ORE or TonE (Ferraris et al., 1994, Takenaka et al., 1994, Ferraris et al., 1996, Mallee et al., 1997, Rim et al., 1997, Ferraris et al., 1999, Miyakawa et al., 1999a, Ito et al., 2004).

Transactivation of NFAT5 results in transcription and translation of genes that induce upregulation of compatible organic osmolytes, including sorbitol, betaine and inositol (Figures 1.4 and 1.5) (Burg et al., 1997, Gallazzini et al., 2006). Knocking out NFAT5 expression or dominant-negative expression of NFAT5 has several kidney and non-kidney related consequences. If both alleles of NFAT5 is deleted, mice generally die at embryonic stage (Go et al., 2004, Lopez-Rodriguez et al., 2004). Among these NFAT5 knockout mice, few survive and display characteristic downregulation of NFAT5 target genes (Lopez-Rodriguez et al., 2004). On the other hand, heterozygous deletion of NFAT5 results in diminished number of lymphoid cells and suppressed antigen-specific antibody production (Go et al., 2004). Dominant negative overexpression of inactive NFAT5 results in cataract formation in lenses of mice after birth and fiber cells in these lenses show the characteristics of hyperosmotic stress (Wang et al., 2005).

### 1.4.1. Structure of NFAT5

NFAT5 is found as homodimer on its target DNA (Figures 1.7 and 1.8) (Stroud et al., 2002). Binding mode of each immunoglobulin like monomer to DNA, is very close to those of that of RHR of NFAT and NF $\kappa$ B families (Muller et al., 1995, Chen et al., 1998b, Miyakawa et al., 1999b). In this similarity, NFAT5 is more like NFAT than NF $\kappa$ B, based on backbone superposition and sequence identity (Cramer et al., 1997). Nonetheless, the orientation of N-terminal and C-terminal of NFAT5 differs significantly from those of NFAT1 and has increased similarity to the binding mode of NF $\kappa$ B to DNA (Ghosh et al., 1995, Cramer et al., 1997, Chen et al., 1998a, Chen et al., 1998b, Chen et al., 1998c, Miyakawa et al., 1999b). Moreover, NFAT5 has two dimer interfaces unlike NF $\kappa$ B-DNA complexes, which have only one (Figures 1.7 and 1.8).

NFAT5 homodimer binds to DNA through interaction of N-terminal of one monomer (Stroud et al., 2002). AB loop region in N-terminal, which contain amino acid residues of Arg217, Arg226, Glu223, Tyr 220, as well as, Gln364 from the linker region between N and C-terminals are responsible for binding to DNA in sequence specific manner (Stroud et al., 2002). AB loop is also conserved in NFAT and NF $\kappa$ B family of transcription factors (Stroud et al., 2002).

NFAT5 homodimer is maintained through two dimer interfaces located in between N and C-terminal regions (Stroud et al., 2002). For C-terminal dimer interface, hydrophobic residues, Leu372, Ile390, Leu422, Ile429 and Phe388 of each monomer resides at the center of the interface and polar residues Asn426, His424, His427, Lys373, Glu 386 and Ser375 makes the necessary hydrogen bonding and electrostatic interactions (Stroud et al., 2002). Among these, in this thesis, Lys 373 has been proposed to be potential SIRT1 target, when acetylated, hence SIRT1 may have important implications in NFAT5 dimerization (See heading 3.7. In silico prediction of lysine 282 of NFAT5 as a potential SIRT1 target site). For N-terminal interface,  $\alpha$ -helix loop from each monomer, including Arg315, Ala317, Asp318 and Glu320 makes up the dimerization interface. Dimerization of NFAT5 is independent of hyperosmotic stress, and is essential for DNA binding, phosphorylation and

transactivation of the osmotic stress related genes (Lopez-Rodriguez et al., 2001, Lee et al., 2002, Lopez-Rodriguez et al., 2004).

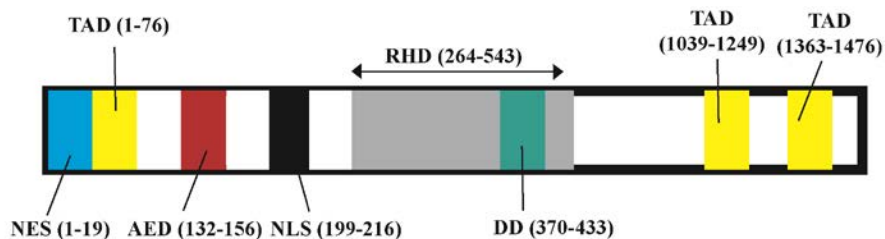


Figure 1.7. Structure of NFAT5. NES: Nuclear export sequence, TAD: Transactivation domain, AED: Auxillary export sequence, NLS: Nuclear export sequence, RHD: Rel homology domain, DD: Dimerization domain

#### 1.4.2. Regulation of NFAT5 mRNA and protein

Hyperosmotic stress upregulates NFAT5 mRNA in several cell types in a transient manner, peaking in between 4<sup>th</sup> and 12<sup>th</sup> (Ko et al., 1997, Woo et al., 2000a, Cai et al., 2005). This increase in NFAT5 mRNA is due stabilization of the 5'-UTR, thus, this condition clearly explains the increase in NFAT5 mRNA without any change in its transcriptional rate (Cai et al., 2005). Parallel to the stabilization of NFAT5 mRNA, NFAT5 protein accumulates and translocates to the nucleus, upon exposure to hyperosmotic stress (Woo et al., 2000a).

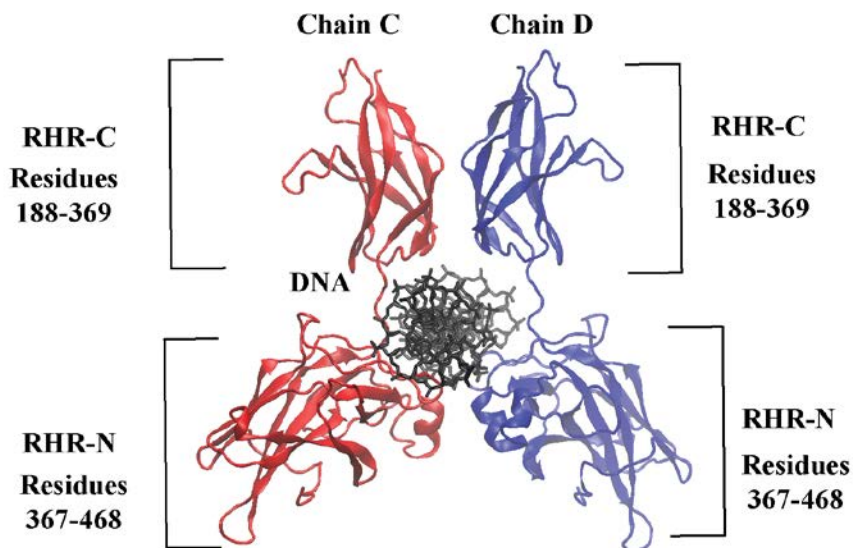


Figure 1.8. Structure of NFAT5-DNA complex, depicted from PDB ID: 1IMH. C-terminal (RHR-N) and N-terminal domains of NFAT5 and their residue number in 1IMH structure is shown. NFAT5 binds to the DNA as homodimer. Chain identifiers and residue numbers are kept as in 1IMH.

### 1.4.3. Regulation of NFAT5 phosphorylation and other post translational modifications

NFAT5 is phosphorylated within 30 minutes of hyperosmotic exposure from serine and tyrosine residues (Dahl et al., 2001). Role of this phosphorylation is still unconvincing due to the fact that no amino acids of NFAT5, are identified to be directly phosphorylated. However, it is likely that, as in other transcription factors, NFAT5 and its dependent events may be regulated by this post translational modification.

DNA binding of NFAT5 may be regulated by serine/threonine phosphorylation since CIP and PP1 phosphatases, suppresses DNA binding of this transcription factor (Aida et al., 1999). However, this effect is not maintained by immunoprecipitated NFAT5, since at this level, it does not respond to enzymatic activity of CIP, and kept its DNA binding intact (Dahl

et al., 2001). Moreover, hyperosmotic stress has displayed increased phosphorylation in NFAT5 residues 548 to 1531 (NFAT5, isoform C), which contains residues 872 to 1271 (NFAT5, isoform C), responsible for its transactivation (Ferraris et al., 2002b). Inhibitors of serine/threonine kinases has been shown to suppress this phosphorylation, however if it is a direct or indirect effect, is still a matter of debate (Ferraris et al., 2002b). Moreover, it has been suggested to be indirect, since NFAT5 transactivation domain has been presented to have no changes in phosphorylation upon hyperosmotic exposure (Lee et al., 2003). Nevertheless, there are other site directed mutagenesis studies, proposing direct phosphorylation of NFAT5 (Irarrazabal et al., 2004).

Other than phosphorylation, NFAT5 was proposed to be palmitoylated in which depalmitoylation was shown to accelerate its nuclear translocation (Eisenhaber et al., 2011). In addition, sumoylation of NFAT5 was revealed to inhibit its transactivation (Kim et al., 2014a).

#### **1.4.4. Regulation of intracellular localization of NFAT5**

Transcription factors above 50 kDa cannot directly translocate to nucleus for DNA binding. Therefore, high molecular weight proteins such as NFAT5 contain a NLS to bind importin. Importin carries such molecules into nucleus via actively transporting them through nuclear pores. On the contrary, high molecular weight proteins are translocated to cytoplasm from nucleus, via binding to exportin, through employing their NES containing residues.

Under isosmotic conditions, NFAT5 is in both cytoplasm and nucleus but hyperosmotic stress causes its translocation to nucleus (Miyakawa et al., 1999b, Ko et al., 2000, Lopez-Rodriguez et al., 2001, Tong et al., 2006). Under hypotonic conditions, NFAT5 mainly resides in cytoplasm (Woo et al., 2000a, Tong et al., 2006). Moreover, NFAT5 translocation to nucleus is suppressed by utilization of a widely known, proteasome inhibitor, MG132, proposing the possibility of the presence of an inhibitor of NFAT5, residing in cytoplasm, just like NF $\kappa$ B – I $\kappa$ B interaction (Woo et al., 2000b, Cyert, 2001).

Recombinant NFAT5 containing residues 1 to 547 of N-terminal region (NFAT5, isoform C) translocates to nucleus under hyperosmotic stress, indicating that C-terminal of NFAT5 is not required for nuclear translocation event, under such circumstances (Zhang et al., 2005). NLS also resides within N-terminal amino acids of NFAT5 (Lopez-Rodriguez et al., 1999, Ko et al., 2000). NES is also located in N-terminal of NFAT5, and composes a domain that can be targeted by CRM1 (Tong et al., 2006). In this regard, leptomycin1, a CRM1 inhibitor, has been shown to suppress NFAT5 nuclear export under isosmotic conditions (Tong et al., 2006). However, CRM1 is not responsible for nuclear export for NFAT5 under hypoosmotic stress, since mutations in NES did not altered export under this condition (Tong et al., 2006). On the other hand, AED, auxiliary export domain in N-terminal of NFAT5, maintains the nuclear export under both isosmotic and hypoosmotic conditions (Tong et al., 2006).

Among NFAT5 modulating kinases, ATM has been shown to induce nuclear translocation of NFAT5 under hyperosmotic stress (Zhang et al., 2005). Non-functional ATM causes diminished nuclear translocation of NFAT5 and only N-terminal containing construct of NFAT5 (Zhang et al., 2005). This effect of ATM could be directly on N-terminal of NFAT5 or could be mediated from the TAD domain of NFAT5, since this domain can also control localization of NFAT5 and contains consensus ATM sites for phosphorylation (Ferraris et al., 2002b, Irarrazabal et al., 2004, Ramadoss et al., 2005).

#### **1.4.5. Regulation of NFAT5 transactivational activity**

TADs, the transactivation domains of transcription factors, are the sites of interaction with other proteins for the purpose of enhancement of transcription. In this regard, at basal level, RNA polymerase recruitment is a necessary event for TAD activation. Transactivation of genes is mediated by transcription factors through DNA binding, interaction with other proteins or factors or by modifications at the post translational level. NFAT5 has a hyperosmotic stress responsive TAD in residues between 1039 and 1249 (NFAT5, isoform C) (Ferraris et al., 2002b, Lee et al., 2003). There is also a hyperosmotic stress dependent modulation domain in between residues 618 to 820 of NFAT5 (NFAT5, isoform C), which

acts in synergy with TAD for proper hyperosmotic stress response (Lee et al., 2003). NFAT5 interacts with many protein for transactivation such PKA, p38, Fyn, ATM and PI3K.

PKA, cyclic AMP dependent serine-threonine kinase, transfers phosphate groups to other proteins under high intracellular cyclic AMP concentrations. Nevertheless, this rise in cyclic AMP is not necessary for PKA activation under hyperosmotic stress (Ferraris et al., 2002a). PKA positively regulates NFAT5 under hyperosmotic milieu via increasing its transactivation and results in increased in AR and BGT1 transcription (Ferraris et al., 2002a). In line with these findings, NFAT5 and PKA co-immunoprecipitate (Ferraris et al., 2002a).

p38 is a MAPK that is also activated under hyperosmotic stress. It positively regulates NFAT5 transactivation and increases NFAT5 targets as presented by pharmacological modulator and dominant negative constructs of p38 (Han et al., 1994, Sheikh-Hamad et al., 1998, Nadkarni et al., 1999, Ko et al., 2002). Hyperosmotic stress activates MEKK3 and MAPK kinases, MKK3 and MKK6, which in turn can activate p38 (Cuenda et al., 1996, Meier et al., 1996, Uhlik et al., 2003, Kang et al., 2006). TAB1 also mediates autoactivation of p38 under hyperosmotic stress (Kang et al., 2006). Moreover, some of the p38 population within the cell interacts with OSM, which also interacts with actin, GTPase Rac, MEKK3 and MKK3 under hyperosmotic stress (See heading 1.3.1. Hyperosmotic environment induced modifications of cytoskeleton).

Fyn is a member of Src family of tyrosine kinases which are regulated via phosphorylation and dephosphorylation events. Phosphorylation from C-terminal tyrosine renders Src family kinases inactive, whereas dephosphorylation events on this tyrosine causes a conformational change and activates these enzymes. Fyn is activated under hyperosmotic stress via mainly via cell shrinkage (Kapus et al., 1999, Reinehr et al., 2004). Several observations indicate the involvement of Fyn for NFAT5 transactivation such that Fyn knockout cells have lower NFAT5 transcriptional activity towards AR gene and pharmacological inhibition or dominant negative expression of Fyn diminish NFAT5 dependent transcription (Ko et al., 2002).

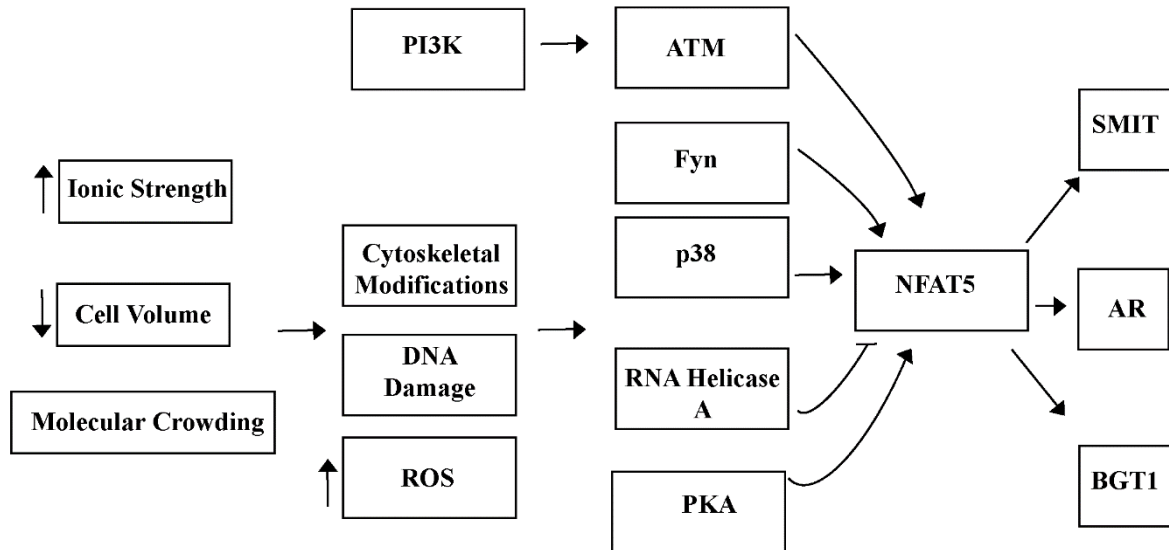


Figure 1.9. High NaCl causes NFAT5 transcriptional activity via several mechanisms and upregulates osmoprotective gene expression, including AR, SMIT and BGT1.

ATM, is a DNA backbone breakage sensitive serine threonine kinase, phosphorylates several intracellular targets such as p53 and BRCA1 upon DNA damage, and induce DNA repair for cell survival. ATM is also activated under hyperosmotic stress and positively regulates NFAT5 transactivation (Irrarrazabal et al., 2004). In this regard, pharmacological modulators of ATM and experiments done on ATM knockout cells has shown findings that loss of ATM results in suppressed NFAT5 transactivation, decreased NFAT5 dependent transcription and downregulated NFAT5 targets (Irrarrazabal et al., 2004). ATM also interacts with NFAT5 and have been found acting together with NFAT5 on ORE sites (Irrarrazabal et al., 2004). C-terminal region of NFAT5 contains three serine residues, which are ATM consensus phosphorylation sites (Irrarrazabal et al., 2004) Among these serines, mutation of serine at position 1247 has been suggested to be phosphorylated by ATM for proper NFAT5 transcriptional activity, however direct evidence for phosphorylation of this site is still lacking (Irrarrazabal et al., 2004).

PI3Ks are lipid kinases that transfers phosphate groups to 3' hydroxyl groups of phosphatidylinositol and phosphoinositides. PI3KIA, a class IA PI3K, converts PIP<sub>3</sub> to PIP<sub>2</sub>

and is involved in NFAT5 activation (Engelman et al., 2006). These effects of PI3KIA on NFAT5 are mediated by ATM (Irrarrazabal et al., 2006).

#### **1.4.6. Interactions of NFAT5**

To date, NFAT5 was documented to be part of a bulky complex, which consist of several other partners, such as catalytic subunit of PKA (Ferraris et al., 2002a), ATM (Irrarrazabal et al., 2004), RNA Helicase A (Colla et al., 2006), TAZ (Jang et al., 2012), FSP27 (Ueno et al., 2013), B-catenin (Wang et al., 2013), AP-1 (Irrarrazabal et al., 2008), HSP-90 (Chen et al., 2007) and PARP1 (Chen et al., 2007).

#### **1.4.7. Inhibition of NFAT5**

RNA Helicase A is nuclear protein that is involved in unwinding of DNA and RNA. Independent of this activity, it suppresses NFAT5 activation (Colla et al., 2006). It interacts with dimerization interface at the N terminal of NFAT5 through its N and C-terminals. NFAT5-RNA Helicase A interaction is disrupted upon hyperosmotic exposure.

PARP1, an also inhibitor of transcriptional activity of NFAT5 (Chen et al., 2007), catalyzes poly (ADP-ribosyl)ation of proteins, as well as takes role in DNA repair mechanism using NAD<sup>+</sup> as cofactor (Schreiber et al., 2006). PARP1 expression under hyperosmotic stress has been shown to suppress both transcriptional activity and activity of transactivation residues of NFAT5 (Chen et al., 2007). This inhibitory effect of PARP1 was suggested to be independent of its activity (Chen et al., 2007).

### **1.5. NFAT5, AR and diabetic vascular complications**

During the course diabetes, diabetic patients develop vascular complications of diabetes such as such as atherosclerosis, nephropathy, neuropathy and retinopathy

(Vikramadithyan et al., 2005, Oates, 2008, Kim et al., 2014b, Wei et al., 2014). Hyperglycemia induced by diabetes, increases hyperosmolality of the plasma up to 350 mosmol/kgH<sub>2</sub>O and more frequently, diabetes patients have hyperglycemia at every post-prandial stage, even under good metabolic control (Reaven et al., 1988, Campos et al., 2003, Monnier et al., 2003). During the course of diabetes, the oscillatory increases in plasma concentrations of glucose causes acute upregulations of IL-6, IL-18 and TNF- $\alpha$  (Ceriello et al., 2004). The possible link between hyperosmotic stress and increased cytokine expression have been previously shown in human peripheral blood monocytic cells, which had increased levels of IL-1 and IL-8 under hyperosmotic milieu in the range of 330 to 410 mosmol/kgH<sub>2</sub>O (Shapiro et al., 1997). Moreover, increased NFAT5 at TonE sites have been presented in peripheral blood monocytic cells of diabetic patients (Yang et al., 2006). Remarkably, a hyperosmotic stress dependent target of NFAT5, AR has also been linked to diabetic atherosclerosis (Vikramadithyan et al., 2005). Since AR gene has NFAT5 binding sites in its promoter region, one can deduce that NFAT5 also plays a role in AR dependent axis of diabetic vascular complications. In line with this background studies, we have investigated the regulation of NFAT5 dependent AR expression in U937 monocytes under hyperosmotic stress in this thesis.

### **1.5.1. Diabetic vascular complications**

There are mainly four different hypothesis regarding how microvascular and macrovascular complications of diabetes are mediated by hyperglycemia, as summarized in Figure 1.10;

- 1) Increased polyol pathway, which includes the target of NFAT5, AR
- 2) Increased flux through hexosamine pathway
- 3) Increased activation of Protein Kinase C isoforms
- 4) Increased production of advanced glycation end (AGE) products

With this background, focus will on polyol pathway due to investigation of AR expression in this thesis.

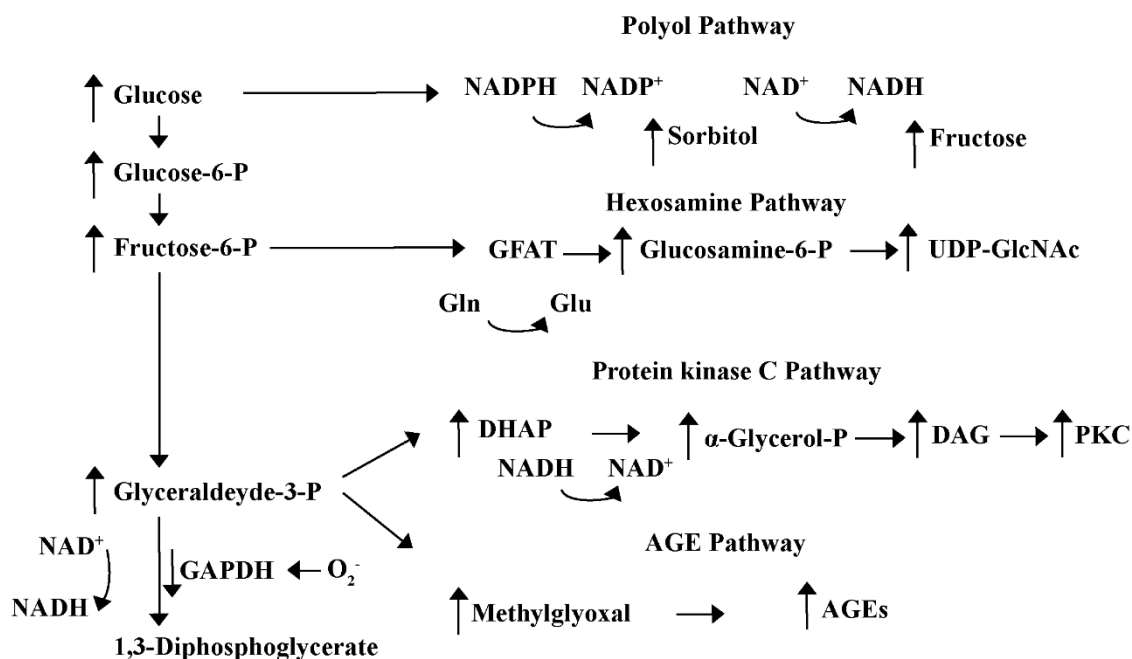


Figure 1.10. Mechanisms of diabetic vascular complications. Excess superoxide from mitochondria inhibits GAPDH, therefore upstream glycolytic intermediates are diverted to glucose overutilization cascades. As a result, excess DHAP is converted to protein kinase C activator, DAG and to methylglyoxal which generates advanced glycation end (AGE) products. On the other hand, increased fructose-6-phosphate concentration causes more proteins to be modified due to overproduction of UDP-N-acetylglucosamine (UDP-GlcNAc). Meanwhile, excess glucose is converted to sorbitol, which depletes NADPH, within the polyol pathway.

### 1.5.2. Role of AR under diabetic vascular complications

AR (E.C: 1.1.1.21), is rate limiting enzyme of the polyol pathway (Figures 1.10 and 1.11). It mainly resides in cytoplasm and catalyzes NADPH dependent reduction of the glucose to sorbitol, along with reduction of atherogenic aldehydes, steroids, phospholipids lipid aldehydes and their glutathione conjugates (Srivastava et al., 2005, Ramana et al., 2010, Vedantham et al., 2012). AR has low affinity to glucose under normal circumstances, but in hyperglycemic environment, this affinity substantially increases (Brownlee, 2001). The product of AR enzymatic activity, sorbitol, is then converted to fructose via SDH, which results in increased NADH/NAD<sup>+</sup> ratio in cytoplasm (Brownlee, 2001). The diabetic vascular complications exacerbated by AR has been reported to be mediated in part, by excess AR activity dependent depletion of NADPH, which is utilized in cellular protection against oxidative stress by glutathione reductase/glutathione peroxidase system (Cheng et al., 1986, Srivastava et al., 2005, Vedantham et al., 2012).

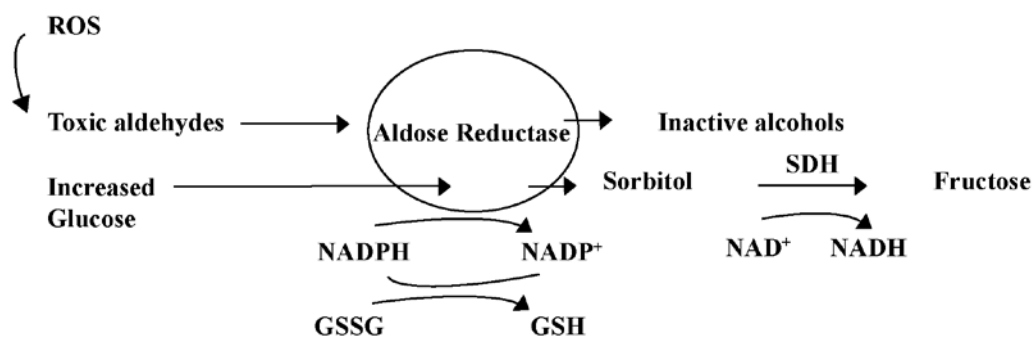


Figure 1.11. Involvement of AR in polyol pathway. Toxic aldehydes generated through ROS formation, and glucose, are utilized by AR. This enzyme converts toxic aldehydes to inactive alcohols and glucose to sorbitol, via employing NADPH as a cofactor. When excess AR flux is present, GSH is depleted leading to oxidative stress, due to overutilization of NADPH by AR. SDH converts sorbitol to fructose.

## 1.6. Protein acetylation and deacetylation

Proteins are frequently modified by acylations which is the attachment of functional groups such as acetylation, formylation, butyrylation, propionylation, succinylation, malonylation, myristoylation, glutarylation and crotonylation through acyl linkages (Figure 1.12) (Zeidman et al., 2009). Among post-translational modifications, acetylation is one of the most abundant modification as nearly 85% of eukaryotic proteins are acetylated (Kouzarides, 2000, Polevoda et al., 2002, Polevoda et al., 2003, Yang, 2004a, Glozak et al., 2005). Several types of amino acids such serine and alanine can be acetylated in a co-translational manner from their N<sup>α</sup>-terminal (Polevoda et al., 2002). Although less common than N<sup>α</sup> type acetylation, N<sup>ε</sup>-acetylation of internal lysines is still an important type of post-translational modification (Polevoda et al., 2003). Essentially this process is highly reversible and involves in mediating several types of cellular process including transcription regulation (Brunet et al., 2004, Faiola et al., 2005), DNA repair (Murr et al., 2006), apoptosis (Cohen et al., 2004, Subramanian et al., 2005), cytokine signaling (Yuan et al., 2005), and nuclear import (Bannister et al., 2000).

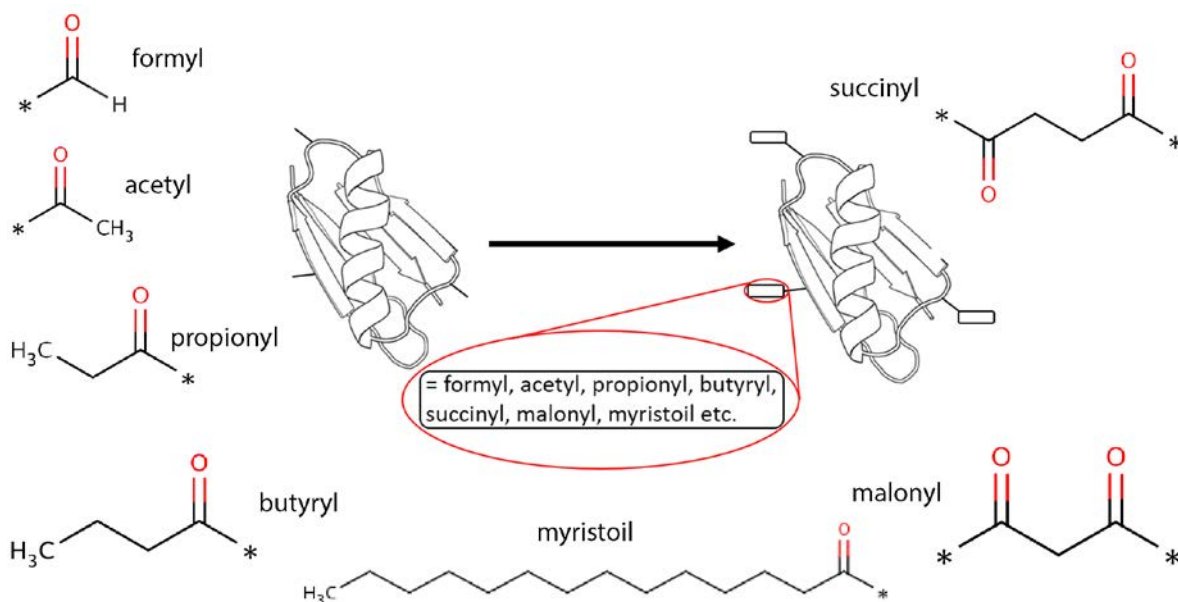


Figure 1.12. Acylation of proteins.

### 1.6.1. Reaction mechanisms of acetylation and deacetylation

Protein acetylation is the enzymatic process of transferring acetyl groups from acetyl coenzyme A (acetyl CoA) to either  $\alpha$ -amino ( $N^\alpha$ ) group of amino-terminal residues or to the  $\epsilon$ -amino group ( $N^\epsilon$ ) of specific internal lysines. Figure 1.13 shows the mechanism of  $N^\epsilon$  acetylation of an internal lysine that is catalyzed by a histone lysine acetylase.

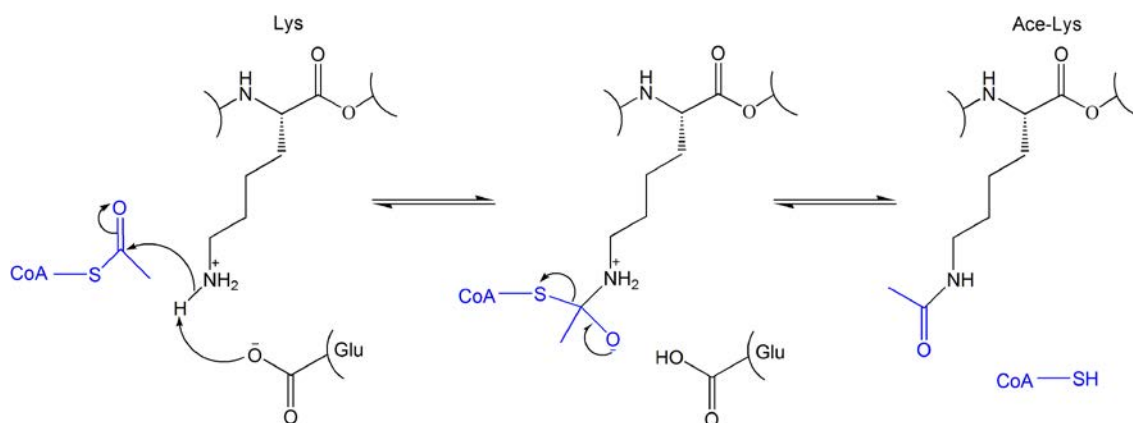


Figure 1.13. Mechanism of lysine acetylation.

In this reaction, acetyl CoA which is the source of the acetyl group is converted to coenzyme A (CoASH). A conserved glutamate residue in acetylase enzymes acts as a general base and activates the lysine  $\epsilon$ -amino group for nucleophilic attack on the carbonyl group of acetyl CoA. Next, an unstable tetrahedral intermediate forms and collapses. The reaction is terminated by the release of acetyl lysine (Ace-Lys) and coenzyme A (CoASH).

This reaction can be reversed by histone deacetylases (HDACs). There are four classes of histone deacetylases (I-IV) that catalyze deacetylation of acetyl lysine. The reaction mechanisms of these deacetylation reactions involve nucleophilic attack of water on the acetyl carbonyl. However the mechanism of activation of water is different for different classes of HDACs. As such, HDAC classes I, II and IV use an active-site metal-dependent mechanism (Figure 1.14), while class III HDACs such as sirtuins operate using a  $NAD^+$

dependent catalytic mechanism (Hallows et al., 2012, Feldman et al., 2013, Hebert et al., 2013) (Figure 1.15).

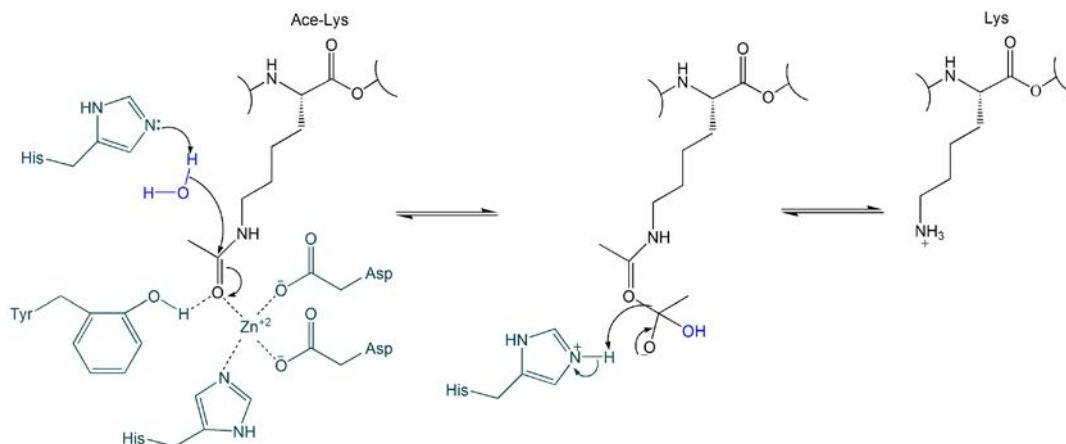


Figure 1.14. Deacetylation by class I, II and IV HDACs.

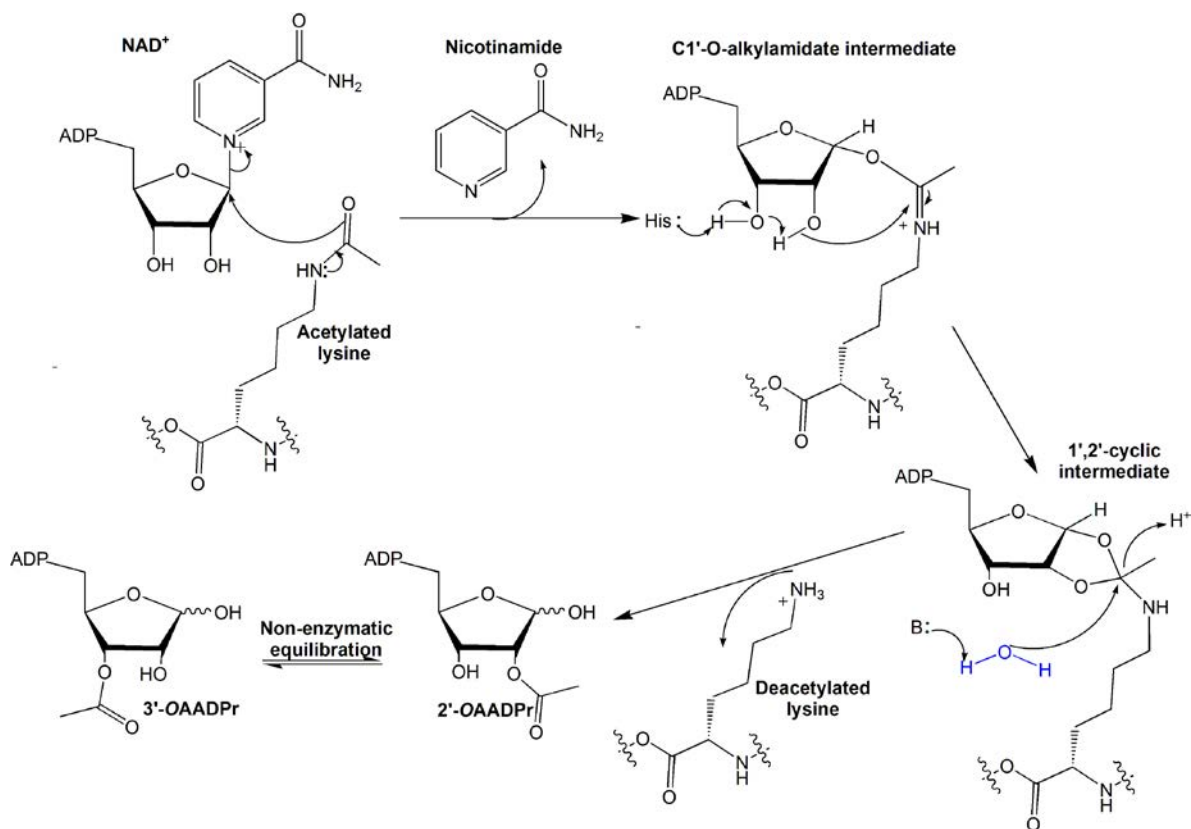


Figure 1.15. Deacetylation by class III HDACs.

### **1.6.2. Roles acetylation and deacetylation in cellular processes**

Hitherto several acetylated proteins along with their selective deacetylases such as sirtuins have been targeted to explain the intricate link between lysine acetylation and cellular metabolism (Finkemeier et al., 2011, Konig et al., 2014). N<sup>ε</sup>-acetylation changes the electrostatic properties of lysine as it neutralizes the positive charge of the lysine. This change would significantly disrupt the hydrogen bonding potential of the positively charged lysine and thus may lead to loss of protein function (Yang, 2004a, Yang, 2004b). On the other hand acetylation of a surface lysine residue might lead to formation a novel interface for protein binding and thus a gain of function will be also proposed in acetylated proteins (Yang, 2004a, Yang, 2004b). Overall such kind of alterations was used to explain the roles played by N<sup>ε</sup>-acetylation of proteins in protein-protein interaction, DNA binding, enzymatic activity, stability and subcellular localization (Bannister et al., 2000, Polevoda et al., 2002, Brunet et al., 2004, Yang, 2004a, Yang, 2004b, Faiola et al., 2005, Glozak et al., 2005, Yuan et al., 2005).

### **1.6.3. NAD<sup>+</sup> dependent deacetylase SIRT1**

Acetylation of proteins is regulated by acetyltransferases, which transfer acetyl groups from acetyl CoA to the ε amino groups of lysines. After discovery of acetyltransferases, their activity has been long thought to be exerted just on histones, which is also countered by histone deacetylases. It is now established histone deacetylases can also target non-histone proteins (Kwon et al., 2008). There are three classes of histone deacetylases in cells, which are divided according to their homologies to repressors of transcription in yeast: 1) Reduced potassium dependency gene 3, 2) A subunit of histone deacetylase A complex 3) Silent information regulator 2 (Cress et al., 2000, North et al., 2004). In humans, there are seven silent information regulator 2 homologues, named as Sirtuins (Frye, 2000).

SIRT1, the closest homologue of silent information regulator 2 of yeast, is a NAD<sup>+</sup> dependent histone/protein deacetylase which has been implicated in wide array of cellular

events including starvation, inflammation, oxidative stress and senescence (Kwon et al., 2008). In part, SIRT1 mediates these cellular events through directly deacetylating several diverse transcription factors including p53 (Vaziri et al., 2001), FOXOs (Motta et al., 2004), Egr-1 (Pardo et al., 2012), p65 (Yeung et al., 2004), NFATc3 (Jia et al., 2014). Due to its control on replicative senescence, it has been proposed to function as a longevity factor, since its overexpression has been shown to suppress p53 through deacetylation (Kaeberlein et al., 1999, Haigis et al., 2006). This role of SIRT1 in longevity has been supported by several lines of evidence on caloric restriction, an inducer of SIRT1 such that caloric restriction increases lifespan several organisms (Lin et al., 2000, Tissenbaum et al., 2001, Rogina et al., 2004, Chen et al., 2005a, Baur et al., 2006, Wang et al., 2006, Milne et al., 2007).

Other than p53, important for the subject of this thesis, SIRT1 deacetylates, Rel family members, p65 and NFATc3, which have been suggested to be negatively regulated directly by SIRT1 (Yeung et al., 2004, Jia et al., 2014). Nevertheless, existence of a similar machinery and its significance on NFAT5 as another Rel family member, still remains as a question. Other than this Rel family linked possibility of NFAT5-SIRT1 axis, in a study exploring SIRT1 substrates through utilization of stable isotope labeling with amino acids in cell culture (SILAC) method stated that NFAT5 could be a possible catalytic target of SIRT1. (Peng et al., 2012). However, the mechanism was not elucidated. More recently, NFAT5 and SIRT1 has been shown to work in synergy under osmotic stress in suppression of prorenin receptor, supporting the probability of an inducement of SIRT1 on NFAT5 (Quadri et al., 2014).

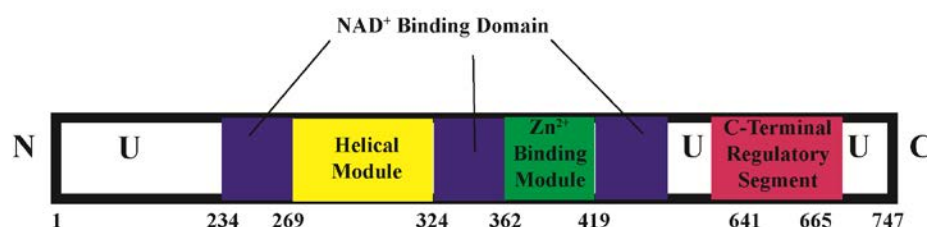


Figure 1.16. Structure of SIRT1.U: Unstructured regions.

#### 1.6.4. Structure of SIRT1

The residues responsible from SIRT1 catalytic activity consists of NAD<sup>+</sup> binding domain, which has a Rossmann fold and other two smaller modules, helical and Zn<sup>2+</sup> binding modules (Figures 1.16 and 1.17) (Davenport et al., 2014). Helical and Zn<sup>2+</sup> binding modules are held together via hydrophobic interface and generates the catalytic core (Davenport et al., 2014). C-terminal regulatory segment complements the Rossmann fold that is responsible for nucleotide binding and this complementation does not affect the structure of catalytic domain (Davenport et al., 2014). Ser265, Asn346, Ile247 and Asp348 are responsible from NAM binding after the deacetylation reaction is completed (Davenport et al., 2014). F414 is responsible from substrate binding (Davenport et al., 2014). H363 is responsible from removal a proton from NAD<sup>+</sup> cofactor (Davenport et al., 2014).

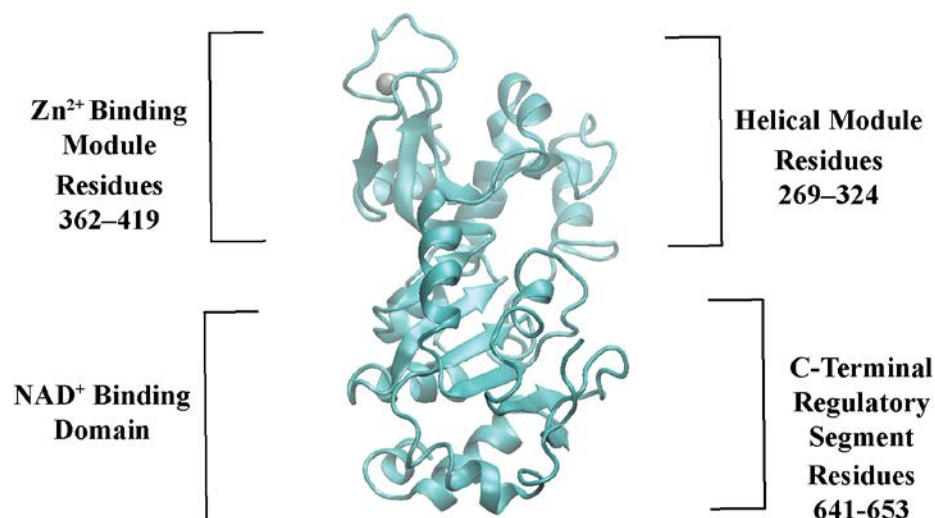


Figure 1.17. Structure of SIRT1, depicted from PDB ID: 4IG9 Chain A. NAD<sup>+</sup> binding domain, Zn<sup>2+</sup> binding module, helical module and C-terminal regulatory segment is shown. Chain identifiers and residue numbers are kept as in 4IG9.

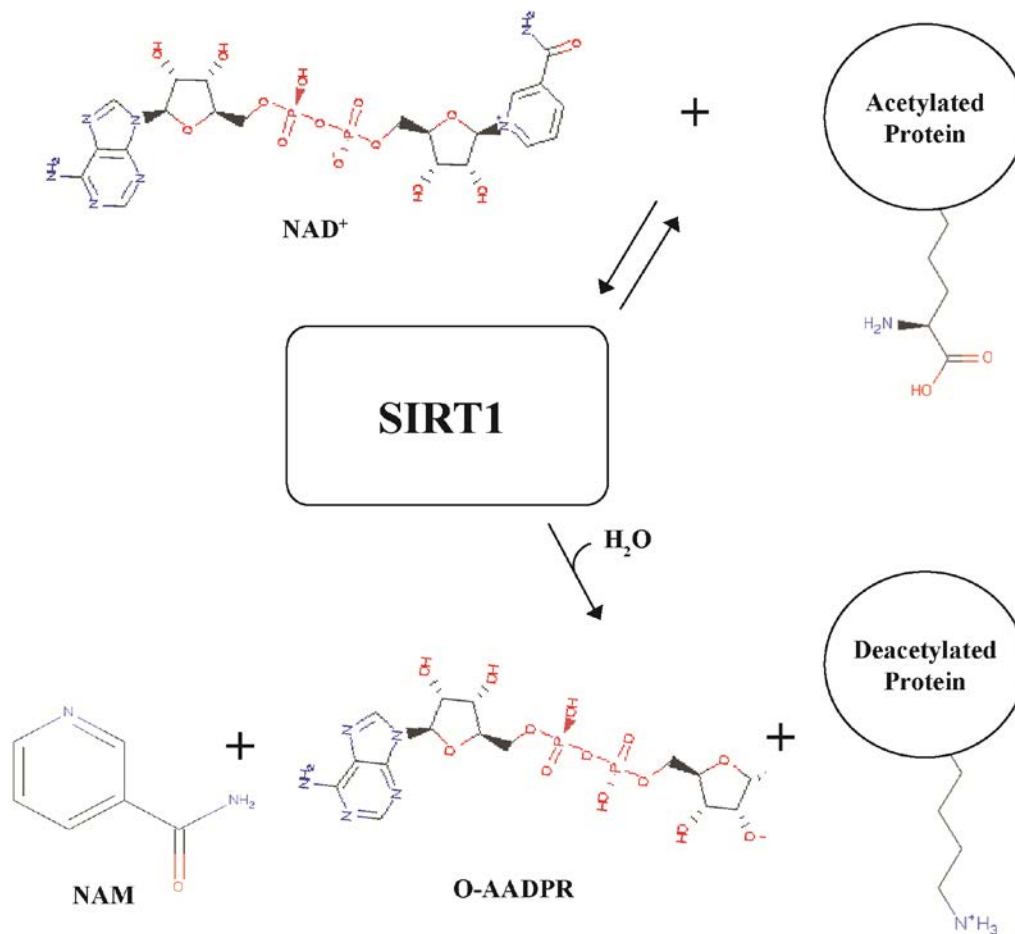


Figure 1.18. Mechanism of SIRT1 based deacetylation of the acetylated protein. In a twostep reaction, SIRT1 uses NAD<sup>+</sup> and releases NAM and AADPR, together with the deacetylated protein. NAD<sup>+</sup> hydrolysis generates the necessary force for the SIRT1 reaction.

### 1.6.5. Enzymatic mechanism of SIRT1

The first reaction which has been identified for sirtuins is the ribosyl transfer reaction in bacteria (Tsang et al., 1998). Through this observation, sirtuins are identified as NAD<sup>+</sup>

dependent deacetylases (Imai et al., 2000, Landry et al., 2000, Tanner et al., 2000, North et al., 2003). In particular, SIRT1 and SIRT6 are involved both in auto-ADP-ribosyltransferase and substrate specific deacetylation reactions (Michishita et al., 2008)

The deacetylation reaction is initiated with amide cleavage from NAD<sup>+</sup> and followed by formation of NAM and ADP-ribose peptide intermediate (Haigis et al., 2010). Then, the intermediates are used for formation of O-AADPR and substrate is deacetylated (Figure 1.18) (Haigis et al., 2010). Amide to ester acyltransfer transfer reactions are not a preferred due to energetics, however hydrolysis of NAD<sup>+</sup> can supply the necessary force for this deacetylation reaction (Sauve et al., 2006, Smith et al., 2008, Sauve, 2009). It has also been proposed that substrate binding induces a conformational change in the enzyme structure that induces a nucleophile of sirtuin to react with NAD<sup>+</sup>, which results in stabilization of ADPR intermediate by the enzyme (Sauve et al., 2006).

#### **1.6.6. Interplay of SIRT1 with NAD<sup>+</sup> dependent poly (ADP-ribose) polymerase, PARP1**

PARP1 is a DNA break sensor and acts upon those breaks spatially and temporally. Moreover, through interacting with other proteins or poly (ADP-ribosyl)ating them, it controls the structure of the chromatin and maintain the integrity of DNA as shown by the studies with inhibition of PARP1 or with PARP1 knockout mice (de Murcia et al., 1997, Wang et al., 1997, Masutani et al., 1999). PARP1 interacts with several DNA related proteins such as histones, topoisomerases, and helicases as well as with NFAT5 for its inhibition (See heading 1.4.7. Inhibition of NFAT5).

PARP1 and SIRT1 both utilize NAD<sup>+</sup> for their catalytic activity. Under physiological, hence, in situations where no DNA damage exist, low PARP1 activity inhibits SIRT1, leading to chromatin decondensation though inducing histone acetylation (Zhang, 2003, Kruszewski et al., 2005). At this level, such an interplay results in activation of gene expression and genomic stability. However under pathological conditions, PARP1 rapidly depletes intracellular NAD<sup>+</sup> for the purpose of DNA repair and results in complete abolishment of SIRT1 activity (Zhang, 2003, Matsushita et al., 2005). This condition leads

to p53 acetylation and results extensively in cell death (Araki et al., 2004, Pillai et al., 2005). Moreover, under such stress condition, PARP1 activity has been shown to be induced by SIRT6 (Mao et al., 2011).

### **1.7. Scope and aim of thesis**

NFAT5, a member of Rel family proteins, is a transcription factor activated upon osmotic stimuli (Aramburu et al., 2006). When cells are exposed to osmotic stress, NFAT5 activates transcription of several osmoadaptive factors that are responsible for accumulation compatible osmolytes including betaine via BGT1, myo-inositol by SMIT and sorbitol by AR (Burg et al., 1996, Aramburu et al., 2006). Osmotic stress dependent activation of NFAT5 was suggested to be mediated by a number of different mechanisms. Osmotic stress increases expressions of NFAT5 protein and mRNA levels (Miyakawa et al., 1999b, Ko et al., 2000), causes translocation of NFAT5 from cytoplasm to nucleus (Miyakawa et al., 1999b, Ko et al., 2000), activates transactivation domain of NFAT5 (Ferraris et al., 2002b) and increases phosphorylation of NFAT5 (Dahl et al., 2001). Other than phosphorylation, NFAT5 was proposed to be palmitoylated in which depalmitoylation was shown to accelerate its nuclear translocation (Eisenhaber et al., 2011). In addition, sumoylation of NFAT5 was revealed to inhibit its transactivation (Kim et al., 2014a). NFAT5 was also documented to be part of a bulky complex, which consist of several other partners, such as catalytic subunit of PKA (Ferraris et al., 2002a), ATM (Irrarrazabal et al., 2004), RNA Helicase A (Colla et al., 2006), TAZ (Jang et al., 2012), FSP27 (Ueno et al., 2013), B-catenin (Wang et al., 2013), AP-1 (Irrarrazabal et al., 2008), HSP-90 (Chen et al., 2007) and PARP1 (Chen et al., 2007). Among these interacting partners, PARP1, an inhibitor of transcriptional activity of NFAT5 (Chen et al., 2007), catalyzes poly (ADP-ribosyl)ation of proteins, as well as plays a role in DNA repair mechanism using NAD<sup>+</sup> as cofactor (Schreiber et al., 2006). In this regard, PARP1 has also been shown to influence several intracellular pathways, reciprocally with a deacetylase, SIRT1 due to utilization of common cofactor NAD<sup>+</sup> (Kauppinen et al., 2013, Luna et al., 2013, Walko Iii et al., 2015). Despite these evidences, likelihood of SIRT1 regulating NFAT5 is still a question to be resolved. Other than previously identified post translational

modifications, impact of possible SIRT1 based deacetylation of NFAT5, also remains unclear.

SIRT1 is a NAD<sup>+</sup> dependent histone/protein deacetylase which has been implicated in wide array of cellular events including starvation, inflammation, oxidative stress and senescence (Kwon et al., 2008). SIRT1 mediates these cellular events in part through directly deacetylating several diverse transcription factors including p53 (Vaziri et al., 2001), FOXOs (Motta et al., 2004), Egr-1 (Pardo et al., 2012), p65 (Yeung et al., 2004), NFATc3 (Jia et al., 2014). Among these transcription factors, Rel family members, p65 and NFATc3 were identified to be negatively regulated by direct SIRT1 dependent deacetylation (Yeung et al., 2004, Jia et al., 2014). Yet, presence of such mechanism and its consequence in another Rel family member, NFAT5, still remains unsettled. Likewise, in a study investigating enzymatic substrates of SIRT1 using SILAC method stated that NFAT5 was a candidate enzymatic target of SIRT1 (Peng et al., 2012). Nonetheless, the intracellular machinery of such targeting has also not been considered until now. More recently, NFAT5 and SIRT1 has been anticipated to work synergistically under osmotic stress towards downregulation of prorenin receptor expression, supporting an influence of SIRT1 activity towards NFAT5 (Quadri et al., 2014). Based on these previous findings, the possibility of SIRT1 based regulation NFAT5 has warranted further studies.

As one of the canonical targets of NFAT5, AR (E.C: 1.1.1.21), the rate limiting enzyme of polyol pathway, catalyzes reduction of the glucose to sorbitol, along with reduction of atherogenic aldehydes, steroids, phospholipids lipid aldehydes and their glutathione conjugates (Srivastava et al., 2005, Ramana et al., 2010, Vedantham et al., 2012). Reduction of glucose to sorbitol by AR, has been established to be osmoprotective in the cells of inner medulla of kidney (Bagnasco et al., 1987, Burg, 1988, Ramasamy et al., 2010). Excess glucose flux through AR was also linked to secondary complications of diabetes such as atherosclerosis, nephropathy, neuropathy and retinopathy (Vikramadithyan et al., 2005, Oates, 2008, Kim et al., 2014b, Wei et al., 2014). These complications has been reported to be mediated in part, by excess AR activity dependent depletion of NADPH, which is utilized in cellular protection against oxidative stress by glutathione reductase/glutathione peroxidase system (Cheng et al., 1986, Srivastava et al., 2005, Vedantham et al., 2012). Besides to these

well-recognized consequences of AR activity in progression of diabetic complications, SIRT1 has been suggested to act as a protective element against these complications (Orimo et al., 2009, He et al., 2010, Kitada et al., 2011, Yang et al., 2011). In a recent study on diabetic human AR overexpressing mice, excess AR flux was also proposed to diminish SIRT1 activity, providing presence of a metabolic link between these proteins (Vedantham et al., 2014). Regardless of these evidences, involvement of SIRT1 in AR expression in monocytes under osmotic stress remains ambiguous, which also prompted this study.

Based on all these findings, in this thesis, we hypothesized that SIRT1 regulates NFAT5 dependent AR expression under hyperosmotic stress.

Specific aims of this theses are indicated as below:

- An osmotic stress model with concurrent expressions of NFAT5 and SIRT1, was generated in U937 monocytes.
- Essential mechanistic details of the model were established by analyzing intracellular localizations of NFAT5 and SIRT1, AR expression and oxidative stress.
- In this model, contribution of SIRT1 activity on AR expression, as well as, stabilization of nuclear NFAT5, were explored using pharmacological modulators.
- By utilizing overexpression and co-transfection of NFAT5 and SIRT1 in HeLa cells, impact of SIRT1 activity on AR and NFAT5 were validated, while its role on DNA binding activity of NFAT5 was demonstrated.
- Using co-immunoprecipitation method, the influence of osmotic stress on NFAT5-SIRT1 interaction was deciphered to comprehend the model more thoroughly.
- Possibility of direct interaction between NFAT5 and SIRT1 was also investigated via in silico analysis. In this regard, deacetylation favored lysine residues of NFAT5 and their binding to SIRT1 substrate binding site were evaluated. Among these lysines, K282 was proposed as the most plausible candidate for SIRT1 activity.

To best of our knowledge, this is the first report investigating the contribution of SIRT1 on NFAT5 dependent AR expression in monocytes under osmotic stress. Overall, here, for

the first time, evidence on identification of novel intracellular SIRT1 target, NFAT5 dependent AR expression, was described.

## **2. MATERIALS AND METHODS**

### **2.1. Materials**

#### **2.1.1. Summary of the materials used in this thesis**

RPMI-1640, DMEM, FBS and antibiotics were purchased from Pan Biotech GmbH (Aidenbach, Germany). MTT Cell Proliferation Kit I, X-tremeGENE 9 DNA transfection reagent, positively charged nylon membranes, protease and phosphatase inhibitor cocktails were purchased from Roche (F. Hoffman-La Roche Ltd., Basel, Switzerland). FITC tagged Annexin V was purchased from Alexis Biochemicals (Enzo Life Sciences Inc., Farmingdale, NY, USA). NFAT5 (H-300), SIRT1 (H-300) and AR (G-1) antibodies were purchased from Santa Cruz Biotechnology Inc. (Dallas, Texas, USA). SIRT1 (1F3), PARP1, myc, Lamin A/C, Beta-Actin, acetyl-lysine, HRP-conjugated anti-rabbit and anti-mouse secondary antibodies were purchased from Cell Signaling Technology Inc. (Beverly, MA, USA). Dynabeads Protein G and chemiluminescent nucleic acid detection module kit were purchased from Life Technologies (Thermo Fisher Scientific Inc., Waltham, MA USA). AR ORE probe was purchased from Integrated DNA Technologies (Coralville, Iowa, USA). NaCl, glucose, mannitol, tris, glycine, and tween-20 were purchased from Molekula Ltd. (Newcastle Upon Tyne, UK).

### **2.1.2. Chemicals and Media**

All chemicals and cell culture media used in this thesis are listed in Appendix A.

### **2.1.3. Antibodies**

All antibodies used in immunoblotting, EMSA, co-immunoprecipitation and enzymes are listed in Appendix B.

### **2.1.4. Molecular biology kits and reagents**

All molecular biology kits used for gene transfection, plasmid isolation, protein analysis, EMSA and co-immunoprecipitation are listed in Appendix C.

### **2.1.5. Expression vectors**

The maps each vector used in overexpression studies are shown in Appendix D.

### **2.1.6. Oligonucleotides**

AR ORE oligonucleotide is listed in Appendix E.

### **2.1.7. Buffers and solutions**

All buffers and solutions, prepared manually are listed in Appendix F.

### **2.1.8. Equipment and computer software**

Equipment, computer software and topology final generated for acetyllysine insertion are listed in Appendix G.

## **2.2. Methods**

### **2.2.1. Cell Culture and Treatments**

U937, human histiocytic lymphoma cell line, was obtained from Professor Giuseppe Poli, cultured in RPMI-1640 with 5 mM glucose, 10% FBS, 2 mM glutamine and 100 IU/ml penicillin/streptomycin. Cultures were maintained at 37°C in a humidified incubator at an atmosphere of 5% CO<sub>2</sub>. Before each experiment, cells were collected by centrifugation at 300g for 5 minutes, resuspended in serum free medium (SFM) and seeded (1,000,000 cells/ml) in 96-well, 6-well, 12-well, 60 mm or 100 mm culture plates depending on the experiment. In all U937 experiments, osmotic agents were applied to cells from main stocks prepared in SFM and an equal amount of SFM were added to the control group. Actual rise in osmolality of the medium was validated using an osmometer (Figure 3.1) (Osmomat 030, Gonatech, Berlin, Germany). Pretreatment with activators and inhibitors were done 1 hour prior to applying osmotic stress agent. For each pretreatment experiments, DMSO (max 0.5 %, v/v) was added to all controls. HeLa cells were cultured in DMEM supplemented with 5 mM glucose, 10% FBS and 100 IU/ml penicillin/streptomycin, maintained in a humidified incubator similar to U937 cells. In all HeLa experiments, osmotic agent was applied to cells from main stock prepared in culture medium.

### **2.2.2. Metabolic activity, cell death and oxidative stress assays**

For metabolic activity assay, U937 cells were seeded in 96-well plates, treated as indicated and analyzed by MTT Cell Proliferation Kit I according to the manufacturer's

instructions. For cell death assay, U937 cells were seeded in 12-well plates, treated as indicated and FITC tagged Annexin V staining was performed according to the manufacturer's protocol. Cells were then quantified by FACS (FACSCanto, Becton Dickinson, Franklin Lakes, NJ, USA) and analyzed by Flowjo software. For oxidative stress assay, U937 cells were seeded in 12 well plates, treated as indicated and stained with 10  $\mu$ M 2',7'-dichlorodihydrofluorescein diacetate (DCFH-DA) for 30 minutes at 37°C. Cells were then collected into flow cytometry tubes, pelleted, washed and resuspended in PBS, analyzed by flow cytometry similar to the analysis of cell death assay.

### **2.2.3. Protein extraction and immunoblotting**

For total protein extraction, cells were treated as indicated in 6-well, 60 mm or 100 mm culture plates and harvested by centrifugation at 300g for 5 min. Cells were then resuspended in 1 ml of ice-cold PBS and transferred into 1.5 ml microcentrifuge tubes and spun at 13200 rpm for 30 seconds. Pellet was lysed by incubation in total cell lysis buffer containing 50 mM Tris-HCl (pH:8.0), 150 mM NaCl, 1% Nonidet P-40 (v/v), 1 mM phenylmethylsulfonyl fluoride (PMSF), protease and phosphatase inhibitors for 30 minutes, followed by centrifugation at 13200 rpm for 10 minutes. Supernatant was collected as total protein extract and stored in -80°C for immunoblotting analysis. For cytoplasmic-nuclear extraction, cells were treated as indicated in 6-well, 60 mm or 100 mm culture plates and harvested by centrifugation at 300g for 5 min. Cells were then resuspended in 1 ml of ice-cold PBS and transferred into 1.5 ml microcentrifuge tubes and spun at 13200 rpm for 30 seconds. For cytoplasmic extraction, pellet was first lysed by incubation in T1 buffer containing 10 mM Hepes-KOH, 2 mM MgCl<sub>2</sub>, 0.1 mM EDTA, 10 mM KCl, 1% Nonidet P-40 (v/v), 1 mM DTT, 0.5 mM PMSF, protease and phosphatase inhibitors for 10 minutes, followed by centrifugation at 13200 rpm for 10 minutes. Supernatant was collected as cytoplasmic extract and stored in -80°C for immunoblotting analysis. For nuclear extraction, remaining pellet was resuspended in T2 buffer containing 50 mM Hepes-KOH, 2mM MgCl<sub>2</sub>, 0.1 mM EDTA, 50 mM KCl, 400 mM NaCl, 10% Glycerol, 1 mM DTT, 0.5 mM PMSF, protease and phosphatase inhibitors for 30 minutes, followed by centrifugation at 13200 rpm

for 20 minutes. Supernatant was collected as nuclear extract and stored in  $-80^{\circ}\text{C}$  for immunoblotting analysis. Proteins (30-100  $\mu\text{g}$ ) were mixed with loading buffer (62.5 mM Tris-HCl pH:6.8, 2% SDS, 10% glycerol, 0.005% bromophenol blue, 5% 2-mercaptoethanol) and separated on 6-12% SDS-PAGE and blotted onto PVDF membranes. Membranes were then blocked with 5% non-fat dry milk (AppliChem GmbH, Darmstadt, Germany) in PBS-Tween20, incubated with primary antibody overnight, followed by washing in PBS-Tween20 and incubation with HRP-conjugated secondary antibody. After the final wash with PBS-Tween20, proteins were analyzed ECL Advance (GE Healthcare Bio-Sciences, Pittsburgh, PA, USA) and exposed to Hyperfilm-ECL (GE Healthcare Bio-Sciences, Pittsburgh, PA, USA).

#### **2.2.4 Measurement of protein concentration**

Protein concentrations were determined by Bio-Rad Protein Assay (Bio-Rad, Munich, Germany) based on Bradford method. Bovine serum albumin (BSA) was used as the protein standard. 5  $\mu\text{g}$  of BSA was diluted 1:1 in 96-well plates for generation of protein standard curve. Samples were diluted 1:100, were also added to 96-well, for protein concentration determination. Absorbance was measured at 595 nm using a spectrophotometer. Protein concentrations were determined using linear fit of BSA based standard curve. For each new protein extraction, a new standard curve was generated from a new assay, was used.

#### **2.2.5. Transfections**

Flag tagged wildtype SIRT1 and flag tagged SIRT1 H363Y were gifts from Michael Greenberg (Addgene plasmid # 1791, # 1792) (Brunet et al., 2004). 6x myc tagged pEGFP NFAT5 (no EGFP) plasmid was a gift from Anjana Rao (Addgene plasmid # 13627) (Lopez-Rodriguez et al., 1999). HeLa cells were transfected either with wildtype flag tagged SIRT1 or catalytically inactive flag tagged SIRT1 H363Y. In co-transfection studies, these SIRT1 plasmids were cotransfected with 6x myc tagged NFAT5. All transfection experiments were done using X-tremeGENE 9 DNA transfection reagent, according to the manufacturer's

instructions. Depending on the experiment, empty backbone plasmids were also transfected as negative transfection control and indicated as mock. Transfections were confirmed by immunoblotting of the tag or protein itself.

#### **2.2.6. Electrophoretic mobility shift assay (EMSA)**

HeLa cells were co-transfected with 6x myc tagged NFAT5 alone or either with wildtype flag tagged SIRT1 or with catalytically inactive flag tagged SIRT1. 5' biotinylated and double stranded osmotic response element (ORE) DNA probe which contains bp -1,238 to -1,104 of human aldose reductase gene, were used as previously described [15, 47]. Briefly, 5 µg of total protein extract were combined with 50 fmol of labeled ORE probe in 20 µl of reaction mixture, containing 1 µg of poly (dA-dT). After 30 minutes of incubation at room temperature, products were separated on 0.4% SeaKem Gold agarose (Lonza Group Ltd, Basel, Switzerland) gels in 0.5X TBE buffer at 4°C. Then, products were transferred to positively charged nylon membranes and crosslinked. Probe was detected by chemiluminescent nucleic acid detection module kit, according to the manufacturer's instructions. For supershift analysis, 1 µg of NFAT5 antibody was added to reaction mixture and incubated 1 hour at 4°C prior to the addition of ORE probe.

#### **2.2.7. Co-immunoprecipitation**

U937 cells were treated as indicated and total cell lysates of 500-1000 µg were first precleared with 25 µl of Dynabeads Protein G for 30 minutes at room temperature and remaining supernatants were then immunoprecipitated with 1 µg NFAT5 (H-300) or 3 µg SIRT1 (H-300) primary antibodies at 4°C overnight on a rocking platform. Next, immune complexes containing NFAT5 and SIRT1 interacting proteins, were captured with 25 µl of Dynabeads Protein G for 30 minutes at room temperature. Immunoprecipitates then were washed three times with total cell lysis buffer and were analyzed by immunoblotting.

### 2.2.8. Prediction of acetylated lysines of NFAT5

The primary amino acid sequence of the available NFAT5 structure (PDB entry: 1IMH Chain C) was used in prediction of lysine acetylation sites. 10 different algorithms were used; KacePred (Suo et al., 2013b), PAIL (Li et al., 2006), ASEB (Li et al., 2012b, Wang et al., 2012), Predmod (Basu et al., 2009), BRABSB-PHKA (Shao et al., 2012), PSKAcePred (Suo et al., 2012), PLMLA (Shi et al., 2012), PHOSIDA (Gnad et al., 2010), EnsemblePail (Xu et al., 2010) and Lys Acet (Li et al., 2009), which are, to our knowledge, the most frequently and widely used/cited methods for prediction of lysine acetylation sites. Threshold values were taken as stringent as possible for all predictions (Table 3.1). The lysines were selected if they were predicted by at least one algorithm. Overall 21 out of 22 lysine residues in NFAT5 were predicted to be acetylated at least by one algorithm.

Identification of site-specific acetylated substrates is fundamental for deciphering the molecular mechanism and dynamics of acetylation process (Hartl et al., 2015). Such efforts are critical to comprehend the interplay between lysine acetylation and cellular metabolism. Experimental methods such as mass spectroscopy that provide strong evidence regarding the position of acetylated lysine have been traditionally used to for identification of specific internal lysine residues that are acetylated (Lundby et al., Bizzozero, 1995). However the cost associated with such kind of experimental methods bears a burden to these studies (Li et al., 2014). Due to the difficulties faced in identification of lysine-acetyl-transferase substrates, experimental determination of acetylated internal lysine sites remains as also a challenge to molecular biologist (Sadoul et al., 2011, Suo et al., 2013a). Nevertheless, with the current advancements in computational approaches, a number of *in silico* methods for prediction of acetylation sites have been developed. These methods have attracted great attention for their convenience and fast-speed, along with their reasonable prediction accuracy (Li et al., 2014). Here a summarization of the computational resources for prediction of lysine acetylation and also acetylation databases will be made. These algorithms and databases could be used to predict internal lysine residues that are to be N<sup>ε</sup>-acetylated in a given protein, representing alternative and easier methods than experimentation to identify acetyl lysine sites in proteins.

### 2.2.8.1. Detailed methodology of algorithms for acetyllysine prediction

*KAcePred* (Lysine-K acetylation prediction) is one of the most recent algorithm for prediction of acetylation states of a human protein by inputting only the amino acid sequence (Kim et al., Yip et al., 2004, Li et al., 2014). For each protein, *KAcePred* web server uses the constructed lysine acetylation prediction model by which the model assigns a score for each lysine residue. To get a finer predictive performance and decrease computational costs, the developers combined position specific scoring matrix profiles along with the best nine physicochemical properties to be used as an optimal sequence encoding scheme.

*PAIL* (Prediction of Acetylation on Internal Lysines) is another method that uses empirical data from 249 experimentally proven acetylated lysines on 92 different proteins (Li et al., 2006). For prediction, they used Bayesian discriminant method and obtained accuracies as high as 89.21% at the highest threshold. *PAIL* algorithm has been validated by Jack-knife validation and *n*-fold (6-, 8-, and 10-fold) cross-validations, confirming its accuracy and robustness for predicting N $\epsilon$ -acetylation on lysines.

*ASEB* (acetylation set enrichment based), available as a computer program and webserver also uses experimentally validated 280 CBP/p300 and 84 GCN5/PCAF family of proteins with acetylated lysine sites (Li et al., 2012b, Wang et al., 2012). *ASEB* can predict novel acetylated sites based on their similarity with the known acetyl lysine in given protein sets. The method has also been both computationally and experimentally validated, suggesting it as a reliable method for prediction of acetyl lysine sites (Li et al., 2012a). Moreover, the webserver of *ASEB* provides additional features such as integration of protein–protein interaction information to enhance prediction accuracy (Li et al., 2014).

*BRBSB-PHKA* is another *in silico* online tool for Prediction of potential Human Lysine (K) Acetylation (PHKA) sites from protein sequences (Li et al., 2009). The bioinformatics approach is based on Bi-Relative Binomial Score Bayes (BRBSB) combined with support vector machines (SVMs). *BRBSB-PHKA* yields, on average, an accuracy of 85.58% in the case of 5-fold cross validation.

In a similar approach, *EnsemblePail* also predicts acetylation on internal lysines using SVM methodology (Xu et al., 2010). Its accuracy is 93.66% which is higher than *BRBSB-PHKA* in the case of 10-fold cross validation.

*PLMLA* is an online platform designed for prediction of potential lysine methylation and acetylation from protein sequences (Shi et al., 2012). In this method an encoding scheme based on grouped weight and position weight amino acid composition are applied to extract sequence information and physicochemical properties around lysine sites. *PLMLA* incorporates protein sequence information, secondary structure and amino acid properties. The prediction accuracy for acetyl lysine is 83.08%.

Another algorithm, *Predmod*, combines experimental methods with clustering analysis of protein sequences to predict acetylation based on the sequence characteristics of acetylated lysines within histones (Basu et al., 2009). *NetAcet* (Kiemer et al., 2005) and *N-Ace* (Lee et al., 2010) can also be used for prediction of acetylation sites. In particular *NetAcet* predicts N-terminal sites while *N-Ace* uses SVM algorithm to predict internal lysine acetylation.

Lastly, *LysAcet* (Li et al., 2009), which is possibly the most comprehensive algorithms for prediction acetyl lysine sites incorporates almost all currently available lysine acetylation data and uses SVM method. When compared with other methods or existing tools, *LysAcet* is the best predictor of lysine acetylation, with the highest K-fold (5- and 10-) and jackknife cross-validation accuracies.

### **2.2.9. FoldX calculations**

Protein design tool FoldX (version 3b51) was used to assess the impact of acetylation and deacetylation mimicry mutations on the stability of NFAT5-DNA complex (PDB entry: 1IMH) (Guerois et al., 2002, Schymkowitz et al., 2005a, Schymkowitz et al., 2005b). This tool predicts stability change in protein-DNA complex based on unfolding free energy difference ( $\Delta\Delta G$ ) between wild type and mutant structures. The 21 lysine residues predicted to be acetylated in the NFAT5-DNA complex (1IMH) were individually mutated to glutamine for acetylation mimicry and to arginine for deacetylation mimicry to reveal the impact of the acetylation/deacetylation on the intermolecular interactions. During calculations, the temperature was set to 310K and average of nine runs was used to compute the  $\Delta\Delta G$ . This method suggests that  $\Delta\Delta G$  values  $>0.5$  kcal/mol may be accepted as destabilizing mutations, whereas values  $<-0.5$  kcal/mol may be accepted as stabilizing

mutations.  $\Delta\Delta G$  values in between 0.5 and  $-0.5$  kcal/mol were suggested as insignificant change due to mutations. In line with these thresholds of the method, threshold of  $+0.5$  kcal/mol was used for selection of deacetylation favored lysines since  $\Delta\Delta G$  values lower than  $+0.5$  kcal/mol either had no effect or more stabilizing for NFAT5-DNA complex. Lysine to glutamine and lysine to arginine mutations has been previously used to mimic acetylated and deacetylated forms of lysine residues, respectively (Matsuzaki et al., 2005, Schwer et al., 2006).

### **2.2.10. Structure Preparation and Docking**

The crystal structures of NFAT5 (PDB entry: 1IMH Chain C), of p65 (PDB entry: 1NFI Chain A) and of SIRT1 (PDB entry: 4IG9 Chain A) were used for docking. First, acetyl group was inserted to lysine 200, 230, 241, 282, 373, and 431 of NFAT5 and lysine 310 of p65. Next, all NFAT5, p65 as well as SIRT1 structures were individually energy minimized in 20000 steps. The crystal waters and the metal ions found in the crystal structures were kept during docking. NFAT5 and p65 were used as the ligand while SIRT1 was kept as the receptor. Acetylated lysines and substrate binding site of SIRT1, phenylalanine 414 were defined as active residues. The initial poses for the NFAT5-SIRT1 and p65-SIRT1 complexes were determined using HADDOCK (version 2.1). This method predicts the dominant complexes of proteins with known 3D structures with support for a wide range of experimental data (de Vries et al., 2010). HADDOCK was used here because it can deal with side-chain and backbone flexibility, and thus performs better compared with other protein-protein docking algorithms (Moreira et al., 2010). The complex configurations obtained from docking were analyzed according to their clusters and HADDOCK scores. In choosing the final configuration of the complex, the structure in the top cluster with the highest HADDOCK score was selected, in which any atom of the acetylated lysines of NFAT5 and p65 resided within  $3 \text{ \AA}$  of any atom of F414 of SIRT1.

### **2.2.11. Molecular dynamics simulations**

Molecular dynamics (MD) simulations were performed using seven complex structures obtained from docking step. As the positive control, p65-SIRT1 complex was used in MD simulations. The NFAT5-SIRT1 complexes and p65-SIRT1 complex composed of 8722 and 9058 atoms were placed in water boxes with dimensions of 150x150x100 and 155x75x80 Å<sup>3</sup> respectively. Then the systems were ionized with a 100 mM NaCl solution to a neutral state. The resulting systems were used in MD simulations using the NAMD program (Phillips et al., 2005) with the CHARMM22 parameters (MacKerell et al., 1998, Brooks et al., 2009) which included correction map (CMAP) for backbone atoms (Feig et al., 2003, MacKerell et al., 2004). Water molecules within the system were treated explicitly using the TIP3P model (Jorgensen et al., 1983). An NpT ensemble was used in MD simulations with periodic boundary conditions, and the long-range Coulomb interactions were computed using the particle-mesh Ewald algorithm. Pressure was maintained at 1 atm and temperature was maintained at 310 K using the Langevin pressure and temperature coupling. A time step of 2 fs was used in all MD simulations. The systems were fully energy minimized in 20,000 steps and carefully equilibrated under constant temperature and volume for 0.5 ns. Then they were heated slowly from 10 K to 310 K in 30 ps before production runs. The production were lasted for 10 ns and repeated twice. Visual molecular dynamics (VMD) (Humphrey et al., 1996) was used for the analysis of trajectories and the visualization of structures. Root mean square displacements (RMSD) for the backbone atoms (C, N, C $\alpha$ ) and residue-wise root mean square fluctuations (RMSF) of C $\alpha$  atoms were measured and shown in Figures 3.15, 3.16 and 3.17.

### **2.2.12. Statistical Analysis**

All in vitro results were representative of at least three independent experiments. All numerical data were shown as mean  $\pm$  SEM. Statistical significance was analyzed with student's t-test. P values of <0.05 and <0.01 were shown as \* or \*\*, respectively.

### **2.2.13. Densitometric analysis**

Densitometric values for immunoblotting and EMSA analysis were calculated using Image J.

### **2.2.14. Illustrations**

All illustrations in all sections including Introduction, Results, Discussion and Conclusion were designed using Adobe Photoshop CS5 & CS6, Adobe illustrator CS5 & CS6, VMD and MS Office 2007 and 2010.

### **3. RESULTS**

#### **3.1. Osmotic stress model to study the role of SIRT1 on NFAT5**

##### **3.1.1. 16 hours of 100 mM NaCl treatment generates osmotic stress dependent intracellular stress**

Medium osmolality of RPMI 1640 was measured using an osmometer to validate the generation of hyperosmotic environment by addition of osmotic agents (Figure. 3.1). Results indicated that hyperosmotic environment can be generated using glucose, NaCl and mannitol.

An osmotic stress model that can simultaneously induce high expressions of intrinsic NFAT5 and SIRT1, was generated. To achieve this goal, two different agents, revealed to upregulate NFAT5 expression, 25 mM glucose and 100 mM NaCl, have been employed on U937 cells (Figures 3.2 and 3.3) (Yang et al., 2006, Hernandez-Ochoa et al., 2012, Kuper et al., 2012, Park et al., 2014, Quadri et al., 2014). The selection criteria were set as follows; a) osmotic stress dependent intracellular stress was present (Figure 3.2), b) osmotic stress dependent increased expressions of NFAT5 and SIRT1 were present (Figure 3.3). To differentiate for osmotic stress independent effects of the agents, osmotic control treatments were included in analysis (Figures 3.2 and 3.3).

Metabolic activity and cell death were examined at the 48<sup>th</sup> hour of osmotic stress in U937 cells for assessing osmotic stress dependent intracellular stress (Figure 3.2). 25 mM

glucose, but not its osmotic controls 12.5 mM NaCl and 25 mM mannitol, designated significantly higher metabolic activity (~30%) indicating that increased metabolic activity was independent of osmotic stress (Figure 3.2). 25 mM glucose or its osmotic controls demonstrated no significant change to cell death, as expected (Figure 3.2). 100 mM NaCl and its osmotic control, 200 mM mannitol displayed decreased metabolic activity, ~75% and ~22%, respectively (Figure 3.2). Cell death were also increased to ~22% in 100 mM NaCl treatment and to ~45% in its osmotic control group (Figure 3.2). Thus, exposing U937 cells to 100 mM NaCl for 48 hours, but not to 25 mM glucose, induced intracellular stress, in part due to osmotic stress.

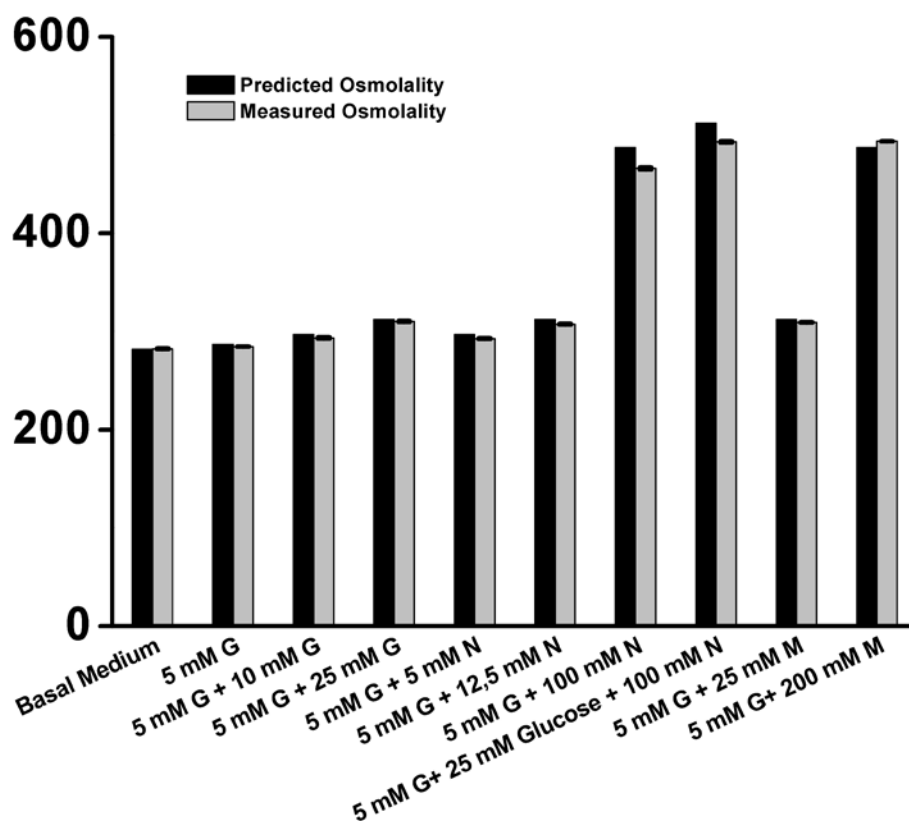


Figure 3.1. Measurement of osmolality of RPMI 1640 for validation of generation of hyperosmotic environment. Each solute was added to RPMI-1640 as in treatments and osmolality was measured using an osmometer. (G: Glucose; N: Sodium Chloride; M: Mannitol). Basal medium of RPMI 1640 without glucose had an osmolality of 282 mOsm/kg. Each solute added should have risen this osmolality to a predicted level (x-axis and black

bars). If the predicted osmolality matched the measured osmolality (gray), then it is concluded that the solute added medium is hyperosmotic to the basal medium. Addition of each solute is shown in x-axis. Y-axis shows the osmolality in mOsm/kg.

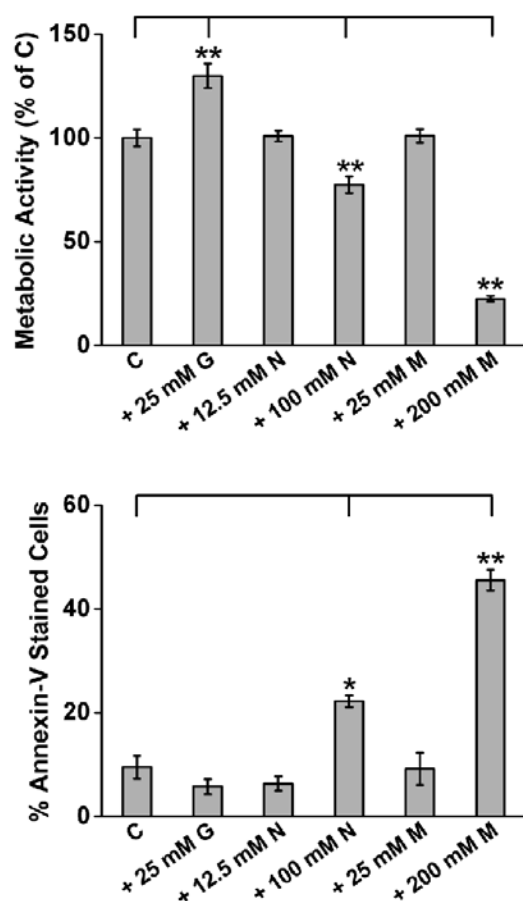


Figure 3.2. 48 hours of 100 mM NaCl treatment generates osmotic stress dependent intracellular stress. Control (C) refers to U937 cells treated with low glucose, serum free medium for 48 hours. Rest of the groups refers U937 cells treated with additional amount of the osmotic stress agent for 48 hours. (G: Glucose; N: Sodium Chloride; M: Mannitol). To differentiate osmotic stress independent effects of the osmotic stress inducers, 12.5 mM N and 25 mM M were used as osmotic controls for 25 mM G, whereas 200 mM M was used as osmotic control for 100 mM N. Data were expressed as mean  $\pm$  SEM,  $n=3$ , \* $p<0.05$ ; \*\* $p<0.01$ ; compared to control group. (Upper panel) 100 mM N, but not 25 mM G, diminished metabolic activity partly due to osmotic stress. Metabolic activity status was analyzed by MTT based colorimetric assay. Average absorbance values of the control were

set as 100%. (Lower panel) 100 mM N, but not 25 mM G, caused increased cell death partly due to osmotic stress. Cell death was analyzed by Annexin-V staining followed by flow cytometry.

### **3.1.2. 16 hours of 100 mM NaCl treatment simultaneously upregulates NFAT5 and SIRT1 in osmotic stress dependent manner**

For the second step of selection, NFAT5 and SIRT1 expressions were examined at the 48<sup>th</sup> hour after addition of each agent to U937 cells for assessing whether if osmotic stress dependent increased expressions of these proteins were present (Figure 3.3). 25 mM glucose, but not its osmotic controls induced NFAT5 expression, indicating this increase was independent of osmotic stress (Figure 3.3). Moreover, SIRT1 expression was undetectable after addition of 25 mM glucose or its osmotic controls (Figure 3.3) On the contrary, 100 mM NaCl or its osmotic control, increased expressions of NFAT5 and SIRT1, indicating that accumulation of these proteins was partly due to osmotic stress (Figure 3.3). As a result, 100 mM NaCl was selected as a convenient osmotic stress model for studying the role of SIRT1 on NFAT5.

Time dependent analysis for the osmotic stress model was conducted in U937 cells to select a time point in which peak expressions of NFAT5 and SIRT1 simultaneously took place (Figure 3.3). Since PARP1 was previously known to negatively regulate NFAT5 and SIRT1, expressions of PARP1 and its activator, SIRT6 were analyzed during this step to control our system against PARP-SIRT1 crosstalk (Chen et al., 2007, Mao et al., 2011, Kauppinen et al., 2013, Luna et al., 2013, Walko Iii et al., 2015). NFAT5 and SIRT1 bands were peaked at 16<sup>th</sup> hour, while at earlier time points of osmotic stress, they were faintly detectable (Figure 3.3). Upregulation of PARP1 and SIRT6 expressions coincided with that of NFAT5 and SIRT1 at 16<sup>th</sup> hour (Figure 3.3). Osmotic stress model induced similar expression trends for NFAT5, SIRT1, SIRT6 and PARP1, which all peaked at 16<sup>th</sup> hour. These trends indicated the possibility that NFAT5 dependent events may be under interplay of SIRT1 and PARP1 in this model. Nevertheless, 16<sup>th</sup> hour was selected for further studies due to simultaneous upregulation of NFAT5 and SIRT1.

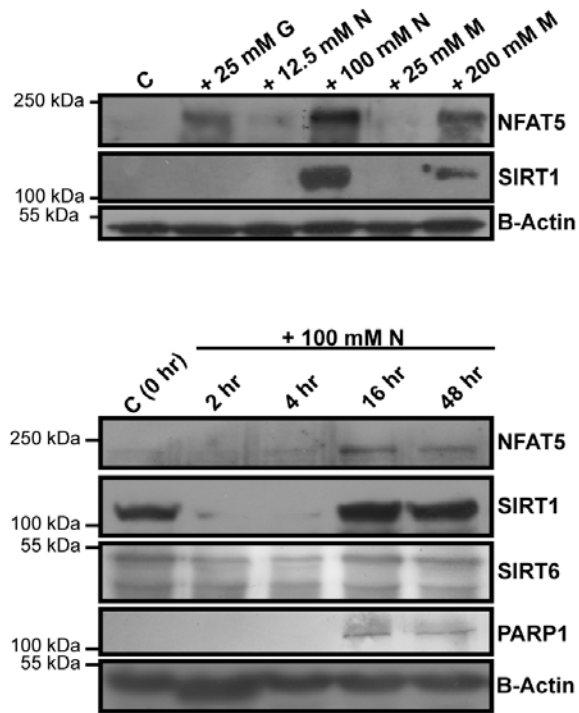


Figure 3.3. 16 hours of 100 mM NaCl treatment simultaneously upregulates NFAT5 and SIRT1 in osmotic stress dependent manner. Control (C) refers to U937 cells treated with low glucose, serum free medium for 48 hours in upper panel and for 0 hour in lower panel. Rest of the groups refers U937 cells treated with additional amount of the osmotic stress agent for 48 hours in upper panel and at indicated time points in lower panel (G: Glucose; N: Sodium Chloride; M: Mannitol). To differentiate osmotic stress independent effects of the osmotic stress inducers, 12.5 mM N and 25 mM M were used as osmotic controls for 25 mM G, whereas 200 mM M was used as osmotic control for 100 mM N. (Upper panel) 100 mM N was a suitable osmotic stress agent, but not 25 mM G, due to simultaneous upregulation of NFAT5 and SIRT1. Expressions were analyzed via immunoblotting of total protein extracts. (Lower panel) 16 hours of 100 mM N treatment increased expressions of NFAT5, SIRT1, SIRT6 and PARP1 simultaneously. Expressions were analyzed via immunoblotting of total proteins extracts.

## **3.2. SIRT1 activity contributes to AR expression during osmotic stress in U937 and HeLa cells**

### **3.2.1. Osmotic stress model dependent changes on intracellular NFAT5 and SIRT1 localizations, AR expression and oxidative stress generation**

After selection of type and timing of osmotic stress model, functionality of the model was questioned in terms of intracellular NFAT5 and SIRT1 localizations, AR expression and oxidative stress generation, as a downstream event of AR activity (Figures 3.4 and 3.5). In order to get more detailed insight on functionality; first, time course of intracellular localizations of NFAT5 and SIRT1 during osmotic stress in U937 cells were investigated. After 4 hours, NFAT5 expression was almost completely nuclear, whereas at later time points, it was concentrated more in cytoplasm, with declining trend in nucleus (Figure 3.4). Interestingly, SIRT1 was completely cytoplasmic at all-time points, with peaking at 16<sup>th</sup> hour, parallel to NFAT5 (Figure 3.4). Based on these data, it was clear that after 16 hours of osmotic stress, simultaneously increased but cytoplasmic expressions of NFAT5 and SIRT1 could be achieved (Figure 3.4).

Although, common intracellular localization may maximize the possibility of interaction between these proteins, it raised the question whether if NFAT5 was functional at this timing of osmotic stress. In order to elaborate the functionality of NFAT5, expression of its target protein, AR was examined at 4<sup>th</sup> and 16<sup>th</sup> hour of osmotic stress in U937 cells (Figure 3.5). AR expression increased at 4<sup>th</sup> hour compared to untreated control when NFAT5 was almost completely nuclear, whereas it was downregulated at 16<sup>th</sup> hour, parallel to increased cytoplasmic NFAT5 (Figures 3.4 and 3.5). To confirm downregulation of AR at 16<sup>th</sup> hour, oxidative stress levels were checked at 4<sup>th</sup> and 16<sup>th</sup> hour of osmotic stress in U937 cells (Figure 3.5). Parallel to expression patterns of AR, oxidative stress has increased at 4<sup>th</sup> hour compared to untreated control but declined at 16<sup>th</sup> hour of osmotic stress (Figure 3.5). Henceforth, our osmotic stress model consisted of increased cytoplasmic NFAT5 and SIRT1, decreased AR expression and decreased oxidative stress in U937 cells (Figures 3.4 and 3.5).

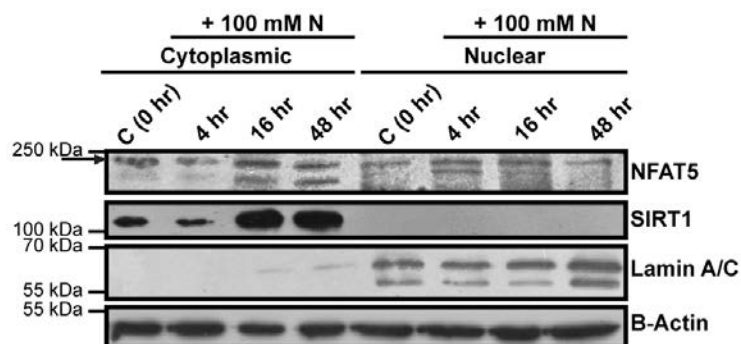


Figure 3.4. Osmotic stress dependent changes on intracellular NFAT5 and SIRT1 localizations. Control (C) group refers U937 cells treated with low glucose, serum free medium at indicated time points. 100 mM N refers to U937 cells treated with 100 mM NaCl (N), at indicated time points. Increased cytoplasmic NFAT5 and SIRT1 expression could be achieved after 16 hours of 100 mM N treatment. Expressions were analyzed via immunoblotting of cytoplasmic and nuclear extracts. Beta-Actin was used as cytoplasmic, whereas Lamin A/C was used as nuclear loading control.

### 3.2.2. SIRT1 activity promotes AR expression during 16 hours of 100 mM NaCl treatment in U937 cells

After functionality of the model was deciphered, the role of SIRT1 activity on AR expression was investigated. AR expressions under osmotic stress were examined using pharmacological inhibitor and activator of SIRT1 (Figure 3.6). AR expression was also studied using PARP1 inhibitor to check out crosstalk of PARP1 on this model (Figure 3.6). SIRT1 specific inhibitor, Ex-527 (10  $\mu$ M), downregulated, but SIRT1 activator, resveratrol (5 and 50  $\mu$ M) and PARP1 inhibitor, 3-aminobenzamide (1 mM), upregulated AR expression compared to the osmotic stress only control (Figure 3.6). It was apparent that SIRT1 activity promoted but PARP1 activity was inhibitory on the expression of AR in osmotic stress model.

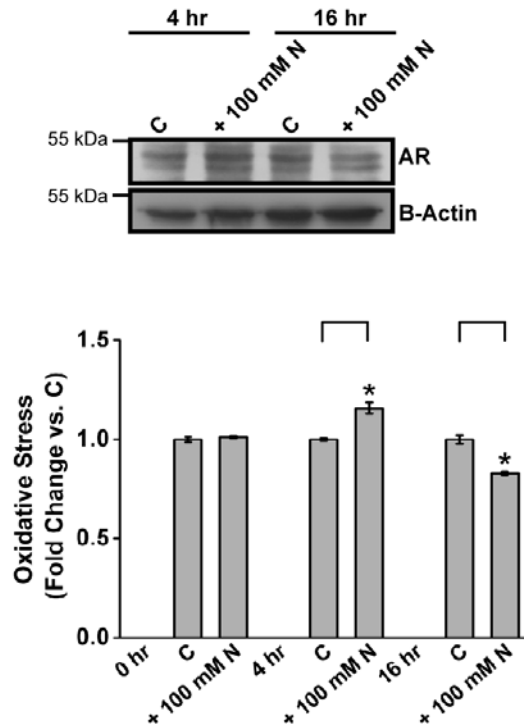


Figure 3.5. Osmotic stress dependent changes on AR expression and oxidative stress generation. Control (C) group refers U937 cells treated with low glucose, serum free medium at indicated time points. 100 mM N refers to U937 cells treated with 100 mM NaCl (N), at indicated time points. Data were expressed as mean  $\pm$  SEM,  $n=3$ , \* $p<0.05$ ; \*\* $p<0.01$  compared to control group in lower panel. (Upper panel) AR expression was downregulated after 16 hours of 100 mM N treatment. Expressions were analyzed via immunoblotting in total protein extracts. (Lower panel) Oxidative stress, downstream event of AR activity, was diminished after 16 hours of 100 mM N treatment. Oxidative stress was analyzed by DCFH-DA staining, followed by flow cytometry.

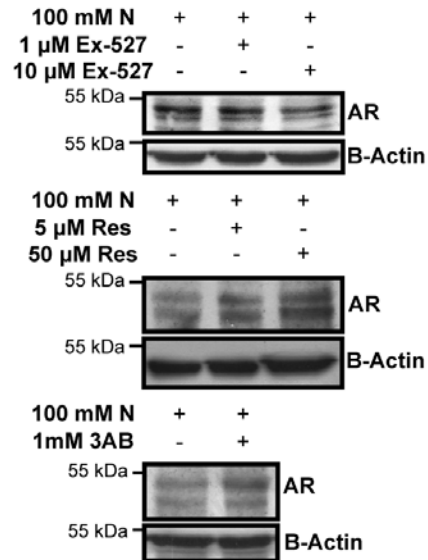


Figure 3.6. SIRT1 activity promotes AR expression during 16 hours of 100 mM NaCl treatment in U937 cells. 100 mM N refers to U937 cells treated with 100 mM NaCl for 16 hours. SIRT1 inhibitor (Ex-527), downregulated, but SIRT1 activator (Resveratrol: Res) and PARP1 inhibitor (3-aminobenzamide: 3AB) upregulated AR expression during 16 hours of 100 mM N treatment. U937 cells were pretreated with solvent or the pharmacological agent for 1 hour, followed by 16 hours of 100 mM N treatment. Expressions were analyzed via immunoblotting in total protein extracts.

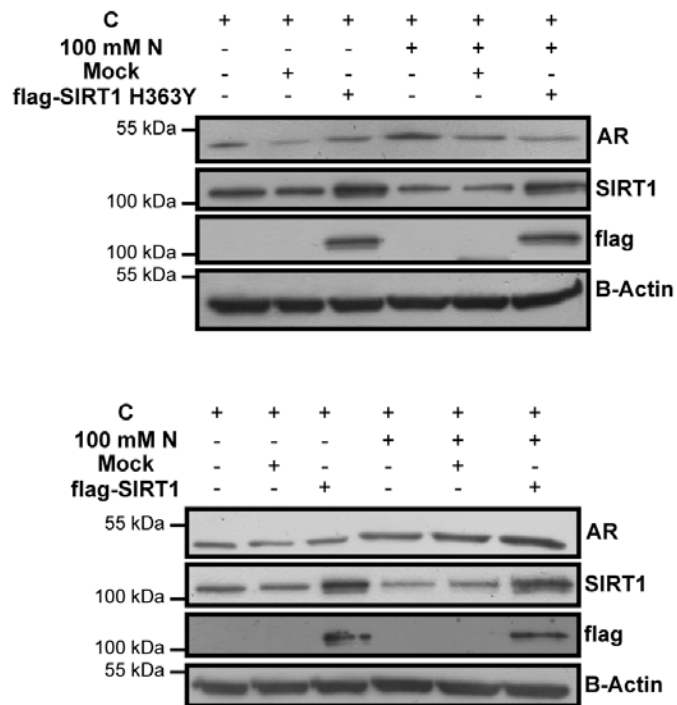


Figure 3.7. SIRT1 activity promotes AR expression during 16 hours of 100 mM NaCl treatment in HeLa cells. Control (C) group refers HeLa cells treated with low glucose, serum containing medium. 100 mM N refers to HeLa cells treated with 100 mM NaCl (N) for 16 hours. Overexpression of SIRT1 catalytic mutant (H363Y) downregulated, whereas overexpression of wild type SIRT1 upregulated AR expression in HeLa cells during 16 hours of 100 mM N treatment. HeLa cells were left untransfected or transfected either with mock (backbone plasmid) or with flag tagged SIRT1 (flag-SIRT1 H363Y in (upper panel) or with wild type flag-SIRT1 in (lower panel)). 24 hours post-transfection, these cells were either left untreated or treated further with 100 mM N for 16 hours. Expressions were analyzed via immunoblotting in total protein extracts. Expressions of SIRT1 and flag were used for confirmation of overexpression.

### **3.2.3. SIRT1 activity promotes AR expression during 16 hours of 100 mM NaCl treatment in HeLa cells**

For the purpose of validating the role SIRT1 activity on AR, analysis of AR expression was conducted during 16 hours of 100 mM NaCl treatment in HeLa cells overexpressing SIRT1 catalytic mutant (H363Y), as well as, its wildtype counterpart (Figure 3.7). In this cell line, 16 hours of osmotic stress displayed increased AR expression compared to untreated, untransfected control, unlike the response of U937 cells (Figure 3.7). Analogous to SIRT1 inhibition in U937 cells, overexpression of SIRT1 catalytic mutant under osmotic stress caused less AR expression compared to mock under osmotic stress. Comparable to the response of U937 cells to SIRT1 activation, overexpression of wildtype SIRT1 under osmotic stress resulted in even higher AR expression compared to mock under osmotic stress (Figure 3.7). This outcome was not apparent in HeLa cells under isosmotic conditions, indicating osmotic stress dependent modulation of AR expression by SIRT1 catalytic activity (Figure 3.7). Based on these findings, it was concluded that enzymatic activity of SIRT1 enhances AR expression in U937 and HeLa cells under osmotic stress.

### **3.3. SIRT1 activity enhances nuclear NFAT5 stabilization during osmotic stress in U937 and HeLa cells**

#### **3.3.1. SIRT1 activity augments stabilization of nuclear NFAT5 in U937 cells**

Given the observation that AR expression was regulated by pharmacological modulation of SIRT1 activity in the osmotic stress model, underlying mechanism of this regulation was explored by analyzing intracellular localization of NFAT5. Expression of nuclear NFAT5 was reduced in osmotic stress only group compared to untreated control in U937 cells, confirming the reduction of AR expression in this model (Figures. 3.5, 3.8 and 3.9). While low dose (1  $\mu$ M) Ex527, a specific SIRT1 inhibitor, lowered cytoplasmic and nuclear levels of NFAT5, high dose (10  $\mu$ M) of Ex527 further decreased cytoplasmic NFAT5 with completely abolishing nuclear NFAT5 (Figure 3.8). Low dose (5  $\mu$ M) or high dose (50

$\mu\text{M}$ ) of resveratrol, a widely accepted SIRT1 activator, decreased cytoplasmic NFAT5, while increasing nuclear NFAT5 stabilization (Figure 3.8). Inhibiting PARP1 via 3-aminobenzamide (3AB) with low (1mM) or high (2 mM) doses also induced almost complete translocation of NFAT5 to nucleus in this model (Figure 3.9). These observations clearly indicated that SIRT1 activity promotes, while PARP1 activity suppresses nuclear accumulation of NFAT5 in osmotic stress model, confirming the AR expression patterns obtained with these agents (Figures. 3.6, 3.8 and 3.9).

Inhibiting SIRT1 with Ex527 caused higher SIRT1 expression, but activating SIRT1 with resveratrol, or inhibiting PARP1 resulted in lower SIRT1 expression (Figures 3.8 and 3.9). This findings also indicated that the possibility that SIRT1 activity may regulate its own expression within the osmotic stress model.

### **3.3.2. SIRT1 activity augments stabilization of nuclear NFAT5 in HeLa cells**

For confirming of the role of SIRT1 activity on stabilization of nuclear NFAT5, localization of NFAT5 was also examined under 16 hours of osmotic stress in HeLa cells overexpressing SIRT1 catalytic mutant (H363Y), as well as, its wildtype counterpart (Figure 3.9). Osmotic stress increased nuclear NFAT5 expression compared to untreated mock control in HeLa cells, confirming the upregulation of AR expression in this cell line (Figures 3.7 and 3.9). Overexpression of SIRT1 catalytic mutant under osmotic stress showed less NFAT5 expression in nucleus compared to mock under osmotic stress (Figure 3.9). On contrary, overexpression of wildtype SIRT1 under osmotic stress displayed similar nuclear NFAT5 expression compared to mock under osmotic stress (Figure 3.9). These results clearly validated the AR expression patterns observed with these overexpression plasmids under osmotic stress (Figure 3.7). Hence, it was established that enzymatic activity of SIRT1 contributed to nuclear stabilization of NFAT5 in U937 and HeLa cells under 16 hours of osmotic stress.

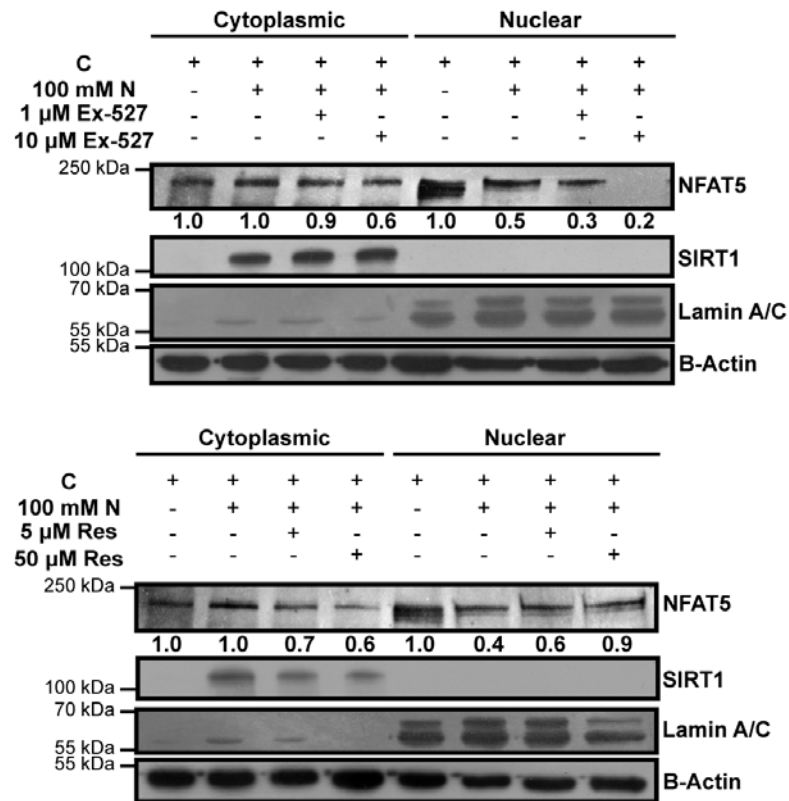


Figure 3.8. SIRT1 activity augments stabilization of nuclear NFAT5 in U937 during 16 hours 100 mM N treatment. Control (C) refers U937 cells treated with low glucose, serum free medium for 16 hours. 100 mM N refers to U937 cells treated with 100 mM NaCl (N) for 16 hours. U937 cells were pretreated either with solvent or pharmacological agent for 1 hour, followed by 16 hours of 100 mM N treatment. Expressions were analyzed via immunoblotting in cytoplasmic and nuclear extracts. Each NFAT5 band was analyzed by densitometry and normalized using Beta-Actin bands for cytoplasmic and Lamin A/C band for nuclear expressions. Normalized intensity of control NFAT5 bands in cytoplasm or nucleus were set to 1 for comparison to other groups. (Upper panel) Specific SIRT1 inhibitor, Ex-527 suppressed nuclear NFAT5 stabilization, while upregulating SIRT1 expression under osmotic stress. (Lower panel) SIRT1 activator, resveratrol, induced higher nuclear NFAT5 expression, while decreasing SIRT1 expression under osmotic stress.

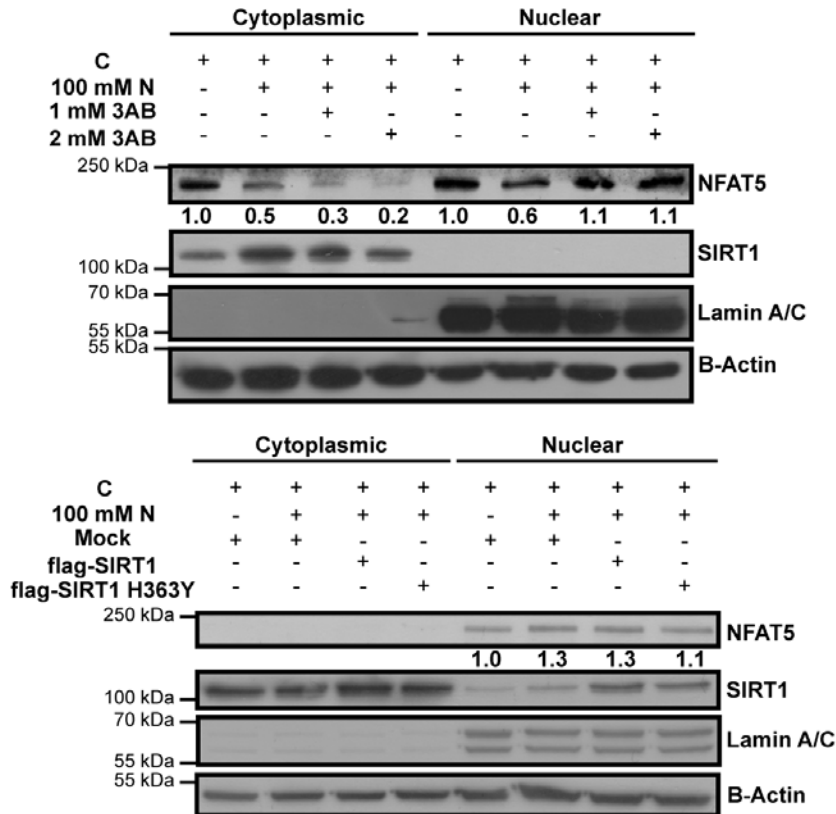


Figure 3.9. Validation of SIRT1 based stabilization of nuclear NFAT5 in U937 and HeLa cells during 16 hours 100 mM N treatment. Control (C) refers U937 cells treated with low glucose, serum free medium for 16 hours in upper panel. 100 mM N refers to U937 cells treated with 100 mM NaCl (N) for 16 hours in upper panel. U937 cells were pretreated either with solvent or pharmacological agent for 1 hour, followed by 16 hours of 100 mM N treatment in upper panel. Expressions were analyzed via immunoblotting in cytoplasmic and nuclear extracts. Each NFAT5 band was analyzed by densitometry and normalized using Beta-Actin bands for cytoplasmic and Lamin A/C band for nuclear expressions. Normalized intensity of control NFAT5 bands in cytoplasm or nucleus were set to 1 for comparison to other groups. (Upper panel) Inhibition of PARP1 with 3-aminobenzamide (3AB) promotes translocation of NFAT5 to nucleus, while decreasing SIRT1 expression. Control (C) group refers HeLa cells treated with low glucose, serum containing medium in lower panel. 100 mM N refers HeLa cells treated with 100 mM NaCl (N) for 16 hours in lower panel. (Lower panel) Overexpression of SIRT1 catalytic mutant (H363Y) suppressed, whereas overexpression of wild type SIRT1 displayed similar nuclear NFAT5 expression in HeLa cells during 16 hours

of 100 mM N treatment. HeLa cells were transfected either with mock or with flag-SIRT1 H363Y or with wild type flag-SIRT1. 24 hours post-transfection, these cells were treated further with 100 mM N for 16 hours. Control group was also mock transfected, left untreated and was used as negative control of 16 hours of 100 mM N treatment in lower panel. Expressions were analyzed via immunoblotting in cytoplasmic and nuclear extracts. Expression of SIRT1 was used for confirmation of overexpression.

### **3.4. Enzymatic activity of SIRT1 regulates myc-NFAT5 induced AR expression through stabilizing nuclear NFAT5 and allowing more NFAT5 to bind AR ORE in HeLa cells**

#### **3.4.1. myc-NFAT5 induced AR expression was regulated by SIRT1 activity in HeLa cells**

In order to confirm the role of SIRT1 activity on AR expression, myc-NFAT5 alone or either with wildtype SIRT1 or with catalytic mutant of SIRT1 (H363Y) were overexpressed in HeLa cells and AR expression was inspected (Figure 3.10). Overexpression of myc-NFAT5 induced higher AR expression compared to mock only control (Figure 3.10). Overexpression myc-NFAT5 with wildtype SIRT1 had higher AR expression compared to overexpression of myc-NFAT5 with catalytically inactive SIRT1 (Figure 3.10). In the light of these results, contribution of SIRT1 activity to AR expression was validated.

#### **3.4.2. Stabilization nuclear of myc-NFAT5 expression was regulated by SIRT1 activity in HeLa cells**

Subsequently, with the purpose of confirming the role of SIRT1 on nuclear stabilization of NFAT5, myc-NFAT5 alone or either with wildtype SIRT1 or with catalytic mutant of SIRT1 were overexpressed in HeLa cells and intracellular NFAT5 localization was examined (Figure 3.11). Overexpression of NFAT5 alone or with wildtype SIRT1 had higher NFAT5 accumulation in nucleus compared to mock control (Figure 3.11). Overexpression of myc-NFAT5 with catalytically inactive SIRT1 displayed diminished NFAT5 expression

in nucleus compared to overexpression of NFAT5 alone or to overexpression of NFAT5 with wildtype SIRT1, validating that SIRT1 activity acts as a stabilizer for nuclear of NFAT5 expression (Figure 3.11).

### **3.4.3. DNA binding of myc-NFAT5 to AR ORE was regulated by SIRT1 activity in HeLa cells**

In order to directly link the role of SIRT1 activity to AR expression and to stabilization of nuclear NFAT5, EMSA was performed to examine myc-NFAT5 binding to AR ORE using co-transfection of NFAT5 and SIRT1 in HeLa cells. Specific band that corresponds to myc-NFAT5-ORE complex was identified by using overexpression of myc-NFAT5, supershift analysis and specific competitor (Figure 3.12). This band displayed higher intensity when myc-NFAT5 was overexpressed with wildtype flag SIRT1 compared to overexpression of myc-NFAT5 alone (Figure 3.12, lower panel, lane 2 and 3). Overexpression of myc-NFAT5 with catalytically inactive SIRT1 showed lower intensity band compared to the overexpression of NFAT5 alone (Figure 3.12, lower panel, lane 2 and 4). It was evident that SIRT1 activity stabilized nuclear of NFAT5 and allowed for more NFAT5 to bind to AR ORE region, which ended up with higher AR expression.

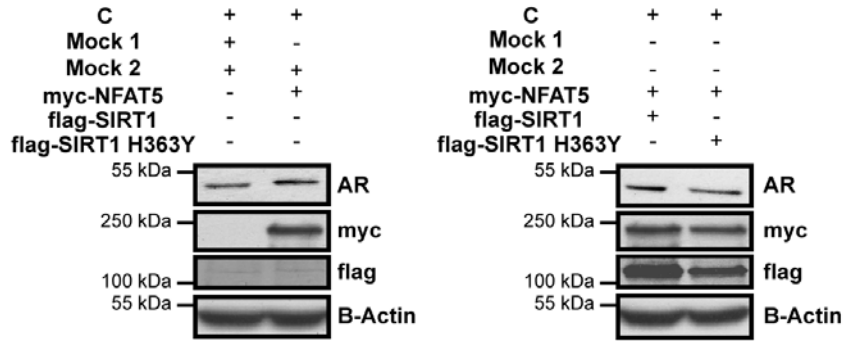


Figure 3.10. myc-NFAT5 induced AR expression was regulated by SIRT1 activity in HeLa cells. Control (C) refers HeLa cells treated with low glucose, serum containing medium. Mock 1 refers to the backbone plasmid of myc-NFAT5, whereas mock 2 refers to the backbone plasmid of flag-SIRT1 (wildtype) and flag-SIRT1 H363Y (catalytically inactive mutant). (Left panel) Overexpression of myc-NFAT5 induced higher AR expression compared to mock. HeLa cells were co-transfected either with mock 1 and mock2 or with myc-NFAT5 with mock 2. 24 hours post transfection, cells were lysed into total protein extracts and expression were via immunoblotting. Expression of myc was used for confirmation of overexpression. Lack of flag expression was shown to confirm that no flag tagged SIRT1 was present in these groups. (Right panel) Overexpression of myc-NFAT with catalytically inactive SIRT1 displayed diminished AR expression compared to overexpression of myc-NFAT5 with wildtype SIRT1. HeLa cells were co-transfected with myc-NFAT5 and wildtype flag SIRT1 or with myc-NFAT5 and flag SIRT1 H363Y. 24 hours post transfection, cells were lysed into total protein extracts and expressions were analyzed via immunoblotting. Expression of myc and flag was used for confirmation of overexpression.

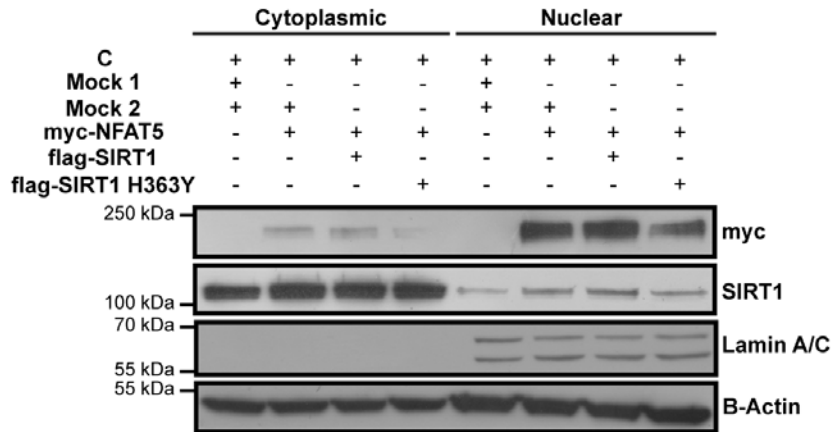


Figure 3.11. Stabilization nuclear of myc-NFAT5 expression was regulated by SIRT1 activity in HeLa cells. Control (C) refers HeLa cells treated with low glucose, serum containing medium. Mock 1 refers to the backbone plasmid of myc-NFAT5, whereas mock 2 refers to the backbone plasmid of flag-SIRT1 (wildtype) and flag-SIRT1 H363Y (catalytically inactive mutant). Overexpression myc-NFAT5 with catalytically inactive SIRT1 showed less nuclear of myc-NFAT5 expression compared to overexpression of myc-NFAT5 alone or to overexpression of myc-NFAT5 with wildtype SIRT1. HeLa cells were transfected with mock 1 and mock 2 (lanes 1 and 5) or with myc-NFAT5 and mock 2 (lanes 2 and 6) or with myc-NFAT5 and flag-SIRT1 (lanes 3 and 7) or with myc-NFAT5 and flag-SIRT1 H363Y (lanes 4 and 8). 24 hours post transfection, cells were lysed into cytoplasmic and nuclear fractions and expressions were analyzed via immunoblotting. Beta-Actin and Lamin A/C were used as loading controls. Expression of myc and SIRT1 were used for confirmation of overexpression.

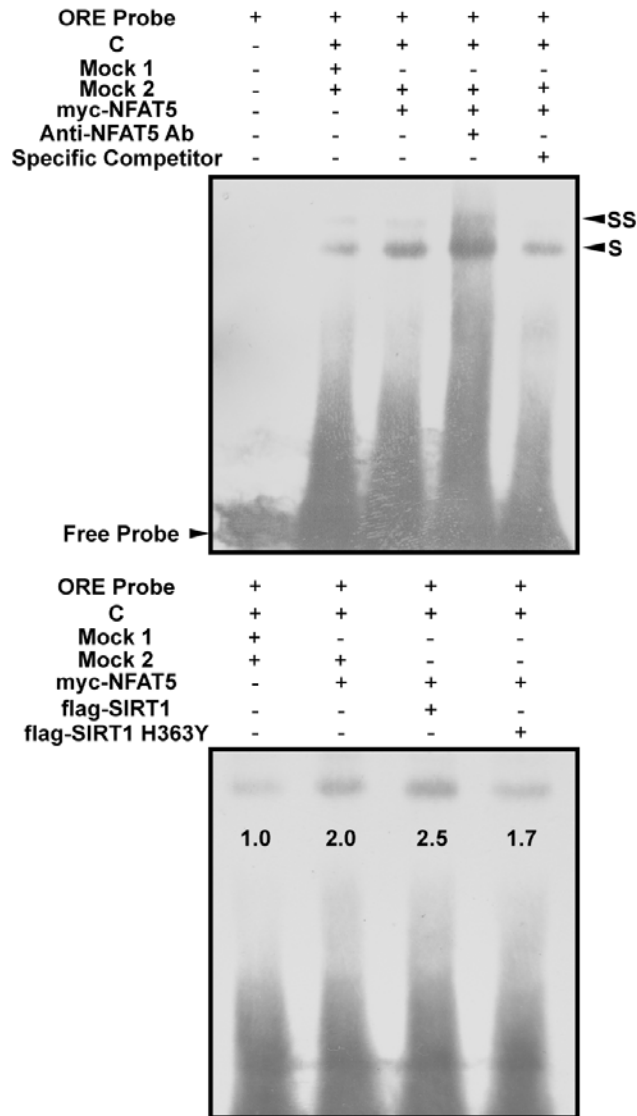


Figure 3.12. DNA binding of myc-NFAT5 to AR ORE was regulated by SIRT1 activity in HeLa cells. Control (C) refers HeLa cells treated with low glucose, serum containing medium. Mock 1 refers to the backbone plasmid of myc-NFAT5, whereas mock 2 refers to the backbone plasmid of flag-SIRT1 (wildtype) and flag-SIRT1 H363Y (catalytically inactive mutant). (Upper panel) myc-NFAT5 binds specifically to AR ORE probe. HeLa cells were transfected with mock 1 and mock 2 (lane 2) or with myc-NFAT5 and mock 2 (lanes 3, 4 and 5). 24 hours post transfection, cells were lysed into total protein extracts and analyzed by EMSA for NFAT5-ORE complex formation. Specificity of the band was assessed by increased intensity due to overexpression of NFAT5 (shown by shift: S) (lane 2), by increased supershift (SS) caused by NFAT5 antibody and elimination of the shift by 40X unlabeled

specific competitor. (Lower panel) Overexpression of myc-NFAT5 with wildtype flag-SIRT1 increased myc-NFAT5-ORE binding, whereas overexpression of myc-NFAT5 with inactive flag-SIRT1 H363Y diminished it. HeLa cells were transfected as in Figure 3.11. 24 hours post transfection, cell were lysed into total protein extracts and analyzed by EMSA for NFAT5-ORE complex formation. For binding analysis, intensities of each specific band were calculated compared to mock control, which was set to 1. Relative intensities were shown below each band.

### **3.5. 16 hours of osmotic stress disrupts the interaction of NFAT5 with SIRT1, but enhances its acetylated lysine status and interaction with PARP1 in U937 cells**

Acetylated lysine status and interactions of NFAT5 containing complex with SIRT1 and PARP1 were examined using co-immunoprecipitation experiments in order to define the underlying mechanism of osmotic stress model of U937 cells. Osmotic stress model disrupted the interaction of NFAT5 containing complex with SIRT1, increased its acetylated lysine status and its interaction with PARP1, indicating that SIRT1 activity was reduced on NFAT5 containing complex (Figure 3.13). In order to confirm that interaction of NFAT5 containing complex with SIRT1 was disrupted, reciprocal co-immunoprecipitation was conducted with SIRT1 antibody, which in turn also displayed diminished NFAT5-SIRT1 interaction (Figure 3.13). This data validated that reduced of AR expression and decreased stabilization of nuclear NFAT5 observed after 16 hours of osmotic stress treatment in U937 cells was due to reduced availability of SIRT1 in NFAT5 containing complex. Moreover, since NFAT5 interaction with PARP1 increased in the osmotic stress model, nuclear translocation of NFAT5 might be regulated by poly-ADP-ribosylation.

Following *in vitro* experiments, *in silico* analysis was conducted to understand if NFAT5 is a direct target of SIRT1. Acetylated lysines of NFAT5 were predicted using ten different algorithms. Using Foldx based stability analysis, the deacetylation favored lysines of NFAT5 that increase the stability of NFAT5-DNA complex, were selected. MD simulations were employed to comprehend if these deacetylation favored lysines could be targeted by SIRT1 substrate binding site.

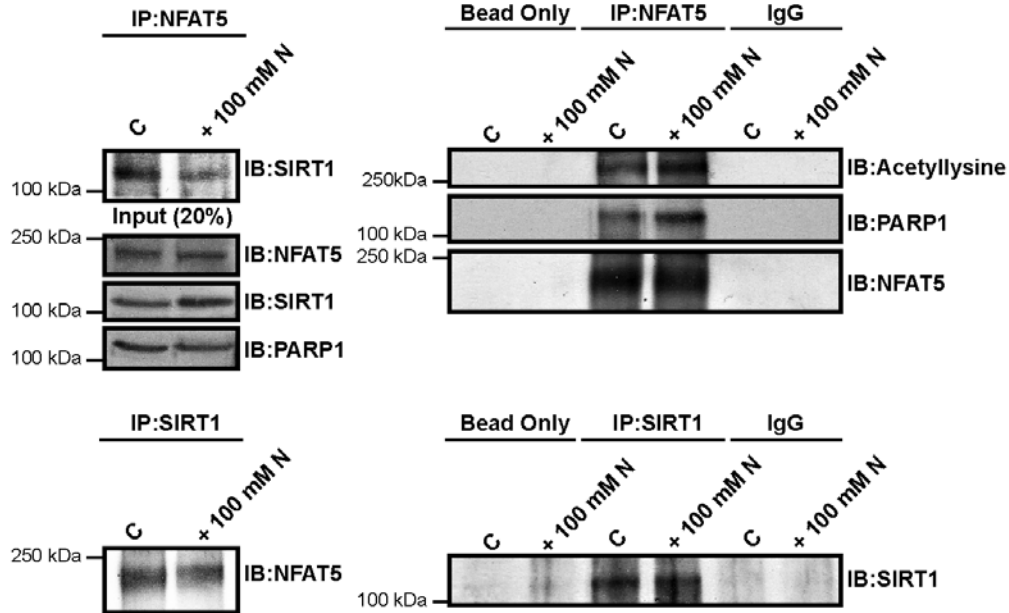


Figure 3.13. 16 hours of osmotic stress weakened the interaction of NFAT5 containing complex with SIRT1, but increased its acetylated lysine status and its interaction with PARP1. Control (C) refers U937 cells treated with low glucose, serum free medium for 16 hours. 100 mM N refers to U937 cells treated with 100 mM NaCl (N) for 16 hours. Input refers to pre-ip immunoblots in which 20% of protein used for immunoprecipitation was analyzed for presence of the interacting partners. (Upper panel) 16 hours of osmotic stress diminished NFAT5-SIRT1 interaction but enhanced acetylated lysine status of NFAT5 and NFAT5-PARP1 interaction. Cells were either left untreated or treated 16 hours with 100 mM N, followed by lysis into total protein extracts. 1  $\mu$ g of NFAT5 antibody was used to immunoprecipitate NFAT5 containing complexes from 500  $\mu$ g of total protein lysate (IP: NFAT5). Immunoprecipitates were then immunoblotted for presence of the targets (IB), using SIRT1, Acetyl-lysine, PARP1 and NFAT5 antibodies. (Lower panel) Reciprocal co-immunoprecipitation confirmed that 16 hours of osmotic stress diminished SIRT1-NFAT5 interaction. Cells were either left untreated or treated 16 hours with 100 mM N, followed by lysis into total protein extracts. 3  $\mu$ g of SIRT1 antibody was used to immunoprecipitate SIRT1 containing complexes from 1000  $\mu$ g of total protein lysate (IP: SIRT1). Immunoprecipitates were then immunoblotted for presence of the targets (IB), using NFAT5 and SIRT1 antibodies. “Bead only” was used to indicate negative control, in which only

beads were used for immunoprecipitation. “IgG” was used to indicate negative control, in which beads and irrelevant antibody was used for immunoprecipitation.

### **3.6. In silico prediction of deacetylated lysines of NFAT5 that stabilize NFAT5-DNA complex**

Since NFAT5 containing complex was identified as a target of SIRT1's deacetylation activity, lysine residues that contribute to stability of NFAT5-DNA complex were investigated. Because only acetylated lysine residues were substrates for deacetylation reaction, possible acetylated lysine residues of NFAT5 were predicted (Table 3.1). Using 10 different algorithms that has been previously developed, 21 of 22 lysine residues of NFAT5 (PDB ID: 1IMH Chain C sequence) were identified to be prone to acetylation (Table 3.1). Acetylation status of these 21 lysine residues were examined in terms of their contribution to the stability of NFAT5-DNA complex. In order to inspect this contribution, these lysines were mutated to glutamine for acetylated lysine mimicry or to arginine for deacetylated lysine mimicry in both monomers of NFAT5 that were bound to target DNA (PDB ID: 1IMH). Stability change of NFAT5-DNA complex due to these mutations was calculated using Foldx method (Figure 3.14). Lysine residues that showed higher  $\Delta\Delta G$  values than +0.5 kcal/mol when converted to glutamine and lower  $\Delta\Delta G$  values than +0.5 kcal/mol when converted to arginine in both NFAT5 monomers were accepted as deacetylation favorable lysine residues (Figure 3.14.). These residues, when kept as deacetylated, maintained or enhanced stability of NFAT5-DNA complex. Given this threshold, lysines at positions 200, 230, 241, 282, 373, and 431 were selected as deacetylation favored lysines of NFAT5 (Figure 3.14).

With the purpose of revealing if these selected lysines were direct targets of SIRT1's deacetylation activity, acetylated lysines were inserted to these selected sites of NFAT5. These acetylated structures were docked to SIRT1 substrate binding site and MD simulations were performed.

<b>1IMH Position #</b>	188	189	200	204	207	230	241	263	282	313	329	330	331	346	373	374	382	392	396	399	431	
Algorithm																						
KacePred <sup>1</sup>					+						+		+								+	
PAIL <sup>2</sup>	+	+	+	+	+	+	+		+		+	+	+		+	+	+		+			
ASEB (CBP/p300) <sup>3</sup>		+				+					+									+		
ASEB (GCN5/PCAF) <sup>3</sup>						+					+											
ASEB (HDAC) <sup>3</sup>						+					+											
Predmod <sup>4</sup>				+		+		+				+	+						+			
BRABSB-PHKA <sup>5</sup>					+				+					+	+	+		+	+			
PSKAcePred <sup>6</sup>				+	+		+	+			+	+	+	+	+	+	+		+	+		
PLMLA <sup>7</sup>				+				+		+				+			+	+	+	+		
PHOSIDA <sup>8</sup>			+	+		+				+							+	+	+			
EnsemblePail <sup>9</sup>			+	+							+				+	+					+	
Lys Acet <sup>10</sup>			+	+		+				+	+	+	+	+	+	+						+

Table 3. 1. Results of acetylated lysine predictions. Possible acetylated lysines of NFAT5 were predicted using ten different algorithms, which names were given in the first column. For prediction, primary amino acid sequence of chain C of NFAT5 structure (PDB ID: 1IMH) were used. The numbers in the first row were used to represent the positions of lysine residues found in NFAT5. The superscripts given as below indicate the threshold values used for prediction algorithms.

<sup>1</sup> Specificity cutoff of 70% was used. <sup>2, 5, 6, 7</sup> Threshold of 0.5 was used. <sup>3</sup> Threshold of <10% was used. <sup>4, 9</sup> High threshold setting was used. <sup>8</sup> Precision (75%) and recall (80%) was used for selection. <sup>10</sup> Linear function and couple features coding scheme was used for selection.

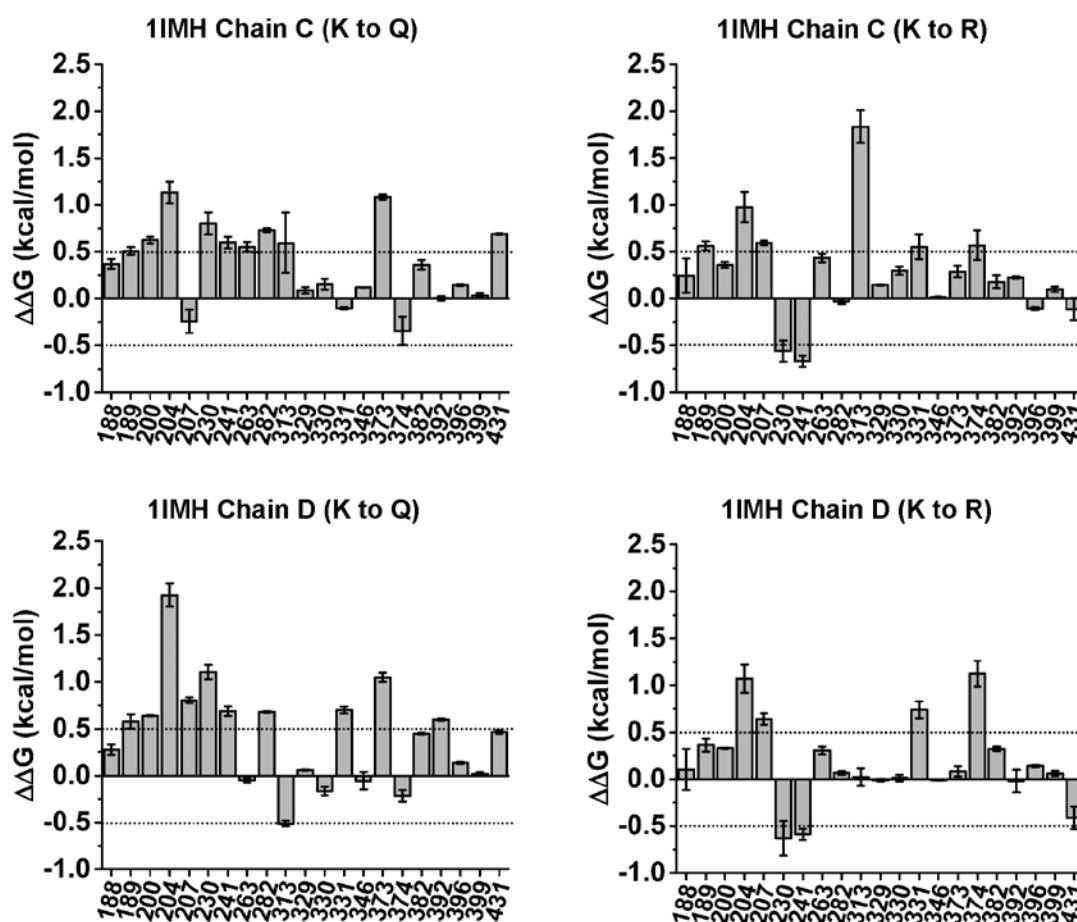


Figure 3.14. Acetylation and deacetylation mimicry mutations of NFAT5 lysine residues regulate the stability of NFAT5-DNA complex. After prediction of possible acetylated lysines of NFAT5 (Table 3.1), each of these predicted lysine residues were converted to glutamine or arginine in both NFAT5 monomers of available NFAT5-DNA complex structure (PDB ID: 1IMH Chain C and Chain D). Lysine (K) to glutamine (Q) mutations were used for acetylated lysine mimicry, whereas lysine to arginine (R) mutations were used for deacetylated lysine mimicry. After each mutation, stability change of NFAT5-DNA complex was calculated using Foldx method, to obtain  $\Delta\Delta G$  values between mutant and wild type structures. Dotted lines at 0.5 and -0.5 kcal/mol  $\Delta\Delta G$  values were used to represent error margins of Foldx method. Lysine residues 200, 230, 241, 282, 373, and 431 showed values higher than +0.5 kcal/mol when mutated to glutamine, whereas they designated values less than +0.5 kcal/mole when converted to arginine, in both monomers of NFAT5 indicating these lysine were more favorable for stability of NFAT5-DNA complex, when kept as

deacetylated. X-axis in all plots indicates position of each lysine in NFAT5-DNA complex structure (PDB ID: 1IMH).

### 3.7. In silico prediction of lysine 282 of NFAT5 as a potential SIRT1 target site

After identification of lysine sites that were favored in deacetylated status, these sites were investigated as possible targets of SIRT1 substrate binding site, using docking and MD simulations (Figures 3.15, 3.16, 3.17, 3.18, 3.19 and 3.20). The selected lysines of NFAT5 (200, 230, 241, 282, 373 and 431) were first acetylated *in silico*. Next, to obtain NFAT5-SIRT1 complexes, these acetylated lysine (AK) containing NFAT5 structures were docked to SIRT1 phenylalanine (F) 414, which has been previously shown for its substrate binding function (Cosgrove et al., 2006, Davenport et al., 2014). For positive control, p65, a previously known SIRT1 target from its K310 were utilized and similarly, AK310 of p65 was docked to F414 of SIRT1 (Yeung et al., 2004). For all these complexes, MD simulations for 10 ns were used and RMSD and RMSF of backbone atoms for stability and flexibility analysis were calculated, respectively (Figures 3.15, 3.16, 3.17). The distance between AK to F414 and RMSF of AK and F414 atoms for *in silico* assessment of binding of AKs in NFAT5 to SIRT1's substrate binding site, were also investigated (Figures 3.18, 3.19, 3.20).

RMSD of backbone atoms converged to a plateau in all simulations, which oscillated in between 2-3 Å range of p65-SIRT1 complex, suggesting that these complexes were stable throughout simulations and were acceptable for data collection (Figure 3.15). According to C $\alpha$  atom fluctuations, AK230, AK241, AK282 and AK373 containing NFAT5-SIRT1 complexes displayed similar flexibility (<6 Å) to p65-SIRT1 complex (Figure 3.16). This similarity in C $\alpha$  atom fluctuations was less pronounced in AK200 and AK431 containing NFAT5-SIRT1 complexes, which have shown higher RMSF values for C $\alpha$  atoms (>6 Å) in residues distant from AK, compared to that of p65 (Figure 3.16). RMSF of C $\alpha$  atoms of SIRT1 in all complexes were almost similar to each other, indicating similar SIRT1 flexibility in all simulations (Figure 3.17). In particular, docked residues (AK200, AK230, AK241, AK282, AK373, AK431 of NFAT5, AK310 of p65 and F414 of SIRT1) showed fluctuations only within limits of 3 Å, implying less mobility in these residues (Figures 3.16

and 3.17). RMSF analysis pointed out that SIRT1 binding decreased mobility of AK residues both in NFAT5 and positive control p65, indicating that the docked residues stay bound to SIRT1 for 10 ns of MD simulations.

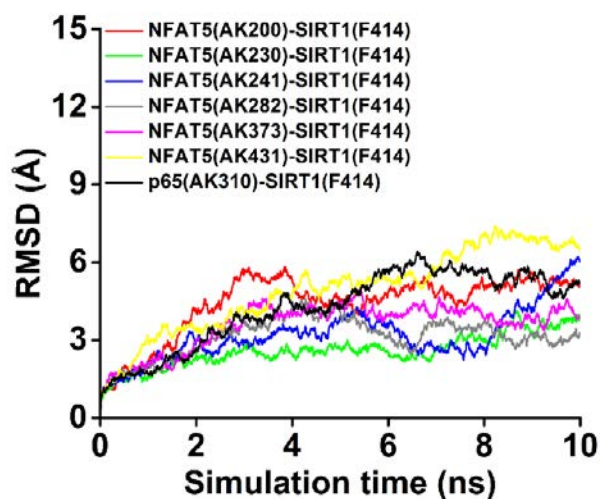


Figure 3.15. RMSD of backbone atoms of p65(AK)-SIRT1(F414) and all NFAT5(AK)-SIRT1 (F414) complexes were calculated from 10 ns of MD simulations, depicted in legend.

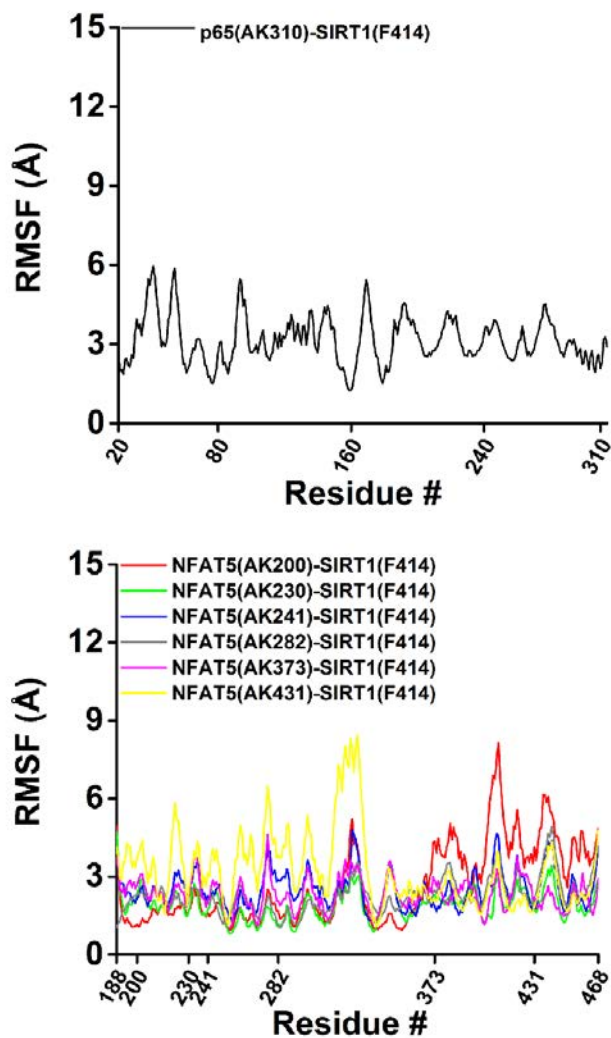


Figure 3.16. RMSF of Ca atoms of p65 in p65(AK)-SIRT1(F414) complex and NFAT5 in all NFAT5(AK)-SIRT1(F414) complexes were calculated from 10 ns of MD simulations, depicted in legends.

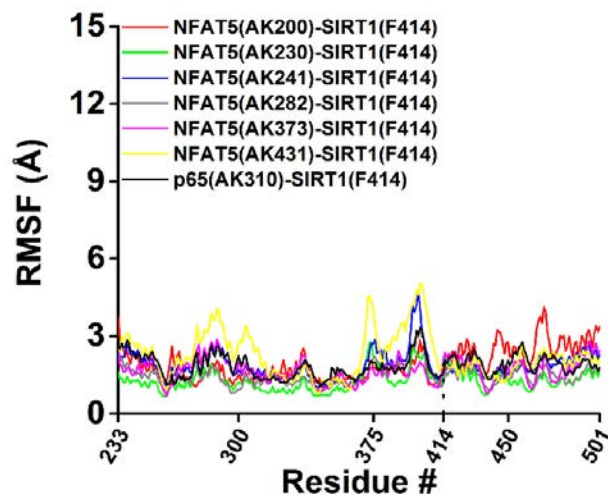


Figure 3.17. RMSF of C $\alpha$  atoms of SIRT1 in p65(AK)-SIRT1(F414) complex and in all NFAT5(AK)-SIRT1(F414) complexes were calculated from 10 ns of MD simulations, depicted in legend.

For *in silico* ranking of AKs of NFAT5 as targets of SIRT1 binding site, distance between AK of NFAT5 to F414 of SIRT1, all atom RMSF of AK and RMSF of F414 of SIRT1 were calculated (Figures 3.18 and 3.19). Only distances between AK373-F414 and AK282-F414 were similar to the distance formed in positive control ( $\sim 6$  Å), proposing these sites as possible targets of SIRT1 binding (Figure 3.18). All atom fluctuations of AK373 and AK282 were also very similar to those observed for AK310 of p65 (Figure 3.19). Among these AK residues, AK 282 had even lower flexibility than the AK of the positive control (Figure 3.19). F414 of SIRT1 in AK282 containing complex also displayed lower fluctuations compared to those observed in positive control (Figure 3.19). The orientation of AK282 to F414 were comparable to that observed for AK 310 of p65 (Figure 3.20). These observations suggested that AK 282 followed by AK 373 as potential substrates for deacetylation reaction catalyzed by SIRT1.

Overall, AK282 of NFAT5 could be considered as a potential SIRT1 target site, since its distance, flexibility and orientation to SIRT1 substrate binding residue was almost completely similar to that of AK 310 of p65 (Figures 3.18, 3.19 and 3.20). Hence, given this *in silico* evidence it is considered that SIRT1 induces a stable DNA binding activity for target

gene expression, possibly through deacetylating one or several lysine in NFAT5, with K282 being the most plausible candidate.

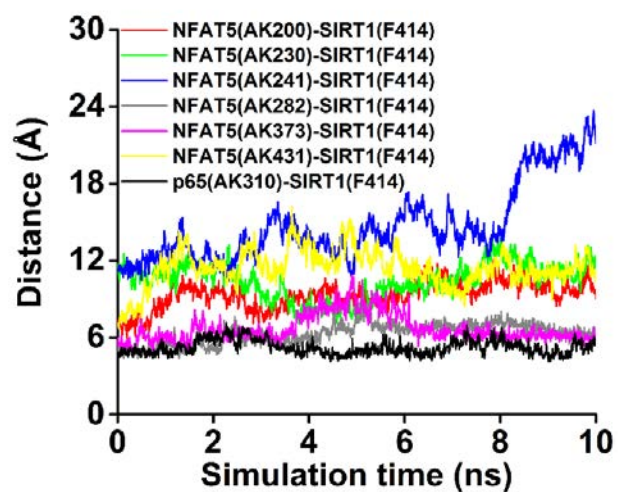


Figure 3.18. AK282 and AK373 of NFAT5 docked to SIRT1 substrate binding site F414 showed similar AK to F414 (gray, magenta and black) distance compared to p65 (AK310)-SIRT1 (F414) complex during 10 ns MD simulations.

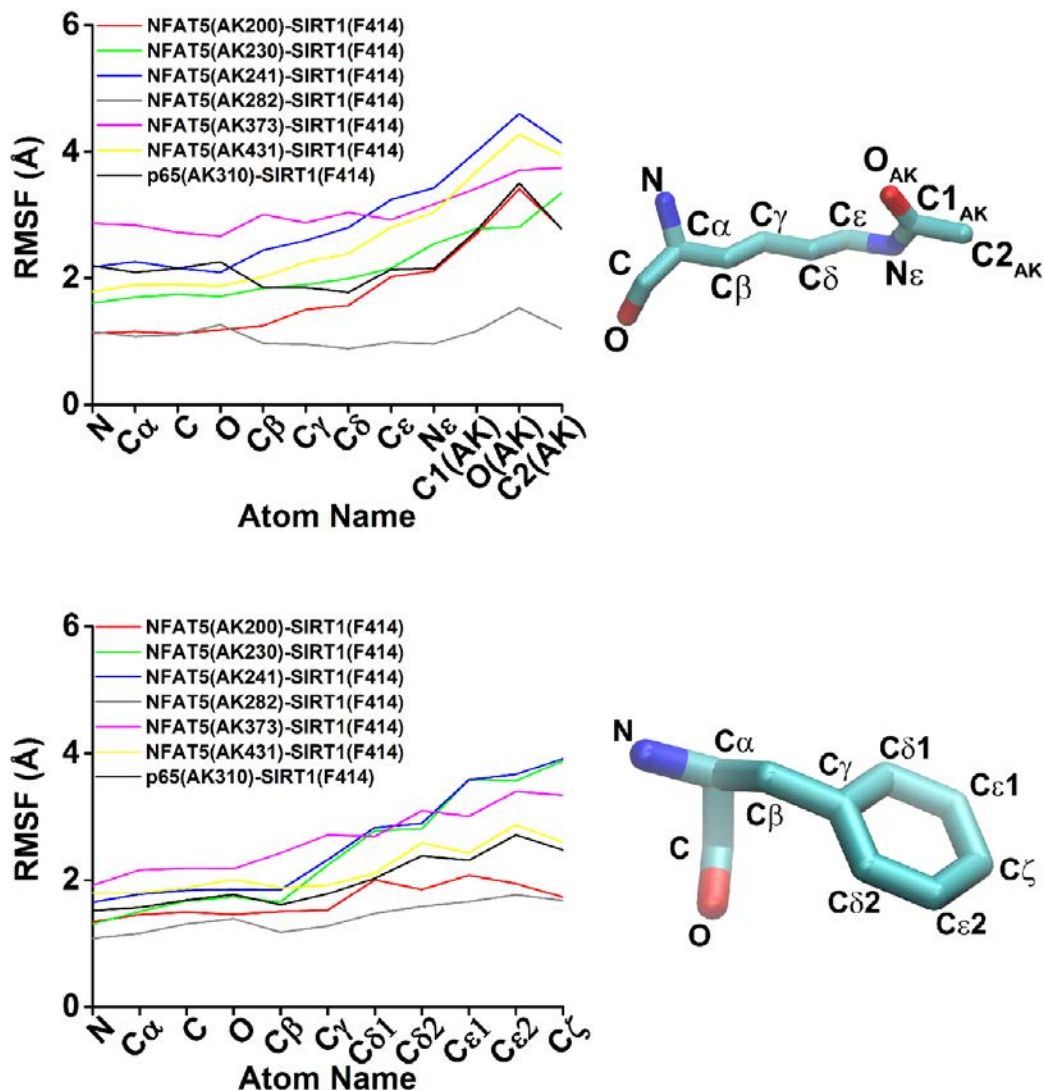


Figure 3.19. AK282 of NFAT5 docked to SIRT1 substrate binding site F414 showed lower RMSF values for AK and F414 atoms, compared to p65 (AK310)-SIRT1 (F414) complex during 10 ns MD simulations. (Upper panel) RMSF of all atoms of AK were calculated during 10 ns of MD simulations in all complexes, depicted in legend. RMSF of AK282 atoms of NFAT5 displayed lower flexibility compared to AK310 of p65. (Lower panel) RMSF of all atoms of SIRT1's F414 were calculated during 10 ns of MD simulations in all complexes, depicted in legend. RMSF of F414 atoms of SIRT1 in NFAT5(AK282)-SIRT1(F414) complex displayed lower flexibility compared to F414 of p65(AK310)-SIRT1(F414) complex. For both panels representatives of AK and F414 with atom names were given near the graphs.

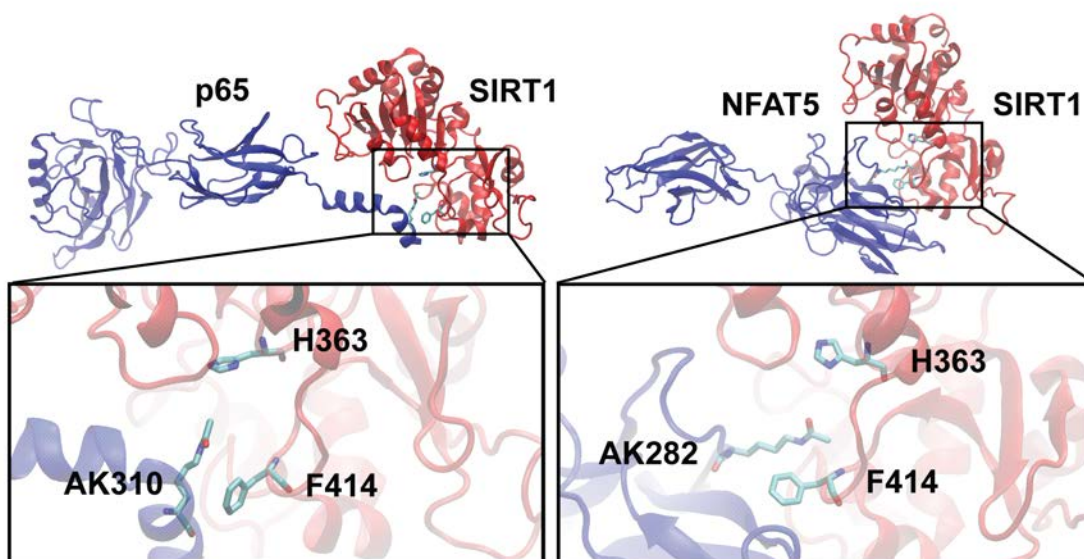


Figure 3.20. Representative snapshots of whole complexes taken from the last 1 ns of simulations were shown in upper panels, while AK282, AK310 and SIRT1 substrate binding site (F414) were shown in lower panels. H363 of SIRT1 was shown for enzymatic cleft positioning. AK282 of NFAT5 approaching close proximity of F414 of SIRT1 (right panel) showed similar orientation to AK310 of p65 approaching to F414 of SIRT1 (left panel) at 10<sup>th</sup> ns of MD simulations.

## 4. DISCUSSION AND CONCLUSION

### 4.1. A unique osmotic stress model

Generation of osmotic stress model was the fundamental step of this study due to selecting osmotic stress specific contribution of the agent to intracellular stress and to expressions of NFAT5 and SIRT1. In order to avoid other specific effects of these agents that might interfere with osmotic stress signaling, osmotic controls were utilized within selection procedure (Figures 3.2 and 3.3) (Burg et al., 2007, Kuper et al., 2012). When compared to its osmotic controls, high glucose treatment increased NFAT5 independent of osmotic stress with lack of SIRT1 expression. Although previous findings suggested similar results such that high glucose increases DNA binding activity of NFAT5 and downregulates SIRT1 expression in monocytes, high glucose was omitted at this step due lack of SIRT1 expression (Yang et al., 2006, de Kreutzenberg et al., 2010, Yun et al., 2012). Similar to our observations, high salt treatment has been recently shown to simultaneously increase expressions of NFAT5 and SIRT1, which led us to utilization of high NaCl in osmotic stress model (Quadri et al., 2014).

Hyperosmotic environment has been shown to be encountered in many diseases, including diabetes, sodium sensitive hypertension and inflammatory bowel disease (Neuhofer, 2010). The functionality of NFAT5 and SIRT1 in terms of AR expression during time course of high salt treatment, which mimics osmotic stress related diseases, holds novel insights for understanding our model. At the initial hours of osmotic challenge, NFAT5 expression was slightly detectable, whereas SIRT1 expression significantly declined, though they both peaked at the 16<sup>th</sup> hour of the osmotic stress (Figure 3.3). Observation of increased NFAT5 expression at 16<sup>th</sup> hour is concordant with previous findings by Woo et al. in which they obtained peak NFAT5 expression between 12<sup>th</sup> and 18<sup>th</sup> hours of osmotic challenge (Woo et al., 2000a). Although peaked expression of NFAT5 was achieved after 16 hours, it became more cytoplasmic, which resulted in less AR expression (Figures 3.4 and 3.5). Interestingly, compared to highly cytoplasmic NFAT5 and SIRT1 expressions at 16 hours, almost completely nucleus localized NFAT5 expression and increased AR expression

coincided with less SIRT1 expression at 4 hours (Figures 3.4 and 3.5). Since SIRT1 activity was identified as a contributing element for NFAT5 dependent AR expression, it was inferred that the fluctuation observed in SIRT1 expression during time course may be explained by the paradigm that SIRT1 activity negatively regulates its own expression (Chen et al., 2005b, Kwon et al., 2008, Yuan et al., 2009, Pardo et al., 2012). In line with this paradigm, in U937 cells under osmotic stress, pharmacological activator of SIRT1, resveratrol and PARP1 inhibitor, 3-aminobenzamide decreased SIRT1 expression, whereas SIRT1 inhibitor, Ex-527 increased it (Figures 3.8 and 3.9). In negative controls of osmotic stress, nuclear NFAT5 and AR expressions were also higher but SIRT1 expressions were either undetectable or less than 16 hours of osmotic stress only group (Figures 3.5, 3.8 and 3.9). Overall, it was apparent that osmotic stress model simultaneously increased expressions of NFAT5 and SIRT1, but increase in expression of SIRT1 was likely to be due to reduction in its activity. This enabled us to study a novel osmotic stress model in which suppression of NFAT5 dependent AR expression was in part due to loss of SIRT1 activity.

#### **4.2. Functional interplay of SIRT1 and PARP1 under osmotic stress**

Our motivation towards investigating the role of SIRT1 on NFAT5 dependent AR expression, was developed due to the fact that previously PARP1, which has documented to work reciprocally with SIRT1, has also been revealed to inhibit NFAT5 transcriptional activity (Chen et al., 2007, Luna et al., 2013). PARP1 and SIRT1 compete for intracellular NAD<sup>+</sup>, hence, these enzymes has been considered to work as antagonists of each other (Rajamohan et al., 2009, Bai et al., 2011). In particular, PARP1 activity has been shown to act on several SIRT1 targets such as p65 and High Mobility Group Box 1 by diminishing SIRT1 activity (Kauppinen et al., 2013, Walko Iii et al., 2015). Based on these previous observations, it was reasoned that possible presence of PARP1 activity could also interfere with our osmotic stress model via lowering SIRT1 activity. Therefore, expressions of PARP1 and its activator SIRT6 were analyzed in time course expression analysis (Figure 3.3). Since peaked expression of PARP1, as well as its activator SIRT6 were found to coincide with those of NFAT5 and SIRT1, it was deduced that our model was vulnerable to a possible

crosstalk from PARP1 activity. In line with this deduction, inhibiting PARP1 with 3AB caused higher nuclear NFAT5 stabilization and AR expression, yielding results parallel to SIRT1 activation by resveratrol (Figures 3.6, 3.8 and 3.9). Co-immunoprecipitation experiments also provided evidence that osmotic stress model of U937 monocytes decreases SIRT1 interaction with NFAT5, increases NFAT5 acetylation status and increases NFAT5-PARP1 interaction (Figure 3.13). These interactions were clearly confirming the presence of PARP1 activity. Crosstalk of PARP1 in the osmotic stress model explains why NFAT5 dependent AR expression could be induced to a certain extent when only SIRT1 was activated. Evidently, it was concluded that NFAT5 dependent AR expression could be under control of PARP1-SIRT1 interplay in osmotic stress model.

#### **4.3. Complementary *in vitro* and *in silico* data for NFAT5 as direct target of SIRT1 enzymatic activity**

Until now, SIRT1 was shown to positively regulate many intracellular targets via direct deacetylation of acetylated lysine residues. It has been previously found that SIRT1 deacetylated Foxo1, which allowed auto transcription of SIRT1 (Xiong et al., 2011). SIRT1 has also displayed deacetylation activity on Tat of human immunodeficiency virus, which resulted in Tat transactivation (Pagans et al., 2005). In another study, deacetylation of the eukaryotic DNA replication initiation factor, Mcm10 by SIRT1, resulted in increased stability and DNA binding of this factor (Fatoba et al., 2013). Parallel to these systems, NFAT5 has been suggested to be a direct SIRT1 deacetylation target using SILAC method (Peng et al., 2012). In line with these previous studies, our *in vitro* and *in silico* approaches shared novel and complementary observations towards understanding of SIRT1 based regulation of NFAT5 in our osmotic stress model. NFAT5 containing complex was identified to be acetylated under osmotic stress, parallel to decrease in its interaction with SIRT1 (Figure 3.13). This observation was validated using 10 different acetylation prediction algorithms in which almost all lysine residues were predicted to be acetylated via at least by one algorithm (Table 3.1). Using co-transfection of NFAT5 and SIRT1 in HeLa cells, it was shown that SIRT1 catalytic activity contributes to the stability of nuclear NFAT5 and its

binding AR ORE probe (Figures 3.11 and 3.12). This *in vitro* finding was also validated using a computational approach, Foldx algorithm, in which six lysine residues, when kept deacetylated, may contribute to the stability NFAT5-DNA complex (Figure 3.14). Among these six residues, at least one lysine residue of NFAT5, K282 has also shown similar distance and even lower flexibility, compared to experimentally proven positive control in MD simulations (Figure 3.18, 3.19 and 3.20). While experimental verification of this residue is necessary, here complimentary *in vitro* and *in silico* evidences were provided such that NFAT5 could be directly deacetylated from at least one residue by SIRT1 and this deacetylation event may contribute to the stabilization of nuclear NFAT5, leading to increased AR expression.

#### **4.4. Proposed Mechanism**

Finally, here a unique mechanism was proposed regulating NFAT5 dependent AR expression in U937 cells under osmotic stress (Figure 4.1). Under 16 hours of osmotic stress, U937 cells tended to display increased cytoplasmic NFAT5 expression, disrupted NFAT5-SIRT1 interaction and decreased AR expression. During this cellular response, inhibiting SIRT1 via its specific inhibitor, EX-527, caused even less NFAT5 expression both in cytoplasm and in nucleus, resulting in decreased AR expression levels. Overexpression of SIRT1 H363Y, catalytically inactive form of SIRT1, in HeLa cells validated the findings of EX-527 and have displayed decreased stabilization of nuclear NFAT5, diminished binding of NFAT5 to AR ORE and decreased AR expression. Activation of SIRT1 via resveratrol displayed increased cytoplasmic to nuclear translocation of NFAT5, leading to increased AR expression in osmotic stress model. Overexpression of wildtype SIRT1 in HeLa cells, kept nuclear NFAT5 stable, while increasing its binding to AR ORE and AR expression. This SIRT1 based regulation could be mediated via direct deacetylation of at least one lysine residue, K282 of NFAT5, based on the *in silico* findings.

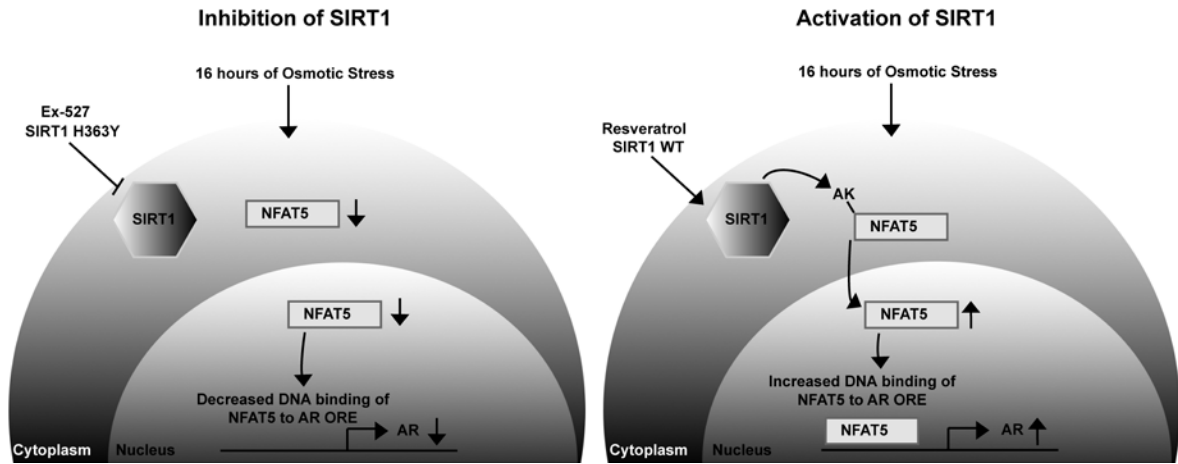


Figure 4.1. Proposed mechanism of SIRT1 based regulation of NFAT5 dependent AR expression in U937 cells under 16 hours of osmotic stress.

#### 4.5. Conclusions

In this study, for the first time, SIRT1 was identified as a novel contributor of NFAT5 dependent AR expression in U937 monocytes under osmotic stress.

- Evidence on SIRT1 based modulation of nuclear NFAT5 stabilization and AR expression in U937 cells under osmotic stress, was provided.
- Key features of this modulation was validated in HeLa cells under osmotic stress.
- NFAT5 and SIRT1 were also discovered to be interacting partners under isosmotic conditions but osmotic stress disrupted this interaction, leading to decreased NFAT5 dependent AR expression in osmotic stress model.
- Using several bioinformatics and computational tools, K282, as a candidate target site of NFAT5, was predicted *in silico* for SIRT1 activity.

#### 4.6. Future Studies

Hyperosmotic environment has been shown to be encountered in many diseases, including diabetes, sodium sensitive hypertension and inflammatory bowel disease. In particular, AR has been shown to mediate micro and macrovascular complications of diabetes. In line with these observations, several AR inhibitors have been developed and tested in clinical trials. Nevertheless, many of these AR inhibitors have been withdrawn from human use due to side effects. Hence, targeting NFAT5, the transcription factor of AR, could stand as a treatment option for AR related diseases. Therefore, our approach, modulation of SIRT1, could be tested to for fine tuning NFAT5 dependent AR expression in future studies.

K282, as a candidate target site of NFAT5, was predicted *in silico* for SIRT1 activity. Based on this result, site-directed mutagenesis studies, followed by luciferase reporter assays for the impact of this mutation on NFAT5 transcriptional activity, could be conducted for *in vitro* verification of this residue. Moreover, K373, which was shown to be involved in NFAT5 dimerization, has also shown properties close to K282. Mutations in K282 may also change solvent exposure of K373 and following accessibility of this residue for SIRT1 activity, therefore K282 may have indirect role on K373 for regulation of NFAT5 dimerization. Further studies using both of these sites will also unravel more detailed mechanism of SIRT1 based regulation of NFAT5 dependent events.

## 5. REFERENCES

- Aida, K., M. Tawata, Y. Ikegishi and T. Onaya (1999). "Induction of rat aldose reductase gene transcription is mediated through the cis-element, osmotic response element (ORE): increased synthesis and/or activation by phosphorylation of ORE-binding protein is a key step." *Endocrinology* 140(2): 609-617.
- Araki, T., Y. Sasaki and J. Milbrandt (2004). "Increased nuclear NAD biosynthesis and SIRT1 activation prevent axonal degeneration." *Science* 305(5686): 1010-1013.
- Aramburu, J., K. Drews-Elger, A. Estrada-Gelonch, J. Minguillon, B. Morancho, V. Santiago and C. Lopez-Rodriguez (2006). "Regulation of the hypertonic stress response and other cellular functions by the Rel-like transcription factor NFAT5." *Biochem Pharmacol* 72(11): 1597-1604.
- Aramburu, J. and C. Lopez-Rodriguez (2009). "Brx shines a light on the route from hyperosmolarity to NFAT5." *Sci Signal* 2(65): pe20.
- Bagnasco, S., R. Balaban, H. M. Fales, Y. M. Yang and M. Burg (1986). "Predominant osmotically active organic solutes in rat and rabbit renal medullas." *J Biol Chem* 261(13): 5872-5877.
- Bagnasco, S., D. Good, R. Balaban and M. Burg (1985). "Lactate production in isolated segments of the rat nephron." *Am J Physiol* 248(4 Pt 2): F522-526.
- Bagnasco, S. M., S. Uchida, R. S. Balaban, P. F. Kador and M. B. Burg (1987). "Induction of aldose reductase and sorbitol in renal inner medullary cells by elevated extracellular NaCl." *Proc Natl Acad Sci U S A* 84(6): 1718-1720.

Bai, P., C. Canto, H. Oudart, A. Brunyanszki, Y. Cen, C. Thomas, H. Yamamoto, A. Huber, B. Kiss, R. H. Houtkooper, K. Schoonjans, V. Schreiber, A. A. Sauve, J. Menissier-de Murcia and J. Auwerx (2011). "PARP-1 inhibition increases mitochondrial metabolism through SIRT1 activation." *Cell Metab* 13(4): 461-468.

Bannister, A. J., E. A. Miska, D. Gorlich and T. Kouzarides (2000). "Acetylation of importin- $\alpha$  nuclear import factors by CBP/p300." *Curr Biol* 10(8): 467-470.

Basu, A., K. L. Rose, J. Zhang, R. C. Beavis, B. Ueberheide, B. A. Garcia, B. Chait, Y. Zhao, D. F. Hunt, E. Segal, C. D. Allis and S. B. Hake (2009). "Proteome-wide prediction of acetylation substrates." *Proc Natl Acad Sci U S A* 106(33): 13785-13790.

Baur, J. A., K. J. Pearson, N. L. Price, H. A. Jamieson, C. Lerin, A. Kalra, V. V. Prabhu, J. S. Allard, G. Lopez-Lluch, K. Lewis, P. J. Pistell, S. Poosala, K. G. Becker, O. Boss, D. Gwinn, M. Wang, S. Ramaswamy, K. W. Fishbein, R. G. Spencer, E. G. Lakatta, D. Le Couteur, R. J. Shaw, P. Navas, P. Puigserver, D. K. Ingram, R. de Cabo and D. A. Sinclair (2006). "Resveratrol improves health and survival of mice on a high-calorie diet." *Nature* 444(7117): 337-342.

Bizzozero, O. A. (1995). "Chemical analysis of acylation sites and species." *Methods Enzymol* 250: 361-379.

Bortner, C. D. and J. A. Cidlowski (1996). "Absence of volume regulatory mechanisms contributes to the rapid activation of apoptosis in thymocytes." *Am J Physiol* 271(3 Pt 1): C950-961.

Brooks, B. R., C. L. Brooks, 3rd, A. D. Mackerell, Jr., L. Nilsson, R. J. Petrella, B. Roux, Y. Won, G. Archontis, C. Bartels, S. Boresch, A. Caffisch, L. Caves, Q. Cui, A. R. Dinner, M. Feig, S. Fischer, J. Gao, M. Hodoscek, W. Im, K. Kuczera, T. Lazaridis, J. Ma, V. Ovchinnikov, E. Paci, R. W. Pastor, C. B. Post, J. Z. Pu, M. Schaefer, B. Tidor, R. M. Venable, H. L. Woodcock, X. Wu, W. Yang, D. M. York and M. Karplus (2009). "CHARMM: the biomolecular simulation program." *Journal of Computational Chemistry* 30(10): 1545-1614.

Brownlee, M. (2001). "Biochemistry and molecular cell biology of diabetic complications." *Nature* 414(6865): 813-820.

Brunet, A., L. B. Sweeney, J. F. Sturgill, K. F. Chua, P. L. Greer, Y. Lin, H. Tran, S. E. Ross, R. Mostoslavsky, H. Y. Cohen, L. S. Hu, H. L. Cheng, M. P. Jedrychowski, S. P. Gygi, D.

A. Sinclair, F. W. Alt and M. E. Greenberg (2004). "Stress-dependent regulation of FOXO transcription factors by the SIRT1 deacetylase." *Science* 303(5666): 2011-2015.

Burg, M. B. (1988). "Role of aldose reductase and sorbitol in maintaining the medullary intracellular milieu." *Kidney Int* 33(3): 635-641.

Burg, M. B., J. D. Ferraris and N. I. Dmitrieva (2007). "Cellular response to hyperosmotic stresses." *Physiol Rev* 87(4): 1441-1474.

Burg, M. B., E. D. Kwon and D. Kultz (1996). "Osmotic regulation of gene expression." *FASEB J* 10(14): 1598-1606.

Burg, M. B., E. D. Kwon and D. Kultz (1997). "Regulation of gene expression by hypertonicity." *Annu Rev Physiol* 59: 437-455.

Bustamante, M., F. Roger, M. L. Bochaton-Piallat, G. Gabbiani, P. Y. Martin and E. Feraille (2003). "Regulatory volume increase is associated with p38 kinase-dependent actin cytoskeleton remodeling in rat kidney MTAL." *Am J Physiol Renal Physiol* 285(2): F336-347.

Cai, Q., J. D. Ferraris and M. B. Burg (2005). "High NaCl increases TonEBP/OREBP mRNA and protein by stabilizing its mRNA." *Am J Physiol Renal Physiol* 289(4): F803-807.

Campos, M. V., M. Bastos, T. Martins, P. Leitao, M. Lemos, M. Carvalheiro and A. Ruas (2003). "[Diabetic hyperosmolality. Retrospective study of 60 cases]." *Acta Med Port* 16(1): 13-19.

Capasso, J. M., C. J. Rivard and T. Berl (2001). "Long-term adaptation of renal cells to hypertonicity: role of MAP kinases and Na-K-ATPase." *Am J Physiol Renal Physiol* 280(5): F768-776.

Capasso, J. M., C. J. Rivard, L. M. Enomoto and T. Berl (2003). "Chloride, not sodium, stimulates expression of the gamma subunit of Na/K-ATPase and activates JNK in response to hypertonicity in mouse IMCD3 cells." *Proc Natl Acad Sci U S A* 100(11): 6428-6433.

Ceriello, A., M. Hanefeld, L. Leiter, L. Monnier, A. Moses, D. Owens, N. Tajima and J. Tuomilehto (2004). "Postprandial glucose regulation and diabetic complications." *Arch Intern Med* 164(19): 2090-2095.

Chen, D., A. D. Steele, S. Lindquist and L. Guarente (2005a). "Increase in activity during calorie restriction requires Sirt1." *Science* 310(5754): 1641.

Chen, F. E., D. B. Huang, Y. Q. Chen and G. Ghosh (1998a). "Crystal structure of p50/p65 heterodimer of transcription factor NF-kappaB bound to DNA." *Nature* 391(6665): 410-413.

Chen, L., J. N. Glover, P. G. Hogan, A. Rao and S. C. Harrison (1998b). "Structure of the DNA-binding domains from NFAT, Fos and Jun bound specifically to DNA." *Nature* 392(6671): 42-48.

Chen, W. Y., D. H. Wang, R. C. Yen, J. Luo, W. Gu and S. B. Baylin (2005b). "Tumor suppressor HIC1 directly regulates SIRT1 to modulate p53-dependent DNA-damage responses." *Cell* 123(3): 437-448.

Chen, Y., M. P. Schnetz, C. E. Irrarrazabal, R. F. Shen, C. K. Williams, M. B. Burg and J. D. Ferraris (2007). "Proteomic identification of proteins associated with the osmoregulatory transcription factor TonEBP/OREBP: functional effects of Hsp90 and PARP-1." *Am J Physiol Renal Physiol* 292(3): F981-992.

Chen, Y. Q., S. Ghosh and G. Ghosh (1998c). "A novel DNA recognition mode by the NF-kappa B p65 homodimer." *Nat Struct Biol* 5(1): 67-73.

Cheng, H. M. and R. G. Gonzalez (1986). "The effect of high glucose and oxidative stress on lens metabolism, aldose reductase, and senile cataractogenesis." *Metabolism* 35(4 Suppl 1): 10-14.

Cohen, H. Y., S. Lavu, K. J. Bitterman, B. Hekking, T. A. Imahiyerobo, C. Miller, R. Frye, H. Ploegh, B. M. Kessler and D. A. Sinclair (2004). "Acetylation of the C terminus of Ku70 by CBP and PCAF controls Bax-mediated apoptosis." *Mol Cell* 13(5): 627-638.

Colla, E., S. D. Lee, M. R. Sheen, S. K. Woo and H. M. Kwon (2006). "TonEBP is inhibited by RNA helicase A via interaction involving the E'F loop." *Biochem J* 393(Pt 1): 411-419.

Cosgrove, M. S., K. Bever, J. L. Avalos, S. Muhammad, X. Zhang and C. Wolberger (2006). "The structural basis of sirtuin substrate affinity." *Biochemistry* 45(24): 7511-7521.

Cramer, P., C. J. Larson, G. L. Verdine and C. W. Muller (1997). "Structure of the human NF-kappaB p52 homodimer-DNA complex at 2.1 A resolution." *EMBO J* 16(23): 7078-7090.

Cress, W. D. and E. Seto (2000). "Histone deacetylases, transcriptional control, and cancer." *J Cell Physiol* 184(1): 1-16.

Cuenda, A., G. Alonso, N. Morrice, M. Jones, R. Meier, P. Cohen and A. R. Nebreda (1996). "Purification and cDNA cloning of SAPKK3, the major activator of RK/p38 in stress- and cytokine-stimulated monocytes and epithelial cells." *EMBO J* 15(16): 4156-4164.

Cyert, M. S. (2001). "Regulation of nuclear localization during signaling." *J Biol Chem* 276(24): 20805-20808.

Dahl, S. C., J. S. Handler and H. M. Kwon (2001). "Hypertonicity-induced phosphorylation and nuclear localization of the transcription factor TonEBP." *Am J Physiol Cell Physiol* 280(2): C248-253.

Davenport, A. M., F. M. Huber and A. Hoelz (2014). "Structural and functional analysis of human SIRT1." *J Mol Biol* 426(3): 526-541.

de Kreutzenberg, S. V., G. Ceolotto, I. Papparella, A. Bortoluzzi, A. Semplicini, C. Dalla Man, C. Cobelli, G. P. Fadini and A. Avogaro (2010). "Downregulation of the longevity-associated protein sirtuin 1 in insulin resistance and metabolic syndrome: potential biochemical mechanisms." *Diabetes* 59(4): 1006-1015.

de Murcia, J. M., C. Niedergang, C. Trucco, M. Ricoul, B. Dutrillaux, M. Mark, F. J. Oliver, M. Masson, A. Dierich, M. LeMeur, C. Walzinger, P. Chambon and G. de Murcia (1997). "Requirement of poly(ADP-ribose) polymerase in recovery from DNA damage in mice and in cells." *Proc Natl Acad Sci U S A* 94(14): 7303-7307.

de Vries, S. J., M. van Dijk and A. M. Bonvin (2010). "The HADDOCK web server for data-driven biomolecular docking." *Nat Protoc* 5(5): 883-897.

Di Ciano, C., Z. Nie, K. Szaszi, A. Lewis, T. Uruno, X. Zhan, O. D. Rotstein, A. Mak and A. Kapus (2002). "Osmotic stress-induced remodeling of the cortical cytoskeleton." *Am J Physiol Cell Physiol* 283(3): C850-865.

Dmitrieva, N. I., D. V. Bulavin and M. B. Burg (2003). "High NaCl causes Mre11 to leave the nucleus, disrupting DNA damage signaling and repair." *Am J Physiol Renal Physiol* 285(2): F266-274.

Dmitrieva, N. I., Q. Cai and M. B. Burg (2004). "Cells adapted to high NaCl have many DNA breaks and impaired DNA repair both in cell culture and in vivo." *Proc Natl Acad Sci U S A* 101(8): 2317-2322.

Dmitrieva, N. I., K. Cui, D. A. Kitchaev, K. Zhao and M. B. Burg (2011). "DNA double-strand breaks induced by high NaCl occur predominantly in gene deserts." *Proc Natl Acad Sci U S A* 108(51): 20796-20801.

Eggermont, J. (2003). "Rho's role in cell volume: sensing, strutting, or signaling? Focus on "Hyperosmotic stress activates Rho: differential involvement in Rho kinase-dependent MLC phosphorylation and NKCC activation"." *Am J Physiol Cell Physiol* 285(3): C509-511.

Eisenhaber, B., M. Sammer, W. H. Lua, W. Benetka, L. L. Liew, W. Yu, H. K. Lee, M. Koranda, F. Eisenhaber and S. Adhikari (2011). "Nuclear import of a lipid-modified transcription factor: mobilization of NFAT5 isoform a by osmotic stress." *Cell Cycle* 10(22): 3897-3911.

Engelman, J. A., J. Luo and L. C. Cantley (2006). "The evolution of phosphatidylinositol 3-kinases as regulators of growth and metabolism." *Nat Rev Genet* 7(8): 606-619.

Faiola, F., X. Liu, S. Lo, S. Pan, K. Zhang, E. Lyman, A. Farina and E. Martinez (2005). "Dual regulation of c-Myc by p300 via acetylation-dependent control of Myc protein turnover and coactivation of Myc-induced transcription." *Mol Cell Biol* 25(23): 10220-10234.

Fatoba, S. T., S. Tognetti, M. Berto, E. Leo, C. M. Mulvey, J. Godovac-Zimmermann, Y. Pommier and A. L. Okorokov (2013). "Human SIRT1 regulates DNA binding and stability of the Mcm10 DNA replication factor via deacetylation." *Nucleic Acids Res* 41(7): 4065-4079.

Feig, M., J. MacKerell, A.D. and I. Brooks, C.L. (2003). " Force field influence on the observation of  $\alpha$ -helical protein structures in molecular dynamics simulations." *Journal of Physical Chemistry B* 107: 2831-2836.

Feldman, J. L., J. Baeza and J. M. Denu (2013). "Activation of the protein deacetylase SIRT6 by long-chain fatty acids and widespread deacylation by mammalian sirtuins." *J Biol Chem* 288(43): 31350-31356.

Ferraris, J. D., P. Persaud, C. K. Williams, Y. Chen and M. B. Burg (2002a). "cAMP-independent role of PKA in tonicity-induced transactivation of tonicity-responsive enhancer/osmotic response element-binding protein." *Proc Natl Acad Sci U S A* 99(26): 16800-16805.

Ferraris, J. D., C. K. Williams, K. Y. Jung, J. J. Bedford, M. B. Burg and A. Garcia-Perez (1996). "ORE, a eukaryotic minimal essential osmotic response element. The aldose reductase gene in hyperosmotic stress." *J Biol Chem* 271(31): 18318-18321.

Ferraris, J. D., C. K. Williams, B. M. Martin, M. B. Burg and A. Garcia-Perez (1994). "Cloning, genomic organization, and osmotic response of the aldose reductase gene." *Proc Natl Acad Sci U S A* 91(22): 10742-10746.

Ferraris, J. D., C. K. Williams, A. Ohtaka and A. Garcia-Perez (1999). "Functional consensus for mammalian osmotic response elements." *Am J Physiol* 276(3 Pt 1): C667-673.

Ferraris, J. D., C. K. Williams, P. Persaud, Z. Zhang, Y. Chen and M. B. Burg (2002b). "Activity of the TonEBP/OREBP transactivation domain varies directly with extracellular NaCl concentration." *Proc Natl Acad Sci U S A* 99(2): 739-744.

Finkemeier, I., M. Laxa, L. Miguet, A. J. Howden and L. J. Sweetlove (2011). "Proteins of diverse function and subcellular location are lysine acetylated in Arabidopsis." *Plant Physiol* 155(4): 1779-1790.

Frye, R. A. (2000). "Phylogenetic classification of prokaryotic and eukaryotic Sir2-like proteins." *Biochem Biophys Res Commun* 273(2): 793-798.

Galizia, L., M. P. Flamenco, V. Rivarola, C. Capurro and P. Ford (2008). "Role of AQP2 in activation of calcium entry by hypotonicity: implications in cell volume regulation." *Am J Physiol Renal Physiol* 294(3): F582-590.

Gallazzini, M., J. D. Ferraris, M. Kunin, R. G. Morris and M. B. Burg (2006). "Neuropathy target esterase catalyzes osmoprotective renal synthesis of glycerophosphocholine in response to high NaCl." *Proc Natl Acad Sci U S A* 103(41): 15260-15265.

Galvez, A., M. P. Morales, J. M. Eltit, P. Ocaranza, L. Carrasco, X. Campos, M. Sapag-Hagar, G. Diaz-Araya and S. Lavandero (2001). "A rapid and strong apoptotic process is triggered by hyperosmotic stress in cultured rat cardiac myocytes." *Cell Tissue Res* 304(2): 279-285.

Garcia-Perez, A. and M. B. Burg (1991). "Renal medullary organic osmolytes." *Physiol Rev* 71(4): 1081-1115.

Garner, M. M. and M. B. Burg (1994). "Macromolecular crowding and confinement in cells exposed to hypertonicity." *Am J Physiol* 266(4 Pt 1): C877-892.

Ghosh, G., G. van Duyne, S. Ghosh and P. B. Sigler (1995). "Structure of NF-kappa B p50 homodimer bound to a kappa B site." *Nature* 373(6512): 303-310.

Glozak, M. A., N. Sengupta, X. Zhang and E. Seto (2005). "Acetylation and deacetylation of non-histone proteins." *Gene* 363: 15-23.

Gnad, F., S. Ren, C. Choudhary, J. Cox and M. Mann (2010). "Predicting post-translational lysine acetylation using support vector machines." *Bioinformatics* 26(13): 1666-1668.

Go, W. Y., X. Liu, M. A. Roti, F. Liu and S. N. Ho (2004). "NFAT5/TonEBP mutant mice define osmotic stress as a critical feature of the lymphoid microenvironment." *Proc Natl Acad Sci U S A* 101(29): 10673-10678.

Greenberg, M. M. (2004). "In vitro and in vivo effects of oxidative damage to deoxyguanosine." *Biochem Soc Trans* 32(Pt 1): 46-50.

Guerois, R., J. E. Nielsen and L. Serrano (2002). "Predicting changes in the stability of proteins and protein complexes: a study of more than 1000 mutations." *J Mol Biol* 320(2): 369-387.

Hager, K., A. Hazama, H. M. Kwon, D. D. Loo, J. S. Handler and E. M. Wright (1995). "Kinetics and specificity of the renal Na<sup>+</sup>/myo-inositol cotransporter expressed in *Xenopus* oocytes." *J Membr Biol* 143(2): 103-113.

Haigis, M. C. and L. P. Guarente (2006). "Mammalian sirtuins--emerging roles in physiology, aging, and calorie restriction." *Genes Dev* 20(21): 2913-2921.

Haigis, M. C. and D. A. Sinclair (2010). "Mammalian sirtuins: biological insights and disease relevance." *Annu Rev Pathol* 5: 253-295.

Hallows, W. C., W. Yu and J. M. Denu (2012). "Regulation of glycolytic enzyme phosphoglycerate mutase-1 by Sirt1 protein-mediated deacetylation." *J Biol Chem* 287(6): 3850-3858.

Han, J., J. D. Lee, L. Bibbs and R. J. Ulevitch (1994). "A MAP kinase targeted by endotoxin and hyperosmolarity in mammalian cells." *Science* 265(5173): 808-811.

Hartl, M., A.-C. König and I. Finkemeier (2015). Identification of Lysine-Acetylated Mitochondrial Proteins and Their Acetylation Sites. *Plant Mitochondria*. J. Whelan and M. W. Murcha, Springer New York. 1305: 107-121.

He, W., Y. Wang, M. Z. Zhang, L. You, L. S. Davis, H. Fan, H. C. Yang, A. B. Fogo, R. Zent, R. C. Harris, M. D. Breyer and C. M. Hao (2010). "Sirt1 activation protects the mouse renal medulla from oxidative injury." *J Clin Invest* 120(4): 1056-1068.

Hebert, A. S., K. E. Dittenhafer-Reed, W. Yu, D. J. Bailey, E. S. Selen, M. D. Boersma, J. J. Carson, M. Tonelli, A. J. Balloon, A. J. Higbee, M. S. Westphall, D. J. Pagliarini, T. A. Prolla, F. Assadi-Porter, S. Roy, J. M. Denu and J. J. Coon (2013). "Calorie restriction and SIRT3 trigger global reprogramming of the mitochondrial protein acetylome." *Mol Cell* 49(1): 186-199.

Hernandez-Ochoa, E. O., P. Robison, M. Contreras, T. Shen, Z. Zhao and M. F. Schneider (2012). "Elevated extracellular glucose and uncontrolled type 1 diabetes enhance NFAT5 signaling and disrupt the transverse tubular network in mouse skeletal muscle." *Exp Biol Med (Maywood)* 237(9): 1068-1083.

Hoffmann, E. K., I. H. Lambert and S. F. Pedersen (2009). "Physiology of cell volume regulation in vertebrates." *Physiol Rev* 89(1): 193-277.

Humphrey, W., A. Dalke and K. Schulten (1996). "VMD: visual molecular dynamics." *J Mol Graph* 14(1): 33-38.

Imai, S., C. M. Armstrong, M. Kaeberlein and L. Guarente (2000). "Transcriptional silencing and longevity protein Sir2 is an NAD-dependent histone deacetylase." *Nature* 403(6771): 795-800.

Irrazabal, C. E., M. B. Burg, S. G. Ward and J. D. Ferraris (2006). "Phosphatidylinositol 3-kinase mediates activation of ATM by high NaCl and by ionizing radiation: Role in osmoprotective transcriptional regulation." *Proc Natl Acad Sci U S A* 103(23): 8882-8887.

Irrazabal, C. E., J. C. Liu, M. B. Burg and J. D. Ferraris (2004). "ATM, a DNA damage-inducible kinase, contributes to activation by high NaCl of the transcription factor TonEBP/OREBP." *Proc Natl Acad Sci U S A* 101(23): 8809-8814.

Irrazabal, C. E., C. K. Williams, M. A. Ely, M. J. Birrer, A. Garcia-Perez, M. B. Burg and J. D. Ferraris (2008). "Activator protein-1 contributes to high NaCl-induced increase in tonicity-responsive enhancer/osmotic response element-binding protein transactivating activity." *J Biol Chem* 283(5): 2554-2563.

Ito, T., Y. Fujio, M. Hirata, T. Takatani, T. Matsuda, S. Muraoka, K. Takahashi and J. Azuma (2004). "Expression of taurine transporter is regulated through the TonE (tonicity-responsive

element)/TonEBP (TonE-binding protein) pathway and contributes to cytoprotection in HepG2 cells." *Biochem J* 382(Pt 1): 177-182.

Jang, E. J., H. Jeong, K. H. Han, H. M. Kwon, J. H. Hong and E. S. Hwang (2012). "TAZ suppresses NFAT5 activity through tyrosine phosphorylation." *Mol Cell Biol* 32(24): 4925-4932.

Jia, Y. Y., J. Lu, Y. Huang, G. Liu, P. Gao, Y. Z. Wan, R. Zhang, Z. Q. Zhang, R. F. Yang, X. Tang, J. Xu, X. Wang, H. Z. Chen and D. P. Liu (2014). "The involvement of NFAT transcriptional activity suppression in SIRT1-mediated inhibition of COX-2 expression induced by PMA/Ionomycin." *PLoS One* 9(5): e97999.

Jin, Z. and W. S. El-Deiry (2005). "Overview of cell death signaling pathways." *Cancer Biol Ther* 4(2): 139-163.

Jorgensen, W. L. and J. D. Madura (1983). "Quantum and statistical mechanical studies of liquids. 25. Solvation and conformation of methanol in water." *Journal of the American Chemical Society* 105(6): 1407-1413.

Kaeberlein, M., M. McVey and L. Guarente (1999). "The SIR2/3/4 complex and SIR2 alone promote longevity in *Saccharomyces cerevisiae* by two different mechanisms." *Genes Dev* 13(19): 2570-2580.

Kang, Y. J., A. Seit-Nebi, R. J. Davis and J. Han (2006). "Multiple activation mechanisms of p38alpha mitogen-activated protein kinase." *J Biol Chem* 281(36): 26225-26234.

Kapus, A., K. Szaszi, J. Sun, S. Rizoli and O. D. Rotstein (1999). "Cell shrinkage regulates Src kinases and induces tyrosine phosphorylation of cortactin, independent of the osmotic regulation of Na<sup>+</sup>/H<sup>+</sup> exchangers." *J Biol Chem* 274(12): 8093-8102.

Kauppinen, T. M., L. Gan and R. A. Swanson (2013). "Poly(ADP-ribose) polymerase-1-induced NAD(+) depletion promotes nuclear factor-kappaB transcriptional activity by preventing p65 de-acetylation." *Biochim Biophys Acta* 1833(8): 1985-1991.

Kempson, S. A., J. M. Edwards and M. Sturek (2006). "Inhibition of the renal betaine transporter by calcium ions." *Am J Physiol Renal Physiol* 291(2): F305-313.

Kempson, S. A. and M. H. Montrose (2004). "Osmotic regulation of renal betaine transport: transcription and beyond." *Pflugers Arch* 449(3): 227-234.

Kiemer, L., J. D. Bendtsen and N. Blom (2005). "NetAcet: prediction of N-terminal acetylation sites." *Bioinformatics* 21(7): 1269-1270.

- Kim, J. A., M. J. Kwon, W. Lee-Kwon, S. Y. Choi, S. Sanada and H. M. Kwon (2014a). "Modulation of TonEBP activity by SUMO modification in response to hypertonicity." *Front Physiol* 5: 200.
- Kim, S. C., R. Sprung, Y. Chen, Y. Xu, H. Ball, J. Pei, T. Cheng, Y. Kho, H. Xiao, L. Xiao, N. V. Grishin, M. White, X.-J. Yang and Y. Zhao "Substrate and Functional Diversity of Lysine Acetylation Revealed by a Proteomics Survey." *Molecular Cell* 23(4): 607-618.
- Kim, S. J., H. Kim, J. Park, I. Chung, H. M. Kwon, W. S. Choi and J. M. Yoo (2014b). "Tonicity response element binding protein associated with neuronal cell death in the experimental diabetic retinopathy." *Int J Ophthalmol* 7(6): 935-940.
- King, L. S., D. Kozono and P. Agre (2004). "From structure to disease: the evolving tale of aquaporin biology." *Nat Rev Mol Cell Biol* 5(9): 687-698.
- Kitada, M., S. Kume, N. Imaizumi and D. Koya (2011). "Resveratrol improves oxidative stress and protects against diabetic nephropathy through normalization of Mn-SOD dysfunction in AMPK/SIRT1-independent pathway." *Diabetes* 60(2): 634-643.
- Ko, B. C., A. K. Lam, A. Kapus, L. Fan, S. K. Chung and S. S. Chung (2002). "Fyn and p38 signaling are both required for maximal hypertonic activation of the osmotic response element-binding protein/tonicity-responsive enhancer-binding protein (OREBP/TonEBP)." *J Biol Chem* 277(48): 46085-46092.
- Ko, B. C., B. Ruepp, K. M. Bohren, K. H. Gabbay and S. S. Chung (1997). "Identification and characterization of multiple osmotic response sequences in the human aldose reductase gene." *J Biol Chem* 272(26): 16431-16437.
- Ko, B. C., C. W. Turck, K. W. Lee, Y. Yang and S. S. Chung (2000). "Purification, identification, and characterization of an osmotic response element binding protein." *Biochem Biophys Res Commun* 270(1): 52-61.
- Konig, A. C., M. Hartl, P. A. Pham, M. Laxa, P. J. Boersema, A. Orwat, I. Kalitventseva, M. Plochinger, H. P. Braun, D. Leister, M. Mann, A. Wachter, A. R. Fernie and I. Finkemeier (2014). "The Arabidopsis class II sirtuin is a lysine deacetylase and interacts with mitochondrial energy metabolism." *Plant Physiol* 164(3): 1401-1414.
- Kouzarides, T. (2000). "Acetylation: a regulatory modification to rival phosphorylation?" *EMBO J* 19(6): 1176-1179.

Kruszewski, M. and I. Szumiel (2005). "Sirtuins (histone deacetylases III) in the cellular response to DNA damage--facts and hypotheses." *DNA Repair (Amst)* 4(11): 1306-1313.

Kultz, D. and D. Chakravarty (2001). "Hyperosmolality in the form of elevated NaCl but not urea causes DNA damage in murine kidney cells." *Proc Natl Acad Sci U S A* 98(4): 1999-2004.

Kuper, C., F. X. Beck and W. Neuhofer (2012). "NFAT5 contributes to osmolality-induced MCP-1 expression in mesothelial cells." *Mediators Inflamm* 2012: 513015.

Kwon, H. M., A. Yamauchi, S. Uchida, A. S. Preston, A. Garcia-Perez, M. B. Burg and J. S. Handler (1992). "Cloning of the cDNA for a Na<sup>+</sup>/myo-inositol cotransporter, a hypertonicity stress protein." *J Biol Chem* 267(9): 6297-6301.

Kwon, H. S. and M. Ott (2008). "The ups and downs of SIRT1." *Trends Biochem Sci* 33(11): 517-525.

Landry, J., J. T. Slama and R. Sternglanz (2000). "Role of NAD(+) in the deacetylase activity of the SIR2-like proteins." *Biochem Biophys Res Commun* 278(3): 685-690.

Lang, K. S., S. Fillon, D. Schneider, H. G. Rammensee and F. Lang (2002). "Stimulation of TNF alpha expression by hyperosmotic stress." *Pflugers Arch* 443(5-6): 798-803.

Leaf, A. (1959). "Maintenance of concentration gradients and regulation of cell volume." *Ann N Y Acad Sci* 72(12): 396-404.

Lee, S. D., E. Colla, M. R. Sheen, K. Y. Na and H. M. Kwon (2003). "Multiple domains of TonEBP cooperate to stimulate transcription in response to hypertonicity." *J Biol Chem* 278(48): 47571-47577.

Lee, S. D., S. K. Woo and H. M. Kwon (2002). "Dimerization is required for phosphorylation and DNA binding of TonEBP/NFAT5." *Biochem Biophys Res Commun* 294(5): 968-975.

Lee, T.-Y., J. B.-K. Hsu, F.-M. Lin, W.-C. Chang, P.-C. Hsu and H.-D. Huang (2010). "N-Ace: Using solvent accessibility and physicochemical properties to identify protein N-acetylation sites." *Journal of Computational Chemistry* 31(15): 2759-2771.

Levine, R. L. (2002). "Carbonyl modified proteins in cellular regulation, aging, and disease." *Free Radic Biol Med* 32(9): 790-796.

Levine, R. L., N. Wehr, J. A. Williams, E. R. Stadtman and E. Shacter (2000). "Determination of carbonyl groups in oxidized proteins." *Methods Mol Biol* 99: 15-24.

- Li, A., Y. Xue, C. Jin, M. Wang and X. Yao (2006). "Prediction of Nepsilon-acetylation on internal lysines implemented in Bayesian Discriminant Method." *Biochem Biophys Res Commun* 350(4): 818-824.
- Li, S., H. Li, M. Li, Y. Shyr, L. Xie and Y. Li (2009). "Improved prediction of lysine acetylation by support vector machines." *Protein Pept Lett* 16(8): 977-983.
- Li, T., Y. Du, L. Wang, L. Huang, W. Li, M. Lu, X. Zhang and W.-G. Zhu (2012a). "Characterization and Prediction of Lysine (K)-Acetyl-Transferase Specific Acetylation Sites." *Molecular & Cellular Proteomics* 11(1).
- Li, T., Y. Du, L. Wang, L. Huang, W. Li, M. Lu, X. Zhang and W. G. Zhu (2012b). "Characterization and prediction of lysine (K)-acetyl-transferase specific acetylation sites." *Mol Cell Proteomics* 11(1): M111 011080.
- Li, Y., M. Wang, H. Wang, H. Tan, Z. Zhang, G. I. Webb and J. Song (2014). "Accurate in silico identification of species-specific acetylation sites by integrating protein sequence-derived and functional features." *Sci. Rep.* 4.
- Lin, S. J., P. A. Defossez and L. Guarente (2000). "Requirement of NAD and SIR2 for life-span extension by calorie restriction in *Saccharomyces cerevisiae*." *Science* 289(5487): 2126-2128.
- Liu, Q., S. Guntuku, X. S. Cui, S. Matsuoka, D. Cortez, K. Tamai, G. Luo, S. Carattini-Rivera, F. DeMayo, A. Bradley, L. A. Donehower and S. J. Elledge (2000). "Chk1 is an essential kinase that is regulated by Atr and required for the G(2)/M DNA damage checkpoint." *Genes Dev* 14(12): 1448-1459.
- Liu, X., B. C. Bandyopadhyay, T. Nakamoto, B. Singh, W. Liedtke, J. E. Melvin and I. Ambudkar (2006). "A role for AQP5 in activation of TRPV4 by hypotonicity: concerted involvement of AQP5 and TRPV4 in regulation of cell volume recovery." *J Biol Chem* 281(22): 15485-15495.
- Lopez-Rodriguez, C., C. L. Antos, J. M. Shelton, J. A. Richardson, F. Lin, T. I. Novobrantseva, R. T. Bronson, P. Igarashi, A. Rao and E. N. Olson (2004). "Loss of NFAT5 results in renal atrophy and lack of tonicity-responsive gene expression." *Proc Natl Acad Sci U S A* 101(8): 2392-2397.

Lopez-Rodriguez, C., J. Aramburu, L. Jin, A. S. Rakeman, M. Michino and A. Rao (2001). "Bridging the NFAT and NF-kappaB families: NFAT5 dimerization regulates cytokine gene transcription in response to osmotic stress." *Immunity* 15(1): 47-58.

Lopez-Rodriguez, C., J. Aramburu, A. S. Rakeman and A. Rao (1999). "NFAT5, a constitutively nuclear NFAT protein that does not cooperate with Fos and Jun." *Proc Natl Acad Sci U S A* 96(13): 7214-7219.

Luna, A., M. I. Aladjem and K. W. Kohn (2013). "SIRT1/PARP1 crosstalk: connecting DNA damage and metabolism." *Genome Integr* 4(1): 6.

Lundby, A., K. Lage, Brian T. Weinert, Dorte B. Bekker-Jensen, A. Secher, T. Skovgaard, Christian D. Kelstrup, A. Dmytriiev, C. Choudhary, C. Lundby and Jesper V. Olsen "Proteomic Analysis of Lysine Acetylation Sites in Rat Tissues Reveals Organ Specificity and Subcellular Patterns." *Cell Reports* 2(2): 419-431.

Luo, G., M. S. Yao, C. F. Bender, M. Mills, A. R. Bladl, A. Bradley and J. H. Petrini (1999). "Disruption of mRad50 causes embryonic stem cell lethality, abnormal embryonic development, and sensitivity to ionizing radiation." *Proc Natl Acad Sci U S A* 96(13): 7376-7381.

MacKerell, J., A.D. , M. Feig and C. L. Brooks (2004). " Improved treatment of the protein backbone in empirical force fields." *Journal of the American Chemical Society* 126: 698-699.

MacKerell, J. A. D., D. Bashford, M. Bellott, R. L. Dunbrack Jr., J. D. Evanseck, M. J. Field, S. Fischer, J. Gao, H. Guo, S. Ha, D. Joseph-McCarthy, L. Kuchnir, K. Kuczera, F. T. K. Lau, C. Mattos, S. Michnick, T. Ngo, D. T. Nguyen, B. Prodhom, I. Reiher, W.E., B. Roux, M. Schlenkrich, J. C. Smith, R. Stote, J. Straub, M. Watanabe, J. Wiorkiewicz-Kuczera, D. Yin and M. Karplus (1998). "All-atom empirical potential for molecular modeling and dynamics studies of proteins." *Journal of Physical Chemistry B* 102: 3586-3616.

Malanga, M. and F. R. Althaus (2005). "The role of poly(ADP-ribose) in the DNA damage signaling network." *Biochem Cell Biol* 83(3): 354-364.

Mallee, J. J., M. G. Atta, V. Lorica, J. S. Rim, H. M. Kwon, A. D. Lucente, Y. Wang and G. T. Berry (1997). "The structural organization of the human Na<sup>+</sup>/myo-inositol cotransporter (SLC5A3) gene and characterization of the promoter." *Genomics* 46(3): 459-465.

Mao, Z., C. Hine, X. Tian, M. Van Meter, M. Au, A. Vaidya, A. Seluanov and V. Gorbunova (2011). "SIRT6 promotes DNA repair under stress by activating PARP1." *Science* 332(6036): 1443-1446.

Masutani, M., H. Suzuki, N. Kamada, M. Watanabe, O. Ueda, T. Nozaki, K. Jishage, T. Watanabe, T. Sugimoto, H. Nakagama, T. Ochiya and T. Sugimura (1999). "Poly(ADP-ribose) polymerase gene disruption conferred mice resistant to streptozotocin-induced diabetes." *Proc Natl Acad Sci U S A* 96(5): 2301-2304.

Matsushita, N., Y. Takami, M. Kimura, S. Tachiiri, M. Ishiai, T. Nakayama and M. Takata (2005). "Role of NAD-dependent deacetylases SIRT1 and SIRT2 in radiation and cisplatin-induced cell death in vertebrate cells." *Genes Cells* 10(4): 321-332.

Matsuzaki, H., H. Daitoku, M. Hatta, H. Aoyama, K. Yoshimochi and A. Fukamizu (2005). "Acetylation of Foxo1 alters its DNA-binding ability and sensitivity to phosphorylation." *Proc Natl Acad Sci U S A* 102(32): 11278-11283.

Meier, R., J. Rouse, A. Cuenda, A. R. Nebreda and P. Cohen (1996). "Cellular stresses and cytokines activate multiple mitogen-activated-protein kinase kinase homologues in PC12 and KB cells." *Eur J Biochem* 236(3): 796-805.

Michea, L., C. Combs, P. Andrews, N. Dmitrieva and M. B. Burg (2002). "Mitochondrial dysfunction is an early event in high-NaCl-induced apoptosis of mIMCD3 cells." *Am J Physiol Renal Physiol* 282(6): F981-990.

Michea, L., D. R. Ferguson, E. M. Peters, P. M. Andrews, M. R. Kirby and M. B. Burg (2000). "Cell cycle delay and apoptosis are induced by high salt and urea in renal medullary cells." *Am J Physiol Renal Physiol* 278(2): F209-218.

Michishita, E., R. A. McCord, E. Berber, M. Kioi, H. Padilla-Nash, M. Damian, P. Cheung, R. Kusumoto, T. L. Kawahara, J. C. Barrett, H. Y. Chang, V. A. Bohr, T. Ried, O. Gozani and K. F. Chua (2008). "SIRT6 is a histone H3 lysine 9 deacetylase that modulates telomeric chromatin." *Nature* 452(7186): 492-496.

Milne, J. C., P. D. Lambert, S. Schenk, D. P. Carney, J. J. Smith, D. J. Gagne, L. Jin, O. Boss, R. B. Perni, C. B. Vu, J. E. Bemis, R. Xie, J. S. Disch, P. Y. Ng, J. J. Nunes, A. V. Lynch, H. Yang, H. Galonek, K. Israelian, W. Choy, A. Iffland, S. Lavu, O. Medvedik, D. A. Sinclair, J. M. Olefsky, M. R. Jirousek, P. J. Elliott and C. H. Westphal (2007). "Small

molecule activators of SIRT1 as therapeutics for the treatment of type 2 diabetes." *Nature* 450(7170): 712-716.

Miyakawa, H., J. S. Rim, J. S. Handler and H. M. Kwon (1999a). "Identification of the second tonicity-responsive enhancer for the betaine transporter (BGT1) gene." *Biochim Biophys Acta* 1446(3): 359-364.

Miyakawa, H., S. K. Woo, S. C. Dahl, J. S. Handler and H. M. Kwon (1999b). "Tonicity-responsive enhancer binding protein, a rel-like protein that stimulates transcription in response to hypertonicity." *Proc Natl Acad Sci U S A* 96(5): 2538-2542.

Monnier, L., H. Lapinski and C. Colette (2003). "Contributions of fasting and postprandial plasma glucose increments to the overall diurnal hyperglycemia of type 2 diabetic patients: variations with increasing levels of HbA(1c)." *Diabetes Care* 26(3): 881-885.

Moreira, I. S., P. A. Fernandes and M. J. Ramos (2010). "Protein-protein docking dealing with the unknown." *J Comput Chem* 31(2): 317-342.

Motta, M. C., N. Divecha, M. Lemieux, C. Kamel, D. Chen, W. Gu, Y. Bultsma, M. McBurney and L. Guarente (2004). "Mammalian SIRT1 represses forkhead transcription factors." *Cell* 116(4): 551-563.

Mountain, I., E. Waelkens, L. Missiaen and W. van Driessche (1998). "Changes in actin cytoskeleton during volume regulation in C6 glial cells." *Eur J Cell Biol* 77(3): 196-204.

Muller, C. W., F. A. Rey, M. Sodeoka, G. L. Verdine and S. C. Harrison (1995). "Structure of the NF-kappa B p50 homodimer bound to DNA." *Nature* 373(6512): 311-317.

Murr, R., J. I. Loizou, Y. G. Yang, C. Cuenin, H. Li, Z. Q. Wang and Z. Herceg (2006). "Histone acetylation by Trrap-Tip60 modulates loading of repair proteins and repair of DNA double-strand breaks." *Nat Cell Biol* 8(1): 91-99.

Nadkarni, V., K. H. Gabbay, K. M. Bohren and D. Sheikh-Hamad (1999). "Osmotic response element enhancer activity. Regulation through p38 kinase and mitogen-activated extracellular signal-regulated kinase kinase." *J Biol Chem* 274(29): 20185-20190.

Nakanishi, T., O. Uyama and M. Sugita (1991). "Osmotically regulated taurine content in rat renal inner medulla." *Am J Physiol* 261(6 Pt 2): F957-962.

Neuhofer, W. (2010). "Role of NFAT5 in inflammatory disorders associated with osmotic stress." *Curr Genomics* 11(8): 584-590.

North, B. J., B. L. Marshall, M. T. Borra, J. M. Denu and E. Verdin (2003). "The human Sir2 ortholog, SIRT2, is an NAD<sup>+</sup>-dependent tubulin deacetylase." *Mol Cell* 11(2): 437-444.

North, B. J. and E. Verdin (2004). "Sirtuins: Sir2-related NAD-dependent protein deacetylases." *Genome Biol* 5(5): 224.

Oates, P. J. (2008). "Aldose reductase, still a compelling target for diabetic neuropathy." *Curr Drug Targets* 9(1): 14-36.

Orimo, M., T. Minamino, H. Miyauchi, K. Tateno, S. Okada, J. Moriya and I. Komuro (2009). "Protective role of SIRT1 in diabetic vascular dysfunction." *Arterioscler Thromb Vasc Biol* 29(6): 889-894.

Pagans, S., A. Pedal, B. J. North, K. Kaehlcke, B. L. Marshall, A. Dorr, C. Hetzer-Egger, P. Henklein, R. Frye, M. W. McBurney, H. Hruby, M. Jung, E. Verdin and M. Ott (2005). "SIRT1 regulates HIV transcription via Tat deacetylation." *PLoS Biol* 3(2): e41.

Pardo, P. S. and A. M. Boriek (2012). "An autoregulatory loop reverts the mechanosensitive Sirt1 induction by EGR1 in skeletal muscle cells." *Aging (Albany NY)* 4(7): 456-461.

Park, J., H. Kim, S. Y. Park, S. W. Lim, Y. S. Kim, D. H. Lee, G. S. Roh, H. J. Kim, S. S. Kang, G. J. Cho, B. Y. Jeong, H. M. Kwon and W. S. Choi (2014). "Tonicity-responsive enhancer binding protein regulates the expression of aldose reductase and protein kinase C delta in a mouse model of diabetic retinopathy." *Exp Eye Res* 122: 13-19.

Pedersen, S. F. and E. K. Hoffmann (2002). "Possible interrelationship between changes in F-actin and myosin II, protein phosphorylation, and cell volume regulation in Ehrlich ascites tumor cells." *Exp Cell Res* 277(1): 57-73.

Peng, L., H. Ling, Z. Yuan, B. Fang, G. Bloom, K. Fukasawa, J. Koomen, J. Chen, W. S. Lane and E. Seto (2012). "SIRT1 negatively regulates the activities, functions, and protein levels of hMOF and TIP60." *Mol Cell Biol* 32(14): 2823-2836.

Phillips, J. C., R. Braun, W. Wang, J. Gumbart, E. Tajkhorshid, E. Villa, C. Chipot, R. D. Skeel, L. Kale and K. Schulten (2005). "Scalable molecular dynamics with NAMD." *Journal of Computational Chemistry* 26(16): 1781-1802.

Pillai, J. B., A. Isbatan, S. Imai and M. P. Gupta (2005). "Poly(ADP-ribose) polymerase-1-dependent cardiac myocyte cell death during heart failure is mediated by NAD<sup>+</sup> depletion and reduced Sir2alpha deacetylase activity." *J Biol Chem* 280(52): 43121-43130.

- Polevoda, B. and F. Sherman (2002). "The diversity of acetylated proteins." *Genome Biol* 3(5): reviews0006.
- Polevoda, B. and F. Sherman (2003). "N-terminal acetyltransferases and sequence requirements for N-terminal acetylation of eukaryotic proteins." *J Mol Biol* 325(4): 595-622.
- Quadri, S. and H. M. Siragy (2014). "Regulation of (pro)renin receptor expression in mIMCD via the GSK-3 $\beta$ -NFAT5-SIRT-1 signaling pathway." *Am J Physiol Renal Physiol* 307(5): F593-600.
- Rajamohan, S. B., V. B. Pillai, M. Gupta, N. R. Sundaresan, K. G. Birukov, S. Samant, M. O. Hottiger and M. P. Gupta (2009). "SIRT1 promotes cell survival under stress by deacetylation-dependent deactivation of poly(ADP-ribose) polymerase 1." *Mol Cell Biol* 29(15): 4116-4129.
- Ramadoss, P. and G. H. Perdew (2005). "The transactivation domain of the Ah receptor is a key determinant of cellular localization and ligand-independent nucleocytoplasmic shuttling properties." *Biochemistry* 44(33): 11148-11159.
- Ramana, K. V. and S. K. Srivastava (2010). "Aldose reductase: a novel therapeutic target for inflammatory pathologies." *Int J Biochem Cell Biol* 42(1): 17-20.
- Ramasamy, R. and I. J. Goldberg (2010). "Aldose reductase and cardiovascular diseases, creating human-like diabetic complications in an experimental model." *Circ Res* 106(9): 1449-1458.
- Reaven, G. M., C. Hollenbeck, C. Y. Jeng, M. S. Wu and Y. D. Chen (1988). "Measurement of plasma glucose, free fatty acid, lactate, and insulin for 24 h in patients with NIDDM." *Diabetes* 37(8): 1020-1024.
- Reinehr, R., S. Becker, A. Hongen and D. Haussinger (2004). "The Src family kinase Yes triggers hyperosmotic activation of the epidermal growth factor receptor and CD95." *J Biol Chem* 279(23): 23977-23987.
- Rim, J. S., S. Tanawattanacharoen, M. Takenaka, J. S. Handler and H. M. Kwon (1997). "The canine sodium/myo-inositol cotransporter gene: structural organization and characterization of the promoter." *Arch Biochem Biophys* 341(1): 193-199.
- Rogina, B. and S. L. Helfand (2004). "Sir2 mediates longevity in the fly through a pathway related to calorie restriction." *Proc Natl Acad Sci U S A* 101(45): 15998-16003.

Rosette, C. and M. Karin (1996). "Ultraviolet light and osmotic stress: activation of the JNK cascade through multiple growth factor and cytokine receptors." *Science* 274(5290): 1194-1197.

Sadoul, K., J. Wang, B. Diagouraga and S. Khochbin (2011). *The Tale of Protein Lysine Acetylation in the Cytoplasm*.

Santos, B. C., A. Chevaile, M. J. Hebert, J. Zagajeski and S. R. Gullans (1998). "A combination of NaCl and urea enhances survival of IMCD cells to hyperosmolality." *Am J Physiol* 274(6 Pt 2): F1167-1173.

Santos, B. C., J. M. Pullman, A. Chevaile, W. J. Welch and S. R. Gullans (2003). "Chronic hyperosmolarity mediates constitutive expression of molecular chaperones and resistance to injury." *Am J Physiol Renal Physiol* 284(3): F564-574.

Sauve, A. A. (2009). "Pharmaceutical strategies for activating sirtuins." *Curr Pharm Des* 15(1): 45-56.

Sauve, A. A., C. Wolberger, V. L. Schramm and J. D. Boeke (2006). "The biochemistry of sirtuins." *Annu Rev Biochem* 75: 435-465.

Schreiber, V., F. Dantzer, J. C. Ame and G. de Murcia (2006). "Poly(ADP-ribose): novel functions for an old molecule." *Nat Rev Mol Cell Biol* 7(7): 517-528.

Schwer, B., J. Bunkenborg, R. O. Verdin, J. S. Andersen and E. Verdin (2006). "Reversible lysine acetylation controls the activity of the mitochondrial enzyme acetyl-CoA synthetase 2." *Proc Natl Acad Sci U S A* 103(27): 10224-10229.

Schymkowitz, J., J. Borg, F. Stricher, R. Nys, F. Rousseau and L. Serrano (2005a). "The FoldX web server: an online force field." *Nucleic Acids Res* 33(Web Server issue): W382-388.

Schymkowitz, J. W., F. Rousseau, I. C. Martins, J. Ferkinghoff-Borg, F. Stricher and L. Serrano (2005b). "Prediction of water and metal binding sites and their affinities by using the Fold-X force field." *Proc Natl Acad Sci U S A* 102(29): 10147-10152.

Shao, J., D. Xu, L. Hu, Y. W. Kwan, Y. Wang, X. Kong and S. M. Ngai (2012). "Systematic analysis of human lysine acetylation proteins and accurate prediction of human lysine acetylation through bi-relative adapted binomial score Bayes feature representation." *Mol Biosyst* 8(11): 2964-2973.

Shapiro, L. and C. A. Dinarello (1997). "Hyperosmotic stress as a stimulant for proinflammatory cytokine production." *Exp Cell Res* 231(2): 354-362.

Sheen, M. R., S. W. Kim, J. Y. Jung, J. Y. Ahn, J. G. Rhee, H. M. Kwon and S. K. Woo (2006). "Mre11-Rad50-Nbs1 complex is activated by hypertonicity." *Am J Physiol Renal Physiol* 291(5): F1014-1020.

Sheikh-Hamad, D., J. Di Mari, W. N. Suki, R. Safirstein, B. A. Watts, 3rd and D. Rouse (1998). "p38 kinase activity is essential for osmotic induction of mRNAs for HSP70 and transporter for organic solute betaine in Madin-Darby canine kidney cells." *J Biol Chem* 273(3): 1832-1837.

Sheikh-Hamad, D., W. N. Suki and W. Zhao (1997). "Hypertonic induction of the cell adhesion molecule beta 1-integrin in MDCK cells." *Am J Physiol* 273(3 Pt 1): C902-908.

Shi, S. P., J. D. Qiu, X. Y. Sun, S. B. Suo, S. Y. Huang and R. P. Liang (2012). "PLMLA: prediction of lysine methylation and lysine acetylation by combining multiple features." *Mol Biosyst* 8(5): 1520-1527.

Smith, B. C., W. C. Hallows and J. M. Denu (2008). "Mechanisms and molecular probes of sirtuins." *Chem Biol* 15(10): 1002-1013.

Srivastava, S. K., K. V. Ramana and A. Bhatnagar (2005). "Role of aldose reductase and oxidative damage in diabetes and the consequent potential for therapeutic options." *Endocr Rev* 26(3): 380-392.

Stadtman, E. R. and R. L. Levine (2000). "Protein oxidation." *Ann N Y Acad Sci* 899: 191-208.

Strange, K. (2004). "Cellular volume homeostasis." *Adv Physiol Educ* 28(1-4): 155-159.

Street, T. O., D. W. Bolen and G. D. Rose (2006). "A molecular mechanism for osmolyte-induced protein stability." *Proc Natl Acad Sci U S A* 103(38): 13997-14002.

Stroud, J. C., C. Lopez-Rodriguez, A. Rao and L. Chen (2002). "Structure of a TonEBP-DNA complex reveals DNA encircled by a transcription factor." *Nat Struct Biol* 9(2): 90-94.

Subramanian, C., A. W. Opipari, Jr., X. Bian, V. P. Castle and R. P. Kwok (2005). "Ku70 acetylation mediates neuroblastoma cell death induced by histone deacetylase inhibitors." *Proc Natl Acad Sci U S A* 102(13): 4842-4847.

- Suo, S.-B., J.-D. Qiu, S.-P. Shi, X. Chen, S.-Y. Huang and R.-P. Liang (2013a). "Proteome-wide Analysis of Amino Acid Variations That Influence Protein Lysine Acetylation." *Journal of Proteome Research* 12(2): 949-958.
- Suo, S. B., J. D. Qiu, S. P. Shi, X. Chen, S. Y. Huang and R. P. Liang (2013b). "Proteome-wide analysis of amino acid variations that influence protein lysine acetylation." *J Proteome Res* 12(2): 949-958.
- Suo, S. B., J. D. Qiu, S. P. Shi, X. Y. Sun, S. Y. Huang, X. Chen and R. P. Liang (2012). "Position-specific analysis and prediction for protein lysine acetylation based on multiple features." *PLoS One* 7(11): e49108.
- Takenaka, M., A. S. Preston, H. M. Kwon and J. S. Handler (1994). "The tonicity-sensitive element that mediates increased transcription of the betaine transporter gene in response to hypertonic stress." *J Biol Chem* 269(47): 29379-29381.
- Tanner, K. G., J. Landry, R. Sternglanz and J. M. Denu (2000). "Silent information regulator 2 family of NAD- dependent histone/protein deacetylases generates a unique product, 1-O-acetyl-ADP-ribose." *Proc Natl Acad Sci U S A* 97(26): 14178-14182.
- Tissenbaum, H. A. and L. Guarente (2001). "Increased dosage of a sir-2 gene extends lifespan in *Caenorhabditis elegans*." *Nature* 410(6825): 227-230.
- Tong, E. H., J. J. Guo, A. L. Huang, H. Liu, C. D. Hu, S. S. Chung and B. C. Ko (2006). "Regulation of nucleocytoplasmic trafficking of transcription factor OREBP/TonEBP/NFAT5." *J Biol Chem* 281(33): 23870-23879.
- Tosteson, D. C. and J. F. Hoffman (1960). "Regulation of cell volume by active cation transport in high and low potassium sheep red cells." *J Gen Physiol* 44: 169-194.
- Tsang, A. W. and J. C. Escalante-Semerena (1998). "CobB, a new member of the SIR2 family of eucaryotic regulatory proteins, is required to compensate for the lack of nicotinate mononucleotide:5,6-dimethylbenzimidazole phosphoribosyltransferase activity in cobT mutants during cobalamin biosynthesis in *Salmonella typhimurium* LT2." *J Biol Chem* 273(48): 31788-31794.
- Uchida, S., A. Yamauchi, A. S. Preston, H. M. Kwon and J. S. Handler (1993). "Medium tonicity regulates expression of the Na(+)- and Cl(-)-dependent betaine transporter in Madin-Darby canine kidney cells by increasing transcription of the transporter gene." *J Clin Invest* 91(4): 1604-1607.

Ueno, M., W. J. Shen, S. Patel, A. S. Greenberg, S. Azhar and F. B. Kraemer (2013). "Fat-specific protein 27 modulates nuclear factor of activated T cells 5 and the cellular response to stress." *J Lipid Res* 54(3): 734-743.

Uhlik, M. T., A. N. Abell, N. L. Johnson, W. Sun, B. D. Cuevas, K. E. Lobel-Rice, E. A. Horne, M. L. Dell'Acqua and G. L. Johnson (2003). "Rac-MEKK3-MKK3 scaffolding for p38 MAPK activation during hyperosmotic shock." *Nat Cell Biol* 5(12): 1104-1110.

Vaziri, H., S. K. Dessain, E. Ng Eaton, S. I. Imai, R. A. Frye, T. K. Pandita, L. Guarente and R. A. Weinberg (2001). "hSIR2(SIRT1) functions as an NAD-dependent p53 deacetylase." *Cell* 107(2): 149-159.

Vedantham, S., R. Ananthakrishnan, A. M. Schmidt and R. Ramasamy (2012). "Aldose reductase, oxidative stress and diabetic cardiovascular complications." *Cardiovasc Hematol Agents Med Chem* 10(3): 234-240.

Vedantham, S., D. Thiagarajan, R. Ananthakrishnan, L. Wang, R. Rosario, Y. S. Zou, I. Goldberg, S. F. Yan, A. M. Schmidt and R. Ramasamy (2014). "Aldose reductase drives hyperacetylation of Egr-1 in hyperglycemia and consequent upregulation of proinflammatory and prothrombotic signals." *Diabetes* 63(2): 761-774.

Vikramadithyan, R. K., Y. Hu, H. L. Noh, C. P. Liang, K. Hallam, A. R. Tall, R. Ramasamy and I. J. Goldberg (2005). "Human aldose reductase expression accelerates diabetic atherosclerosis in transgenic mice." *J Clin Invest* 115(9): 2434-2443.

Walko Iii, T. D., V. Di Caro, J. Piganelli, T. R. Billiar, R. S. Clark and R. K. Aneja (2015). "Poly(ADP-Ribose) Polymerase 1-Sirtuin 1 Functional Interplay Regulates LPS-Mediated High Mobility Group Box 1 Secretion." *Mol Med* 20(1): 612-624.

Wang, L., Y. Du, M. Lu and T. Li (2012). "ASEB: a web server for KAT-specific acetylation site prediction." *Nucleic Acids Res* 40(Web Server issue): W376-379.

Wang, Q., Y. Zhou, P. Rychahou, C. Liu, H. L. Weiss and B. M. Evers (2013). "NFAT5 represses canonical Wnt signaling via inhibition of beta-catenin acetylation and participates in regulating intestinal cell differentiation." *Cell Death Dis* 4: e671.

Wang, Y., B. C. Ko, J. Y. Yang, T. T. Lam, Z. Jiang, J. Zhang, S. K. Chung and S. S. Chung (2005). "Transgenic mice expressing dominant-negative osmotic-response element-binding protein (OREBP) in lens exhibit fiber cell elongation defect associated with increased DNA breaks." *J Biol Chem* 280(20): 19986-19991.

Wang, Y. and H. A. Tissenbaum (2006). "Overlapping and distinct functions for a *Caenorhabditis elegans* SIR2 and DAF-16/FOXO." *Mech Ageing Dev* 127(1): 48-56.

Wang, Z. Q., L. Stingl, C. Morrison, M. Jantsch, M. Los, K. Schulze-Osthoff and E. F. Wagner (1997). "PARP is important for genomic stability but dispensable in apoptosis." *Genes Dev* 11(18): 2347-2358.

Wehner, F., H. Olsen, H. Tinel, E. Kinne-Saffran and R. K. Kinne (2003). "Cell volume regulation: osmolytes, osmolyte transport, and signal transduction." *Rev Physiol Biochem Pharmacol* 148: 1-80.

Wei, J., Y. Zhang, Y. Luo, Z. Wang, S. Bi, D. Song, Y. Dai, T. Wang, L. Qiu, L. Wen, L. Yuan and J. Y. Yang (2014). "Aldose reductase regulates miR-200a-3p/141-3p to coordinate Keap1-Nrf2, Tgfbeta1/2, and Zeb1/2 signaling in renal mesangial cells and the renal cortex of diabetic mice." *Free Radic Biol Med* 67: 91-102.

Woo, S. K., S. C. Dahl, J. S. Handler and H. M. Kwon (2000a). "Bidirectional regulation of tonicity-responsive enhancer binding protein in response to changes in tonicity." *Am J Physiol Renal Physiol* 278(6): F1006-1012.

Woo, S. K., D. Maouyo, J. S. Handler and H. M. Kwon (2000b). "Nuclear redistribution of tonicity-responsive enhancer binding protein requires proteasome activity." *Am J Physiol Cell Physiol* 278(2): C323-330.

Xiao, Y. and D. T. Weaver (1997). "Conditional gene targeted deletion by Cre recombinase demonstrates the requirement for the double-strand break repair Mre11 protein in murine embryonic stem cells." *Nucleic Acids Res* 25(15): 2985-2991.

Xiong, S., G. Salazar, N. Patrushev and R. W. Alexander (2011). "FoxO1 mediates an autofeedback loop regulating SIRT1 expression." *J Biol Chem* 286(7): 5289-5299.

Xu, Y., X. B. Wang, J. Ding, L. Y. Wu and N. Y. Deng (2010). "Lysine acetylation sites prediction using an ensemble of support vector machine classifiers." *J Theor Biol* 264(1): 130-135.

Yamamoto, M., M. Z. Chen, Y. J. Wang, H. Q. Sun, Y. Wei, M. Martinez and H. L. Yin (2006). "Hypertonic stress increases phosphatidylinositol 4,5-bisphosphate levels by activating PIP5Kbeta." *J Biol Chem* 281(43): 32630-32638.

Yamauchi, A., S. Uchida, H. M. Kwon, A. S. Preston, R. B. Robey, A. Garcia-Perez, M. B. Burg and J. S. Handler (1992). "Cloning of a Na(+)- and Cl(-)-dependent betaine transporter that is regulated by hypertonicity." *J Biol Chem* 267(1): 649-652.

Yamauchi, A., S. Uchida, A. S. Preston, H. M. Kwon and J. S. Handler (1993). "Hypertonicity stimulates transcription of gene for Na(+)-myo-inositol cotransporter in MDCK cells." *Am J Physiol* 264(1 Pt 2): F20-23.

Yancey, P. H., M. E. Clark, S. C. Hand, R. D. Bowlus and G. N. Somero (1982). "Living with water stress: evolution of osmolyte systems." *Science* 217(4566): 1214-1222.

Yang, B., A. D. Hodgkinson, P. J. Oates, H. M. Kwon, B. A. Millward and A. G. Demaine (2006). "Elevated activity of transcription factor nuclear factor of activated T-cells 5 (NFAT5) and diabetic nephropathy." *Diabetes* 55(5): 1450-1455.

Yang, J., N. Wang, Y. Zhu and P. Feng (2011). "Roles of SIRT1 in high glucose-induced endothelial impairment: association with diabetic atherosclerosis." *Arch Med Res* 42(5): 354-360.

Yang, T., A. Zhang, M. Honeggar, D. E. Kohan, D. Mizel, K. Sanders, J. R. Hoidal, J. P. Briggs and J. B. Schnermann (2005). "Hypertonic induction of COX-2 in collecting duct cells by reactive oxygen species of mitochondrial origin." *J Biol Chem* 280(41): 34966-34973.

Yang, X. J. (2004a). "The diverse superfamily of lysine acetyltransferases and their roles in leukemia and other diseases." *Nucleic Acids Res* 32(3): 959-976.

Yang, X. J. (2004b). "Lysine acetylation and the bromodomain: a new partnership for signaling." *Bioessays* 26(10): 1076-1087.

Yeung, F., J. E. Hoberg, C. S. Ramsey, M. D. Keller, D. R. Jones, R. A. Frye and M. W. Mayo (2004). "Modulation of NF-kappaB-dependent transcription and cell survival by the SIRT1 deacetylase." *EMBO J* 23(12): 2369-2380.

Yip, Y. L., H. Scheib, A. V. Diemand, A. Gattiker, L. M. Famiglietti, E. Gasteiger and A. Bairoch (2004). "The Swiss-Prot variant page and the ModSNP database: A resource for sequence and structure information on human protein variants." *Human Mutation* 23(5): 464-470.

Yuan, J., K. Minter-Dykhouse and Z. Lou (2009). "A c-Myc-SIRT1 feedback loop regulates cell growth and transformation." *J Cell Biol* 185(2): 203-211.

- Yuan, Z. L., Y. J. Guan, D. Chatterjee and Y. E. Chin (2005). "Stat3 dimerization regulated by reversible acetylation of a single lysine residue." *Science* 307(5707): 269-273.
- Yun, J. M., A. Chien, I. Jialal and S. Devaraj (2012). "Resveratrol up-regulates SIRT1 and inhibits cellular oxidative stress in the diabetic milieu: mechanistic insights." *J Nutr Biochem* 23(7): 699-705.
- Zeidman, R., C. S. Jackson and A. I. Magee (2009). "Analysis of protein acylation." *Curr Protoc Protein Sci Chapter 14: Unit 14 12*.
- Zhang, J. (2003). "Are poly(ADP-ribosyl)ation by PARP-1 and deacetylation by Sir2 linked?" *Bioessays* 25(8): 808-814.
- Zhang, Z., N. I. Dmitrieva, J. H. Park, R. L. Levine and M. B. Burg (2004). "High urea and NaCl carbonylate proteins in renal cells in culture and in vivo, and high urea causes 8-oxoguanine lesions in their DNA." *Proc Natl Acad Sci U S A* 101(25): 9491-9496.
- Zhang, Z., J. D. Ferraris, C. E. Irarrazabal, N. I. Dmitrieva, J. H. Park and M. B. Burg (2005). "Ataxia telangiectasia-mutated, a DNA damage-inducible kinase, contributes to high NaCl-induced nuclear localization of transcription factor TonEBP/OREBP." *Am J Physiol Renal Physiol* 289(3): F506-511.
- Zhou, X., J. D. Ferraris and M. B. Burg (2006). "Mitochondrial reactive oxygen species contribute to high NaCl-induced activation of the transcription factor TonEBP/OREBP." *Am J Physiol Renal Physiol* 290(5): F1169-1176.
- Zhou, X., J. D. Ferraris, Q. Cai, A. Agarwal and M. B. Burg (2005). "Increased reactive oxygen species contribute to high NaCl-induced activation of the osmoregulatory transcription factor TonEBP/OREBP." *Am J Physiol Renal Physiol* 289(2): F377-385.
- Zhu, J., S. Petersen, L. Tessarollo and A. Nussenzweig (2001). "Targeted disruption of the Nijmegen breakage syndrome gene NBS1 leads to early embryonic lethality in mice." *Curr Biol* 11(2): 105-109.
- Zou, A. P., N. Li and A. W. Cowley, Jr. (2001). "Production and actions of superoxide in the renal medulla." *Hypertension* 37(2 Pt 2): 547-553.

## APPENDIX A

<b>Name of Chemical</b>	<b>Supplier Company</b>	<b>Catalog #</b>
2-Mercaptoethanol	Fluka, Switzerland	63700
2-7-DCFDA	Sigma, Germany	D6883
3-Aminobenzamide	Sigma, Germany	A0788
Acrylamide/Bis-acrylamide	Sigma, Germany	A3699
Sea Kem Gold Agarose	Lonza, USA	50152
Ammonium persulfate	Sigma, Germany	A3678
Antibiotic solution	Sigma, Germany	P3539
Boric acid	Sigma, Germany	B6768
Bradford solution	Biorad, USA	500-0006
BSA	Amresco, USA	0332
Coomassie Brilliant Blue	Merck, Germany	115444
Developer/Replenisher	Agfa, Belgium	G150
Dulbecco's MEM (DMEM)	Pan, Germany	P04-02500
DMSO	Sigma, Germany	D2650
DTT	Sigma, Germany	D9779
EDTA	Riedel-de Haén, Germany	27248
Ethanol	Riedel-de Haén, Germany	32221
Ethidium Bromide	Merck, Germany	OCO28942
Ex-527	Sigma, Germany	E7034
Fixer	E.O.S. Agfa, Belgium	EKSSH

<b>Name of Chemical</b>	<b>Supplier Company</b>	<b>Catalog #</b>
Fetal Bovine Serum	Pan, Germany	P30-1902
Glucose	Sigma, Germany	G8270
Glycerol	Riedel-de Haén, Germany	15523
Glycine	Molekula,	UK M10795755
HCl	Merck, Germany	100314
HEPES	Molekula, UK	M55704197
Hyperfilm ECL	Amersham, UK	RPN2114K
Isopropanol	Riedel-de Haén, Germany	24137
Kanamycin-sulfate	Applichem, Germany	A1493
KCl	Amresco, USA	0395
KH <sub>2</sub> PO <sub>4</sub>	Riedel-de Haén, Germany	04243
KOH	Riedel-de Haén, Germany	06005
Liquid nitrogen	Karbogaz, Turkey	
Luria Agar	Sigma, Germany	L-3147
Luria Broth	Sigma, Germany	L-3022
Methanol	Riedel-de Haén, Germany	24229
MgCl <sub>2</sub>	Sigma, Germany	M9272
Mannitol	Sigma, Germany	M4125
Milk Diluent concentrate	KPL, USA	50-82-00
Na <sub>2</sub> HPO <sub>4</sub>	Merck, Germany	7558-79-4
NaCl	Duchefa Biochemie, NL	S05205000
NaOH	Merck, Germany	106462

<b>Name of Chemical</b>	<b>Supplier Company</b>	<b>Catalog #</b>
NaPO <sub>4</sub> H <sub>2</sub>	Riedel-de Haén, Germany	04269
NP-40	Sigma, Germany	I3021
Penicilin/Streptomycin	PAN, Germany	P06-07100
phoSTOP phosphatase inhibitor	Roche, Germany	4906837001
PMSF	Sigma, Germany	P7629
Poly dA-dT	Sigma, Germany	P0883
Protease inhibitor cocktail tablet	Roche, Germany	4693124001
PVDF membrane	Roche, Germany	03010040001
Resveratrol	Sigma, Germany	R5010
Sodium Dodecyl Sulphate	Sigma, Germany	L4390
TEMED	Sigma, Germany	T7024
Tris	Molekula, UK	M11946779
Tween® 20	Molekula, UK	18945167

## APPENDIX B

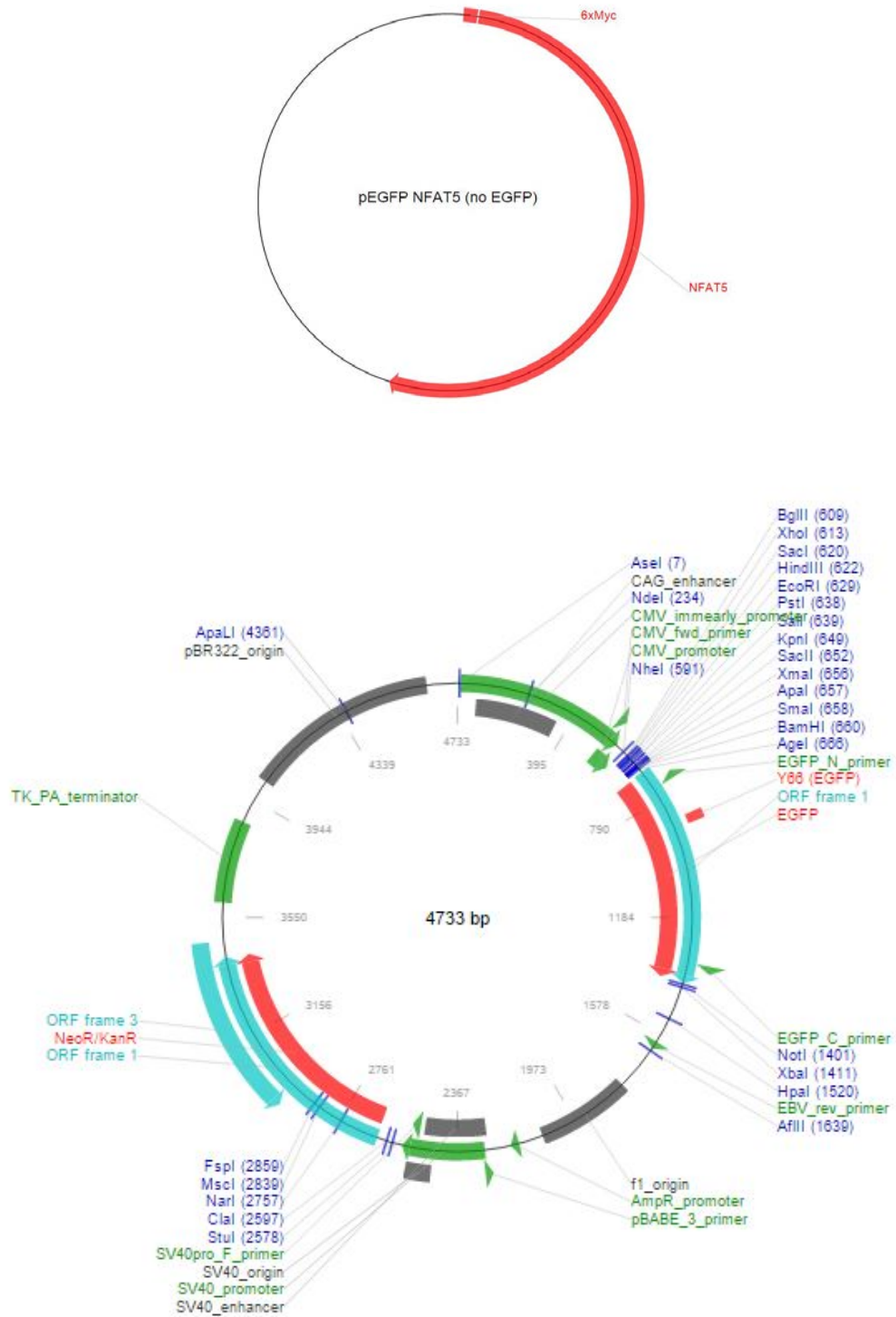
<b>Name</b>	<b>Supplier Company</b>	<b>Catalog #</b>
Anti- $\beta$ -Actin	Cell Signaling, USA	4967
Anti-Flag	Sigma, Germany	F3165
Anti-Lamin A/C	Cell Signaling, USA	2032
Anti-mouse HRP	Cell Signaling, USA	7076
Anti-myc	Cell Signaling, USA	2272
Anti-NFAT5	Santa Cruz, USA	sc-13035
Anti-PARP1	Cell Signaling, USA	9542
Anti-rabbit HRP	Cell Signaling, USA	7074
Anti-SIRT1	Cell Signaling, USA	8469
Anti-SIRT1	Santa Cruz, USA	sc-15404
Anti-SIRT6	Sigma, Germany	SAB4200254
RNase A	Roche, Germany	119915
Trypsin-EDTA	Pan, Germany	P10-0231SP

## APPENDIX C

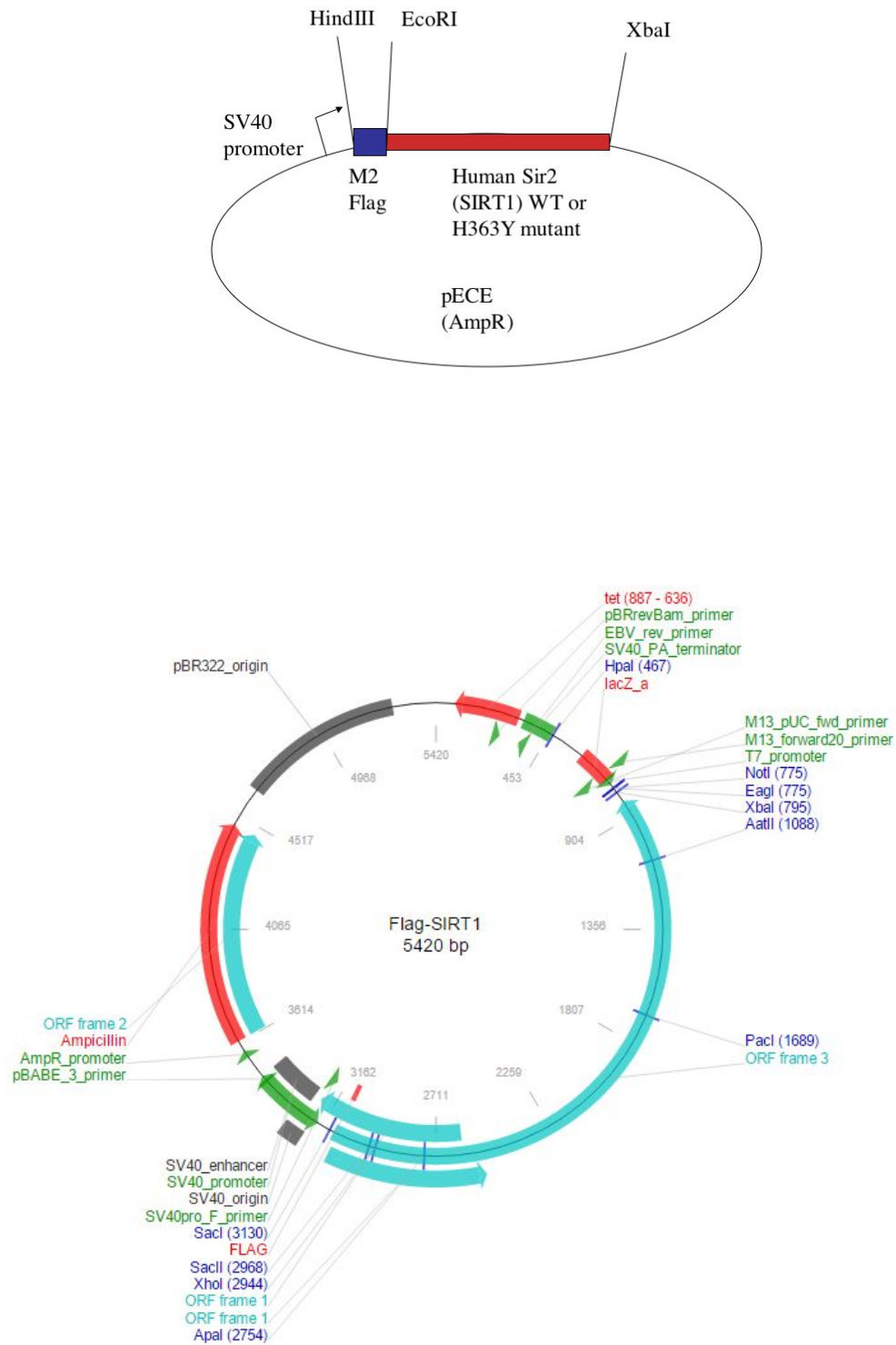
<b>Name</b>	<b>Supplier Company</b>	<b>Catalog #</b>
AnnexinV-FITC	Alexis, USA	ALX-209-250
ECL Advance	Amersham,UK	RPN2209
Genopure plasmid midi kit	Roche, Germany	03143414001
X-TremeGene9	Roche, Germany	06365809001
MTT (Cell Proliferation Kit I)	Roche, Germany	11485007001
PageRuler plus, protein ladder	Fermentas, Lithuania	SM1812
Dynabeads Protein G	Thermo Fisher, USA	10003D
Nucleic acid detection module kit	Thermo Fisher, USA	89880

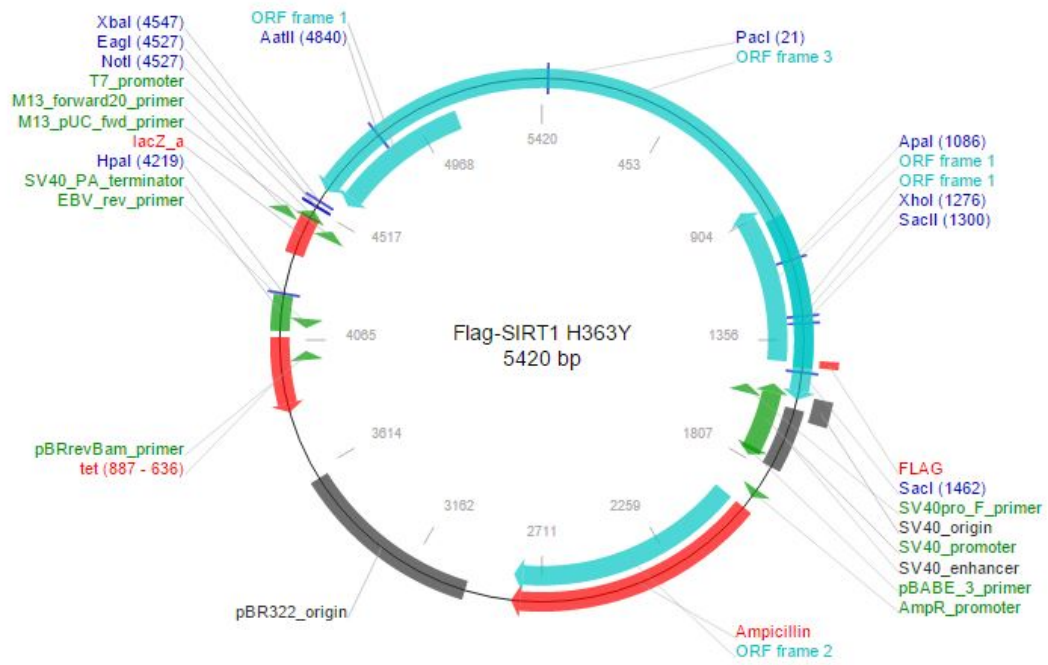
## APPENDIX D

6x myc tagged NFAT5 (Addgene plasmid # 13627) (upper) Vector backbone (lower)



Flag tagged wildtype SIRT1 and flag tagged SIRT1 H363Y (Addgene plasmid # 1791, # 1792)





## APPENDIX E

Osmotic Response Element (ORE) of Human Aldose Reductase Gene (AKR1B1)

5' to 3' Sequence:

AAA GTT ACA TGG AAA AAT ATC TGG GCT AGT CTG TTC TGT ATA AAT TTT  
TCC AGG AGG GAG CAC TTT TAA AGA AAG CAC CAA ATG GAA AAT CAC CGG  
CAT GGA GTT TAG AGA GAC CTG GTG CTT GAG TCA CTA CCA

## APPENDIX F

### **Annealing buffer**

100 mM KAcetate

30 mM HEPES (pH: 7.4)

2 mM MgAcetate

### **Annexin-V staining buffer**

100  $\mu$ l cell suspension in FACS incubation buffer

2  $\mu$ l Annexin-V (Alexis)

### **Blocking solution**

5 g nonfat dried milk

100 ml washing solution

### **Complete lysis buffer**

20 mM Tris-HCl (pH 7.5)

150mM NaCl

NP-40 0.5% (v/v)

0.5 mM PMSF

Protease and phosphatase inhibitor mix

**EMSA binding buffer (5X)**

100 mM HEPES-KOH (pH: 7.9)

5 mM EDTA (pH 7.9)

25% (v/v) glycerol

25 mM MgCl<sub>2</sub>

0,5 M KCl

10 mM DTT (Freshly added)

**EMSA incubation buffer (20µl/sample)**

4 µl EMSA binding buffer

1 µl NP-40

3.45 µl Glycerol (100%)

1 µl BSA (stock: 1mg/ml)

1 µl poly (dA-dT) (stock: 1µg/µl)

Add 5 µg total protein extract and adjust to 20 µl

**FACS incubation buffer**

10 mM HEPES

140 mM NaCl

2.5 mM CaCl<sub>2</sub>

pH: 7.4

**Immunoblotting washing solution**

100 ml PBS (10X)

900 ml ddH<sub>2</sub>O

2ml Tween20 (final: 0.2%)

**Primary antibody incubation solution**

3 ml 5% (w/v) milk blocking solution and 1.5 µg primary antibody

**Running buffer (10X)**

144.1 g glycine

30.3 g Tris

10g SDS

Adjust to 1000ml with ddH<sub>2</sub>O

**Secondary antibody incubation solution**

5ml 5% (w/v) milk blocking solution

1 µg secondary antibody

**T1 Buffer**

10 mM HEPES-KOH (pH: 7.9)

2 mM MgCl<sub>2</sub>.6H<sub>2</sub>O

0.1 mM EDTA

10 mM KCl

1% NP-40

1 mM DTT (freshly added)

0.5 mM PMSF (freshly added)

Complete protease inhibitors (freshly added)

### **T2 Buffer**

50 mM HEPES-KOH (pH: 7.9)

2 mM MgCl<sub>2</sub>·6H<sub>2</sub>O

0.1 mM EDTA

50 mM KCl

400mM NaCl

10% (v/v) Glycerol

1 mM DTT (freshly added)

0.5 mM PMSF (freshly added)

Complete protease inhibitors (freshly added)

### **TBE (10X)**

108 g Tris

55 g Boric acid

40 ml EDTA (pH: 8.0)

**Transfer buffer (stock: 10X)**

144 g glycine

30.3 g Tris

Adjust to 1000ml with ddH<sub>2</sub>O

**Transfer buffer (working: 1X)**

100ml Transfer buffer (10X)

700ml ddH<sub>2</sub>O

200ml Methanol

## APPENDIX G

### Equipments

Autoclave:	Hirayama, Hiclave HV-110, Japan
Balance:	Sartorius, BP211D, Germany
Centrifuge:	Eppendorf, 5415C, Germany
	Eppendorf, 5415D, Germany
	Eppendorf, 5415R, Germany
	Kendro Lab. Prod., Heraeus Multifuge 3L, Germany
	Hitachi, Sorvall RC5C Plus, USA
	Hitachi, Sorvall Discovery 100 SE, USA
	Computer Software: FlowJo V10
	Image J 1.48
	Photoshop CS5, CS6
	Quantity One 4.6.1
	MS Office 2007, 2010
Deepfreezer:	-80°C, Kendro Lab. Prod., Heraeus Hfu486 Basic, Germany
	-20°C, Bosch, Turkey
Distilled water:	Millipore, MilliQ Academic, France
Electrophoresis:	Biorad, USA
Flow cytometer:	BD FACS Conto, USA
Ice Machine:	Scotsman Inc., AF20, USA
Incubator:	Memmert Modell 300 and 600, Germany

Laminar Flow:	Kendro Lab. Prod., Heraeus, HeraSafe HS12, Germany
Magnetic Stirrer:	VELP Scientifica, ARE Heating Magnetic Stirrer, Italy
Microliter Pipette:	Gilson, Pipetman, France
	Mettler Toledo Volumate, USA
	Eppendorf, Germany
pH meter:	WTW, pH540 GLP MultiCal, Germany
Osmometer	Osmomat 030 Gonatech, Germany
Power supply:	Biorad, PowerPac 300, USA
	Wealtec, Elite 300, USA
Refrigerator:	4°C, Bosch, Turkey
Shakers/ mixers:	Forma Scientific, Orbital Shaker 4520, USA
	GFL Shaker 3011, USA
	New Brunswick Sci., Innova 4330, USA
	C25HC Incubator shaker, New Brunswick Scientific, USA
	Gyro rocker SSL3, Stuart, UK
	Thermomixer comfort, Eppendorf, Germany
Spectrophotometer:	Biorad iMark Microplate Absorbance Reader, USA
	ND-1000, Nanodrop, USA
Water bath:	Huber, Polystat cc1, Germany

**Topology for acetyllysine:**

PATCHING FIRS LYSA

RESI LYSA 0.00

GROUP

ATOM N NH1 -0.47

ATOM HN H 0.31

ATOM CA CT1 0.07

ATOM HA HB 0.09

GROUP

ATOM CB CT2 -0.18

ATOM HB1 HA 0.09

ATOM HB2 HA 0.09

GROUP

ATOM CG CT2 -0.18

ATOM HG1 HA 0.09

ATOM HG2 HA 0.09

GROUP

ATOM CD CT2 -0.18

ATOM HD1 HA 0.09

ATOM HD2 HA 0.09

GROUP

ATOM CE CT2 0.21

ATOM HE1 HA 0.05

ATOM HE2 HA 0.05  
 ATOM NZ NH1 -0.61  
 ATOM HZ H 0.30  
 GROUP  
 ATOM CY C 0.51  
 ATOM OY O -0.51  
 GROUP  
 ATOM CAY CT3 -0.27  
 ATOM HY1 HA 0.09  
 ATOM HY2 HA 0.09  
 ATOM HY3 HA 0.09  
 GROUP  
 ATOM C C 0.51  
 ATOM O O -0.51  
 BOND CB CA CG CB CD CG CE CD NZ CE  
 BOND CY CAY CY NZ CAY HY1 CAY HY2 CAY HY3  
 BOND N HN N CA C CA  
 BOND C +N CA HA CB HB1 CB HB2 CG HG1  
 BOND CG HG2 CD HD1 CD HD2 CE HE1 CE HE2  
 DOUBLE O C  
 DOUBLE OY CY  
 BOND NZ HZ  
 IMPR N -C CA HN C CA +N O

IMPR CY CAY NZ OY

IMPR NZ CY CA HZ

CMAP -C N CA C N CA C +N

DONOR HN N

DONOR HZ NZ

ACCEPTOR O C

ACCEPTOR OY CY

!!IC for lysine

IC -C CA \*N HN 1.3482 123.5700 180.0000 115.1100 0.9988

IC -C N CA C 1.3482 123.5700 180.0000 107.2900 1.5187

IC N CA C +N 1.4504 107.2900 180.0000 117.2700 1.3478

IC +N CA \*C O 1.3478 117.2700 180.0000 120.7900 1.2277

IC CA C +N +CA 1.5187 117.2700 180.0000 124.9100 1.4487

IC N C \*CA CB 1.4504 107.2900 122.2300 111.3600 1.5568

IC N C \*CA HA 1.4504 107.2900 -116.8800 107.3600 1.0833

IC N CA CB CG 1.4504 111.4700 180.0000 115.7600 1.5435

IC CG CA \*CB HB1 1.5435 115.7600 120.9000 107.1100 1.1146

IC CG CA \*CB HB2 1.5435 115.7600 -124.4800 108.9900 1.1131

IC CA CB CG CD 1.5568 115.7600 180.0000 113.2800 1.5397

IC CD CB \*CG HG1 1.5397 113.2800 120.7400 109.1000 1.1138

IC CD CB \*CG HG2 1.5397 113.2800 -122.3400 108.9900 1.1143

IC CB CG CD CE 1.5435 113.2800 180.0000 112.3300 1.5350

IC CE CG \*CD HD1 1.5350 112.3300 122.2500 108.4100 1.1141

IC CE CG \*CD HD2 1.5350 112.3300 -121.5900 108.1300 1.1146  
 IC CG CD CE NZ 1.5397 112.3300 180.0000 110.4600 1.4604  
 IC NZ CD \*CE HE1 1.4604 110.4600 119.9100 110.5100 1.1128  
 IC NZ CD \*CE HE2 1.4604 110.4600 -120.0200 110.5700 1.1123  
 IC CD CE NZ HZ 1.5350 110.4600 179.9200 113.1400 1.0065  
 !IC HZ1 CE \*NZ HZ2 1.0404 110.0200 120.2700 109.5000 1.0402  
 !IC HZ1 CE \*NZ HZ3 1.0404 110.0200 -120.1300 109.4000 1.0401  
 !!IC for aceytl  
 IC CY NZ CE CD 1.3482 123.5700 -60.0000 110.4600 1.5350  
 IC CY CE \*NZ HZ 1.4604 110.02 180.0000 45.00 0.9988  
 IC CAY CY NZ CE 1.5397 120.00 180.0000 110.02 1.4604  
 IC NZ CAY \*CY OY 1.5350 120.00 180.0000 120.00 1.2277  
 IC OY CY CAY HY1 1.2277 120.790 180.0000 120.00 1.5435  
 IC OY CY CAY HY2 1.2277 120.7900 60.0000 120.00 1.5435  
 IC OY CY CAY HY3 1.2277 120.7900 -60.0000 120.00 1.5435